University of São Paulo
"Luiz de Queiroz" College of Agriculture

Hydrological modeling of soil-water availability in the Caatinga biome

Everton Alves Rodrigues Pinheiro

Thesis presented to obtain the degree of Doctor of Science. Area: Agricultural Systems Engineering

Piracicaba
2016

Everton Alves Rodrigues Pinheiro
Agronomist

Hydrological modeling of soil-water availability in the Caatinga biome

Advisor:
Prof. Dr. **QUIRIJN DE JONG VAN LIER**

Thesis presented to obtain the degree of Doctor of Science. Area: Agricultural Systems Engineering

Piracicaba
2016

Dados Internacionais de Catalogação na Publicação
DIVISÃO DE BIBLIOTECA - DIBD/ESALQ/USP

Pinheiro, Everton Alves Rodrigues
Hydrological modeling of soil-water availability in the Caatinga biome / Everton Alves Rodrigues Pinheiro. - - Piracicaba, 2016.
90 p. : il.

Tese (Doutorado) - - Escola Superior de Agricultura “Luiz de Queiroz”.

1. Semiárido 2. Evapotranspiração 3. Mudanças climáticas 4. SWAP 5. Balanço hídrico I. Título

CDD 631.432
P654h

To my beloved parents: Elisberto and Maria, for all love and comprehension devoted to me and for their kind understanding towards my career decisions.

To my sisters, Fabiana and Tatiane, for the mutual love.

To Cleidiane, for making herself always present into my life, for all comprehension and patience.

DEDICATED TO THEM

ACKNOWLEDGMENTS

To God, Christ Jesus and Virgin Mary, for life, health and for the opportunity to overcome the life challenges that strengthen my spiritual being, humane and professional.

To Professor Quirijn de Jong van Lier for all knowledge transmitted, patience, openness and professionalism dedicated to this research.

To the "Luiz de Queiroz" College of Agriculture (ESALQ/USP), for providing the necessary resources to finish this thesis.

To FAPESP (São Paulo Research Foundation) for funding this PhD thesis and for providing national scholarship (grant # 2013/08967-8) and for sponsoring my research internship abroad (grant # 2014/06084-4).

To the Department of Biosystems Engineering through its professors, in special, Sergio Oliveira Moraes, Paulo Leonel Libardi, Fábio Ricardo Marin, Sérgio Nascimento Duarte e Jarbas Honório de Miranda.

To the people of the Department of Biosystems Engineering, especially the secretaries Angela Derigi Silva e Davilmar Aparecida Colevatti.

To the Center for Nuclear Energy in Agriculture, for the reception during the entire period of my PhD.

To my Professors and supervisors during my undergraduate course and master course from Federal University of Ceará, especially, Carlos Alexandre Gomes Costa, Cândida Hermínia, Ervino Bleicher e José Carlos de Araújo.

To the group of measurement and modeling of hydrological and sedimentological processes of the semiarid region of Brazil (HIDROSED) for making its dataset available to my research.

To the technicians from FISOL/CENA lab: Robson Arthur e Eduardo Pillot.

To my friends from ESALQ and CENA for the unforgettable talks and scientific discussions: Ali Mehmandoost, Ana Luiza, Ana Paula, André Herman, Angelica Durigon, Ismael Meurer, Leonardo, Lívia Previatello, Marcos Santos, Osvaldo Nogueira, Thaís Rodrigues, Thalita Campos, Verena Benício, Victor Merigueti e Yeleine Almoza.

To my housemates: Alan Bernard, Bruno Lena, Luciano Silveira, Luiz Sobenko, Otávio Neto, Thiago Wendling e Fabrício.

From The Netherlands I would like to thank:

To Professor Klaas Metselaar for his kindness and remarkable scientific contributions devoted to my PhD thesis.

To the Wageningen University, especially *SLM group*, for accepting me as a guest researcher and as part of their scientific team.

To my friends over there who taught me how to cope with a very international group, providing me confidence to share my thoughts and experiences: Ammar Adham, Bélyse Mupfasoni, Berhane Grum, Célia Bento, Demie Moore, Fan Liangxin, Irene Koko, Isaurinda Baptista, Karrar Al-Timiny, Kaveh Hosseini, Lingtong Gai, Mahrooz, Marcien Ndagijimana, Marina Kim, Nadia Jones, Peter Voortman, Raoul Kpegli, Ricardo Silva, Ruben van der Meulen, Saeede Nazari, Sija Stofberg, Vera Silva and Xiaomei Yang.

CONTENTS

RESUMO

Modelagem hidrológica da disponibilidade da água do solo no bioma Caatinga

O Nordeste do Brasil é hidrologicamente caracterizado por secas recorrentes, tornando os recursos hídricos naturais altamente vulneráveis. Nesta região está o bioma Caatinga, ocupando uma área de aproximadamente 800.000 km^2. Cenários de déficit hídrico são projetados para grandes regiões do globo, incluindo o Nordeste brasileiro. Devido às interações entre clima e vegetação, várias pesquisas têm abordado os efeitos das mudanças climáticas sobre os ecossistemas naturais e agrícolas. Neste contexto, as propriedades hidráulicas do solo são essenciais para avaliar o movimento de água, e assim a capacidade de fornecimento de água às plantas. Com base nesta contextualização, os objetivos desta tese são: simular os componentes do balanço hídrico do bioma Caatinga para cenários climáticos atuais e futuros; e avaliar a capacidade de alguns solos em fornecer água às plantas a partir de uma abordagem de potencial de fluxo matricial. Para os cenários climáticos atuais e futuros, simulações hidrológicas foram realizadas com o modelo SWAP, parametrizado para uma microbacia de 12 km^2, inserida em área de Caatinga preservada. A validação das simulações foi processada a partir de medidas diárias do conteúdo de água do solo na profundidade de 0,2 m no período de 2004 a 2012. A capacidade do solo em fornecer água às plantas foi avaliada através da atualização de uma função de potencial de fluxo matricial, que acopla as propriedades hidráulicas do solo, densidade de comprimento radicular e transpiração das plantas, aplicada a um grupo de solos da zona climática semiárida e sub-úmida. Como resultados principais destacam-se: nas condições climáticas atuais, o bioma Caatinga retorna 75% da precipitação anual para a atmosfera como evapotranspiração, particionada entre seus componentes (transpiração, evaporação e intercepção) em 41%, 40% e 19%, respectivamente. Evapotranspiração e temperatura do ar foram sensíveis à umidade do solo durante os períodos de junho-setembro e dezembro-janeiro. Em relação ao cenário climático futuro, a taxa de transpiração foi acrescida em 36%. A evaporação do solo e a interceptação foram reduzidas em 16% e 34%, respectivamente. A quantidade de precipitação devolvida para a atmosfera foi em média 98%. Para ambos os cenários climáticos, é sugerido que os fluxos de água no sistema solo-planta-atmosfera são controlados pela camada superior do solo (0-0,2 m), fornecendo, em média, 80% do total transpirado, indicando que, caso os cenários de disponibilidade hídrica reduzida se confirmem, o bioma Caatinga pode se tornar completamente dependente dos pulsos de água no solo. A partir do potencial de fluxo matricial limitante revelou-se que os solos da região semiárida são capazes de manter o fluxo de água às plantas em taxas potenciais em condições de solo seco (potencial matricial limitante variando de -36 a -148 m), enquanto que, os solos da região mais úmida indicaram severa restrição hidráulica, com potencial matricial limitante maior do que -1,5 m. Ainda para os solos analisados, a atribuição de potencial na superfície da raiz inferior a -150 m não ocasionou aumento de disponibilidade hídrica, indicando que valores menores que -150 m não implicam em uma estratégia viável para suportar baixa disponibilidade hídrica.

Palavras-chave: Semiárido; Evapotranspiração; Mudanças climáticas; SWAP; Balanço hídrico

ABSTRACT

Hydrological modeling of soil-water availability in the Caatinga biome

Northeastern Brazil is hydrologically characterized by recurrent droughts leading to a highly vulnerable natural water resource system. The region contains the Caatinga biome, a sparsely studied ecosystem, covering an area of approximately 800,000 km^2. Reduced water-availability is projected to take place in large regions of the globe, including Northeastern Brazil. Given the strong interactions between climate and vegetation, research has addressed climate change effects on natural and agricultural ecosystems. In this context, soil hydraulic properties are essential to assess soil water flow, and thus the ability of soil to supply water to plants at potential rates under different ranges of pressure head. Based on that, the aims of this thesis are: to increase insight in water balance components for the Caatinga biome, under current and future climate scenarios; and to assess the ability of soils in supplying water to plants by the further development of an existing matric flux potential approach, followed by its application to a group of soils from two Brazilian climatic zones (semi-arid and sub-humid). Both for current and future climate scenarios, hydrological simulations were performed with SWAP model parameterized for a preserved Caatinga basin of 12 km². The validation of the simulations was performed using a dataset of daily soil-water content measurements taken at 0.2 m depth in the period from 2004 to 2012. The soil water supplying capacity was evaluated through a multilayer matric flux potential approach, coupling the soil hydraulic properties, root length density and plant transpiration. Regarding the current climate conditions, the Caatinga biome returns 75% of the annual precipitation to the atmosphere, whereas the partitioning of total evapotranspiration into its components (transpiration, evaporation and interception) on annual basis accounts for 41%, 40% and 19%, respectively. Evapotranspiration and air temperature are most sensitive to soil moisture during the periods June-September and December-January. Concerning the future climate, transpiration was enhanced by 36%, soil evaporation and interception losses reduced by 16% and 34%, respectively. The amount of precipitation returned to the atmosphere was on average 98%. For both climate scenarios, the soil-plant-atmosphere fluxes seem to be controlled by the surface soil layer (0-0.2 m) which provides, on average, 80% of the total transpiration, suggesting that the Caatinga biome may become completely soil-water pulse dominated under scenarios of reduced water availability. The matric flux potential analysis revealed that soils from the semiarid zone were able to deliver water to plants at potential rates under a wider range of bulk soil pressure head (-36 to -148 m), whereas the soils from the wetter zone showed more hydraulic restriction with limiting soil water potential above -1.5 m. For the analyzed soils, only a negligible increase in available water results from decreasing the root water potential below -150 m, therefore, in order to adapt to water-limited conditions, plant species may invest in other adaptive strategies, rather than spending energy in structures that allow a reduction of the lower suction limit in their tissues.

Keywords: Semi-arid; Evapotranspiration; Climate change; SWAP; Water balance

1 INTRODUCTION

According to the Aridity Index (AI), which expresses the ratio between precipitation and potential evapotranspiration, 40% of the earth is covered by drylands. The main hydrological feature of these regions is water shortage for both drinking and ecosystem productivity. Many important issues concerning water availability in drylands remain unclear, which makes it even tougher to develop strategies to cope with water scarcity in order to develop sustainable livelihoods. In general, due to data scarcity, arid and semi-arid regions are poorly investigated and any attempt of doing so is a challenge. A large portion of Northeastern Brazil is covered by semi-arid lands, corresponding to 12% of the Brazilian territory. In an ecosystem approach, the Caatinga is the main biome of Northeast Brazil and the only one that occurs exclusively in Brazil, nonetheless, a reasonably complete picture about its role on climate, water use and ecosystem services is lacking.

The Caatinga biome is important to the Brazilian semi-arid region as a whole for its rich and diverse biota, and beyond the role of being a shelter for several endemic species, the Caatinga biome provides essential services to society such as timber, forage and watershed protection. Regarding the latter, as the population from the Northeastern part of Brazil is highly dependent on surface water reservoirs, the biome is a key component for water security. The hydrological role of this natural ecosystem may be even more required since land surface models, both general and regional, have projected intensified water-scarcity and warmer scenarios across some large regions of the earth, including Northeast Brazil. These scenarios may pose threats on functioning of water-limited ecosystems (changes in composition and structure of forests) as well as on agricultural fields due to less time to biomass productivity as result of shorter crop durations. Therefore, in order to assess strengths and vulnerabilities of current ecosystems, a detailed understanding of soil-plant-atmosphere (SPA) interactions is of utmost importance.

Regarding climate change perspectives of reduced water availability together with higher temperatures, research has addressed the SPA system both experimentally and by using modeling techniques. Although the aim of these investigations has been to understand the interactions within the SPA system as a whole, the plant component (growth and development) received more attention while less attention has been given to the soil and soil hydraulic properties. Due to texture, structure, organic matter content, and other factors, each soil has its own hydraulic architecture that determines the rate of soil-water movement towards plant roots. Hence, under a drying soil and atmosphere, enhanced by climate change,

the different soil abilities of supplying water to plants will play a very important part in the establishment and development of ecosystems and in the regional pattern of hydrological connectivity of land and atmosphere.

In order to acquire more insights in aspects that determine water availability in a water-limited ecosystem, this thesis reports on the hydrological modeling of the spatial and temporal partitioning of the water balance components for a small preserved Caatinga Basin under current and future climate conditions (chapter 2 e 3); and aiming to evaluate the soil ability of supplying water to plants, it also presents the further development of a matric flux potential approach and its application to a group of soils from two Brazilian climatic zones (semi-arid and sub-humid), hydraulically parameterized for the dry range (chapter 4).

2 IMPORTANCE OF SOIL-WATER TO THE CAATINGA BIOME, BRAZIL[1]

Abstract

Northeastern Brazil is hydrologically characterized by recurrent droughts leading to a highly vulnerable natural water resource system. The region contains the Caatinga biome, covering an area of approximately 800,000 km^2. To increase insight in water balance components for this sparsely studied ecosystem, hydrology simulations were performed with the SWAP (Soil Water Atmosphere Plant) model for a Caatinga basin of 12 km^2. SWAP was developed to simulate hydrology under short cycle crops and its parameterization and validation to a diverse ecosystem is a novelty. The validation of the simulations was performed using a dataset of daily soil water content measurements taken at 0.2 m depth in three sites in the basin in the period from 2004 to 2012. Average Nash-Sutcliffe efficiency coefficient for these simulations was 0.57 and Root Mean Square Error of Prediction was 4.3%. The results of the simulations suggest that water components do not diverge statistically among different sites of the biome. The Caatinga biome returns 75% (±17%) of the annual precipitation to the atmosphere, whereas the partitioning of total evapotranspiration into its components (transpiration, evaporation and interception) on annual basis accounts for 41% (±7%), 40% (±6%) and 19% (±3%), respectively. Regarding water availability, the surface soil layer (0.0-0.2 m) is the most important layer in the rooted profile, supplying up to 90% of atmospheric water demand. According to our analysis performed on daily basis, evapotranspiration and air temperature are most sensitive to soil moisture during the periods June-September and December-January.

Keywords: Semi-arid; Evaporation; Evapotranspiration; Hot spots; Hydrology; SWAP; Water balance

2.1 Introduction

A significant part (12%) of the Brazilian territory consists of a semi-arid region, in which the Caatinga biome is dominant. The Caatinga, a complex tropical ecosystem characterized by a wide variety of both herbaceous and arborescent vegetation (PINHEIRO; COSTA; DE ARAÚJO, 2013) is entirely located within Northeastern Brazil, covering an area of approximately 800,000 km^2. Despite its status of Global Wilderness (MITTERMEIER et al., 2002), the amount of scientific research it has attracted is limited (SANTOS, 2011). The seeking for a better hydrological understanding for such an important ecosystem where significant rainfall reduction and increase in air temperature are predicted to take place in the coming years as results of climate change is a need and a challenge.

On a global scale, the tropics are the main source of atmosphere sensible and latent heat (WANG, 2004). Latent heat flux is the most important component of the continental water cycle, capable of returning as much as 60% of all precipitation back to the atmosphere

[1] Chapter published in **Ecohydrology** (2016). DOI: 10.1002/eco.1728

(SCHLESINGER; JASECHKO, 2014), more than half of the solar energy absorbed by land surfaces (TRENBERTH; FASULLO; KIEHL, 2009). However, specific semi-arid regions characterized by a strongly negative atmospheric water balance, like the Caatinga (average precipitation below 900 mm y^{-1} and potential evapotranspiration above 2200 mm y^{-1}), might indicate a hot spot, a location at which soil water content has a substantial impact on precipitation and air temperature (KOSTER et al., 2004, 2006; SENEVIRATNE et al., 2006). Beyond this, the Caatinga biome has been projected by global and regional climate models to face large rainfall reductions and air temperature increase (MARENGO et al., 2012; PESQUERO et al., 2010; SENEVIRATNE et al., 2012).

Modeling results using data from the GLACE, the Global Land-Atmosphere Coupling Experiment (KOSTER et al., 2006) and from IPCC AR4 simulations (SENEVIRATNE et al., 2006) show the Caatinga region in Northeastern Brazil to be such a hot spot for coupling between soil water content and air temperature. These hot spots can significantly impact the near-surface climate, causing very high temperatures and heat waves (FISCHE et al., 2007) because more energy is available for sensible heating when soil water content restricts the total energy converted in latent heat.

Despite the weak support for coupling between soil water content and precipitation based on the GLACE modeling dataset for Northeastern Brazil, this does not rule out the presence of coupling at local scales. The GLACE simulations (KOSTER et al., 2006) focused on the impact of soil water content on subseasonal climate variability for a single year. As highlighted by Seneviratne et al. (2010), climate models contain a high level of uncertainty. To obtain a more complete picture, more investigations using other modeling tools and observational data are needed. A more comprehensive dataset is required to investigate the impact of soil water content on evapotranspiration and indirectly on precipitation. A finer-scale spatial and temporal analysis of the soil water content and meteorological components would allow investigations of the necessary details and also provide a better performance of simulations in current climate models and as well as land-atmosphere interactions. Such an analysis is of utmost importance for semi-arid regions in general, given the scarcity of hydrological data characterized by high spatial variability (COSTA et al., 2012, 2013).

Northeastern Brazil faces recurrent drought episodes which lead to highly vulnerable natural water resource systems and environmental degradation (BARBOSA et al., 2006; DE ARAÚJO; GÜNTNER; BRONSTERT, 2006). Identification of specific soil water content-climate interactions could bring significant improvements in seasonal forecasting and drought monitoring. To address some of the current scientific demands in the field of soil water

content-climate interactions, Seneviratne et al. (2010) performed a broad review and identified a necessity to improve understanding of the main components driven by climate conditions such as soil water, transpiration and evaporation for heterogeneous terrain and regions, including South America. In line with their recommendation and to acquire more insights on water availability upon water-limited ecosystem, the research reports here the spatial and temporal partitioning of the hydrological balance components for a small preserved Caatinga Basin through a hydrological modeling approach using soil physical properties, morphological characteristics of the vegetation and meteorological data.

2.2 Material and Methods

2.2.1 Study area

The study was conducted in the Aiuaba Experimental Basin (AEB), a 12 km^2 integrally-preserved Caatinga watershed (6º42'S; 40º17'W). The AEB is completely located inside the ecological station of Aiuaba, state of Ceará, Brazil, ruled by the Brazilian Federal Environmental Institute. The climate is BSh (semi-arid with low latitude and altitude) according to the Köppen classification, with an average annual class-A pan evaporation of 2500 mm. Average annual rainfall is 549 mm, concentrated between January and May (rainy season). The monthly average temperatures range from 24ºC to 28ºC. The watershed is covered by a dense native vegetation characterized by tree heights typically ranging from 5 to 12 m. The basin has an average slope of 19% and its geology is characterized by the transition from a crystalline complex to a sedimentary formation. The hydrological variables, such as soil water content, rainfall, class A Pan evaporation and brook discharges have been monitored since 2003 by the HIDROSED group (www.hidrosed.ufc.br) with the purpose of studying hydrological and sedimentological processes. More detailed information can be found in de Araújo and Piedra (2009), Medeiros et al. (2009), Medeiros and de Araújo (2014) and Pinheiro et al. (2013).

Based on previous studies (COSTA et al., 2013; GÜNTNER; BRONSTERT, 2004; PINHEIRO et al., 2013), the Aiuaba Experimental Basin (AEB) was subdivided into three systems, denominated soil and vegetation associations or SVA (Figure 2.1). The first association (SVA_1), covered with an Acrisol, occupies 20% of the AEB area, and the average rooting depth of the vegetation is 0.8 m. In the second system (SVA_2, 34% of the experimental area) the soils are classified as Luvisols and the average rooting depth is 0.6 m. SVA_3 has a shallow soil (Regosol) with average rooting depth of 0.4 m, occupying 46% of the

AEB. In each SVA, a location is equipped with a Time Domain Reflectometry sensor (TDR, model *CS616*), installed at the depth of 0.2 m, together with an automatic rainfall gauge.

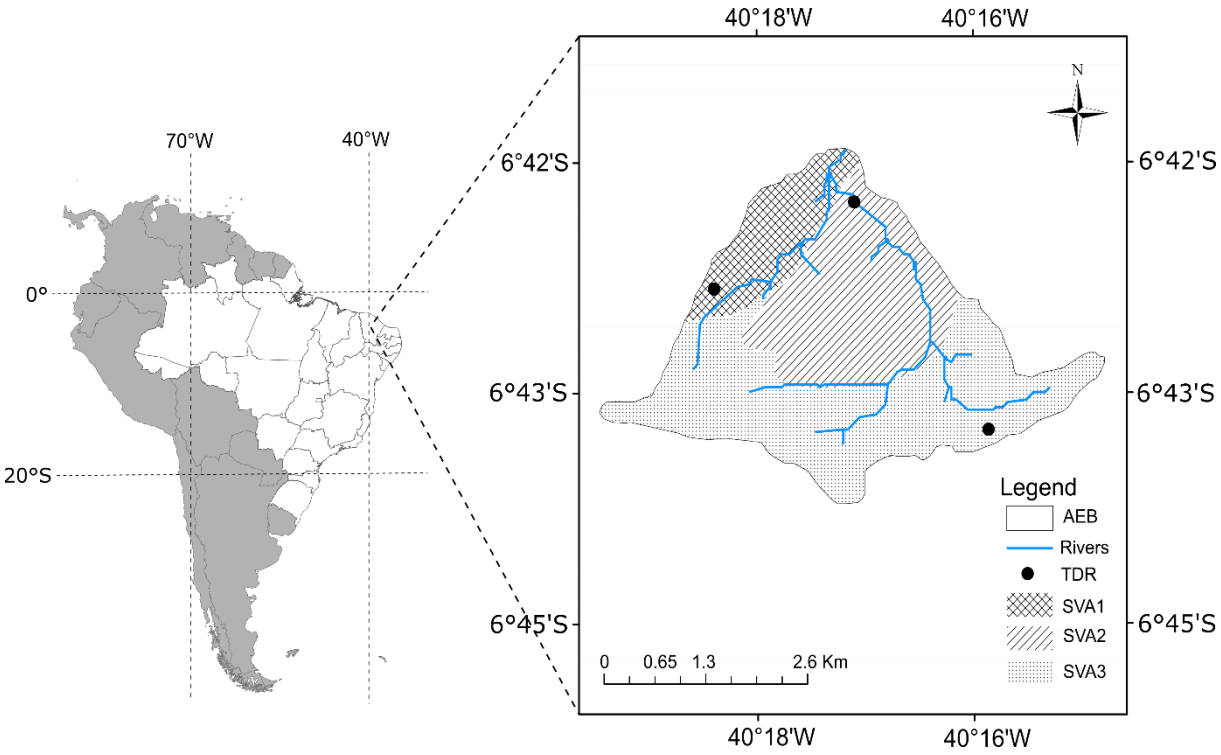

Figure 2.1 – Geographical location of the Aiuaba Experimental Basin (AEB) and its subdivision into three Soil and Vegetation Association (SVA_1, SVA_2 and SVA_3). Dots indicate the location of TDR measurements

2.2.2 Modeling

Hydrological modeling was performed with the SWAP model (KROES et al., 2008), a one-dimensional agro-hydrological model. The model simulates water flow, solute transport and plant growth in a soil–water–atmosphere–plant environment. To calculate the water balance terms, the model employs the Richards equation with a root water extraction sink term:

$$\frac{\partial \theta}{\partial t} = \frac{\partial}{\partial z}\left[K(h)\left(\frac{\partial h}{\partial z} + 1\right)\right] - S(h) \qquad (2.1)$$

in this equation, *t* denotes time *(d)*, *z* is the vertical coordinate taken as positive upwards (cm), *K(h)* is the hydraulic conductivity (cm d^{-1}) and *S(h)* represents the water uptake by plant roots (d^{-1}). Eq. (2.1) is solved numerically describing the *θ-h-K* relation by the Mualem–van Genuchten equations (MUALEM, 1976; VAN GENUCHTEN, 1980). To estimate the sink term S*(h)*, the reduction function proposed by de Jong van Lier et al. (2008; 2013) was used

to simulate root water uptake distribution over depth. This reduction function includes a compensation mechanism such that uptake restrictions in drier layers may be offset by increased uptake from a wetter layer.

The SWAP model was parameterized for the three SVAs with soil hydraulic properties and vegetation parameters. Rainfall was monitored in each SVA, whereas for other meteorological data the regional average was used.

2.2.2.1 Soil hydraulic parameterization

Soil samples were collected in each SVA. A soil profile from each SVA was sampled per 0.2 m thick layer. Following the description of root depth (PINHEIRO; COSTA; de ARAÚJO, 2013), four layers were sampled in SVA_1 and two layers in SVA_2 and SVA_3. Although a third layer should have been sampled in SVA_2, the presence of a very stony layer at the sample spot from about 0.4 m downwards made undisturbed sampling not possible. However, earlier studies (COSTA et al., 2013; PINHEIRO; COSTA; de ARAÚJO, 2013) testify the presence of a third rooted layer (0.4-0.6 m) in other spots of the SVA_2. Therefore, we considered the third layer in our simulations using the hydraulic properties of the second layer. The saturated hydraulic conductivity was measured in seven samples for each layer and water retention was measured for nine different tensions (0.1, 0.2, 0.4, 0.6, 1.0, 3.3, 10, 30 and 150 m) with five replicates per tension for each layer (Table 2.1).

Table 2.1 - Soil physical parameters for the Soil Vegetation Associations: θ_r, θ_s, α, n and K_s according to the van Genuchten equation system. (95% confidence levels between brackets).

Depth	θ_r	θ_s	α	n	K_s
m	--------$m^3\ m^{-3}$---------		cm^{-1}	-	$m\ d^{-1}$
			SVA_1		
0.0-0.2	0.000	0.418	0.068	1.210	2.22
		(0.401-0.435)	(0.039-0.0980)	(1.18-1.23)	(0.65-3.62)
0.2-0.4	0.000	0.440	0.225	1.186	2.50
		(0.430-0.450)	(0.169-0.280)	(1.17-1.20)	(0.50-4.10)
0.4-0.6	0.000	0.433	0.249	1.162	0.36
		(0.415-0.450)	(0.130-0.369)	(1.15-1.18)	(0.01-0.68)
0.6-0.8	0.000	0.415	0.139	1.170	0.16
		(0.403-0.426)	(0.094-0.186)	(1.16-1.18)	(0.06-0.26)
			SVA_2		
0.0-0.2	0.000	0.456	0.246	1.159	3.59
		(0.434-0.477)	(0.107-0.385)	(1.14-1.18)	(0.96-6.01)
0.2-0.4	0.000	0.413	0.128	1.155	5.81
		(0.387-0.439)	(0.024-0.233)	(1.13-1.18)	(1.57-9.60)
			SVA_3		
0.0-0.2	0.000	0.434	0.219	1.299	3.89
		(0.420-0.447)	(0.165-0.273)	(1.28-1.32)	(2.42-5.47)
0.2-0.4	0.000	0.3933	0.294	1.228	7.62
		(0.381-0.406)	(0.205-0.384)	(1.21-1.25)	(1.70-13.68)

2.2.2.2 Vegetation Parameterization

The Caatinga biome is a complex multispecies system with more than 900 known vascular plant species. However, only 60% of the biome area has been surveyed, 20% intensively, making the number of species potentially larger (LEAL et al., 2005). For the AEB, cataloguing only plants with a stem diameter at soil surface level greater than 3 cm resulted in a density of 7700 units/ha (MEDEIROS; DE ARAÚJO; BRONSTERT, 2009). As very few botanical descriptions of the Caatinga biome are available, it does not seem reasonable to consider all species individually for hydrological simulation, and an alternative method was employed to analyze the hydrological processes in the vadose zone. We used a lumped leaf area index approach, i.e. the total leaf area of all species over a unit soil area is assumed to represent the vegetation in terms of interaction with the atmosphere. An exponential extinction coefficient for the aggregated canopy was assumed. This simplification allowed investigation of the soil water balance for the Caatinga biome at soil profile scale.

Temporal and spatial dynamics of the Leaf Area Index

To estimate the temporal and spatial dynamics of the leaf area index, the SEBAL (Surface energy balance algorithm for land) was used (ALLEN; TREZZA; TASUMI, 2002). SEBAL consists of an algorithm validated for different ecosystems around the world. For our purpose, leaf area index (LAI) and albedo were estimated from Landsat 5 satellite images

(eleven in total) downloaded from the website of the Brazilian National Space Research Institute (INPE) (www.inpe.br), covering different periods over time between 2004 and 2012. The period was chosen to match the availability of the dataset of the Aiuaba Experimental Basin (AEB).

Leaf area index estimated by the SEBAL algorithm from eight images was correlated to the mean soil water pressure head at the depth of 0.2 m in the 15-day period before the satellite image for each SVA. Three other images were used to validate the regression models using the Nash-Sutcliffe efficiency index. The soil water content database of the AEB together with soil hydraulic properties allowed us to obtain temporal and spatial dynamics of LAI from 2004 to 2012 for SVA_1 and SVA_2 and from 2004 to 2010 for SVA_3 (PINHEIRO; DE JONG VAN LIER; METSELAAR, 2015).

Root Length Density (RLD)

Soil samples were collected for each SVA, three replicates per layer following the same protocol described for the undisturbed soil samples, using a sample ring with a diameter of 0.1 m (volume $9.43 \cdot 10^{-4}$ m^3). The roots collected in the soil samples were separated from the soil material, digitally scanned and subsequently analyzed for root length and diameter.

Crop Factor for forests

Transpiration crop factors for arable crops are available from literature, but values for more complex systems like forests are scarce. We therefore developed eq. (2.2) (eq. A1.13 from appendix A) from crop growth modeling (VAN DER WERF et al., 2007), describing the crop factor as a function of the extinction coefficient (*k*), the leaf area index (*LAI*), surface soil albedo (α_s) and vegetation albedo (α_v).

$$K_c = \frac{1-\alpha_v-(\alpha_s-\alpha_v)e^{-kLAI}}{1-0.23} \tag{2.2}$$

Values of albedo were estimated from satellite images for both rainy and dry seasons.

Interception losses

To assess the interception losses, the Gash approach (GASH, 1979) was applied, as implemented in SWAP. Required parameters were based on Medeiros, de Araújo and Bronstert (2009), who carried out an experiment (from 2004 to 2006) to evaluate the

interception losses in the Caatinga biome, by monitoring precipitation, throughfall and stem flow in a 100 m² plot inside the AEB.

2.2.3 Evapotranspiration parameterization

Daily ET_o was estimated from Class A Pan data measured in the AEB. About 40% of data were missing, and these were substituted by ET_o estimated using the Hargreaves method as described in Allen et al. (1998). The Hargreaves method was chosen due to its low data requirements (mean, maximum and minimum temperature). The meteorological data used in the Hargreaves method were provided by the Ceará State Foundation of Meteorology and Water Resources (FUNCEME, www.funceme.br).

2.2.4 Simulation, validation and statistical procedures

The SWAP model was run for nine years for SVA_1 and SVA_2 (2004-2012) and for seven years for SVA_3 (2004-2010). After parameterization, the model was run and validated for each SVA. The validation procedures were applied for each SVA, comparing the soil water content measured by the TDR, installed in each SVA at the depth of 0.2 m (totaling 5912 daily measurements), to soil water content simulated by the SWAP model for the same depth. To perform the validation procedure, two statistical parameters were used; Nash and Sutcliffe (1970) efficiency (NSE – eq. 2.3), and the Root Mean Square Error of Prediction (RMSEP – eq. 2.4):

$$NSE = 1 - \frac{\sum_{j}^{i=1}(\theta_i - \hat{\theta}_i)^2}{\sum_{j}^{i=1}(\theta_i - \bar{\theta}_i)^2} \tag{2.3}$$

$$RMSEP = \sqrt{\sum_{i=1}^{n}\frac{(\theta_i - \hat{\theta}_i)^2}{n}} \tag{2.4}$$

where θ_i and $\hat{\theta}_i$ are observed and estimated values of soil water content, respectively; $\bar{\theta}_i$ is mean of the observed soil water content and n is number of observations. NSE ranges from $-\infty$ to 1. If the model prediction capability is lower than simply using the mean measured value as a predictor, then NSE < 0. If the model predicts with a higher accuracy than using the mean observed value, NSE > 0. The closer NSE is to unity, the higher the model efficiency.

In turn, the RMSEP describes the difference between the model simulations and observations in the units of the variable. The closer it is to zero, the higher the model efficiency (LEGATES; MCCABE, 1999).

Another procedure followed in order to analyze the quality of the simulated data was undertaken by drawing the cumulative probability distribution for observed and predicted soil water content. The mathematical description used is known as Chegodayev's method, eq. (2.5). The procedure is described by Chow, Maidment and Mays (1988):

$$P(\theta \geq \theta_m) = \frac{m - 0.3}{n + 0.4} \tag{2.5}$$

where m is a rank of a value in a list ordered by descending magnitude and n is the total number of values.

Statistical analysis was performed using the SPSS 22.0. Water balance components data (precipitation, interception losses, transpiration, evaporation and deep drainage) showed normality and homogeneity of variances according to Kolmogorov-Smirnov (KS) test and Levene's test ($p>0.05$), respectively. Data were analyzed by one-way ANOVA to explore significant differences among the three SVAs for the sets of variables of the water balance components using the Tukey test with a probability value of 0.05.

2.3. Results and Discussion

2.3.1 Spatial and temporal rainfall distribution

Mean annual rainfall for the analyzed period for the three SVAs (2004-2012) was 640, 572 and 694 mm, respectively, and slightly above the long-term average (549 mm). However, despite the size of the watershed, 12 km², for some years a significant difference in rainfall amount among the SVAs could be observed. For instance, in 2007 the measured rainfall in SVA_1 was 740 mm, whereas in SVA_2 it was 34% lower (490 mm) and in SVA_3 it was 80% higher (1330 mm, Figure 2.2).

Besides this spatial variability, Medeiros and de Araújo (2014) also describe a high temporal variability in the rainfall pattern for the same region, where in some years the rainfall is over twice the average.

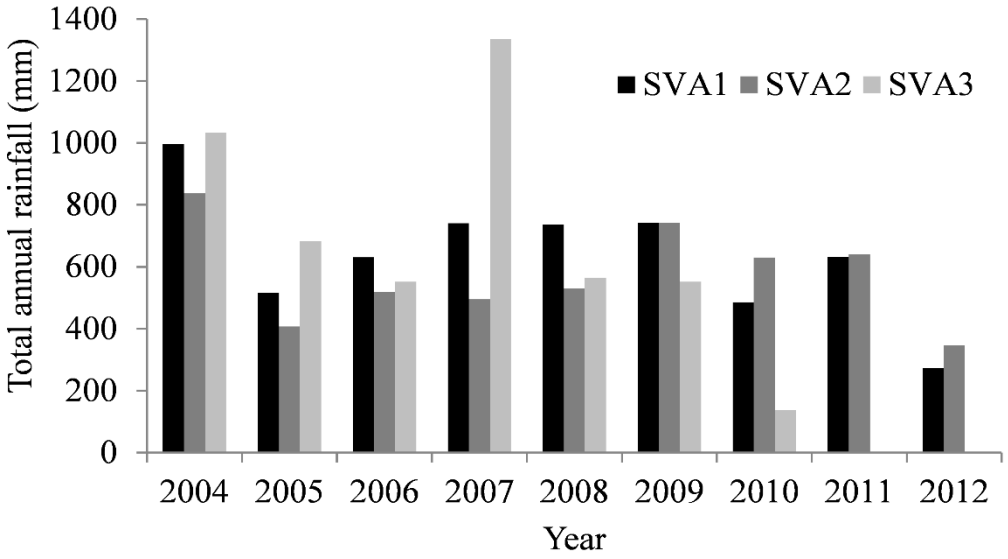

Figure 2.2 – Spatial and temporal variability of the total annual rainfall depth for the studied period (2004-2012 for SVA_1 and SVA_2 and 2004-2010 for SVA_3)

2.3.2 Spatial and temporal dynamics of the leaf area index

Correlations between LAI obtained from SEBAL and mean soil pressure head in the 15-day period before the satellite imaging yielded a range of coefficient of determination from 0.89 to 0.92 and NSE values from 0.76 to 0.94 (Figure 2.3).

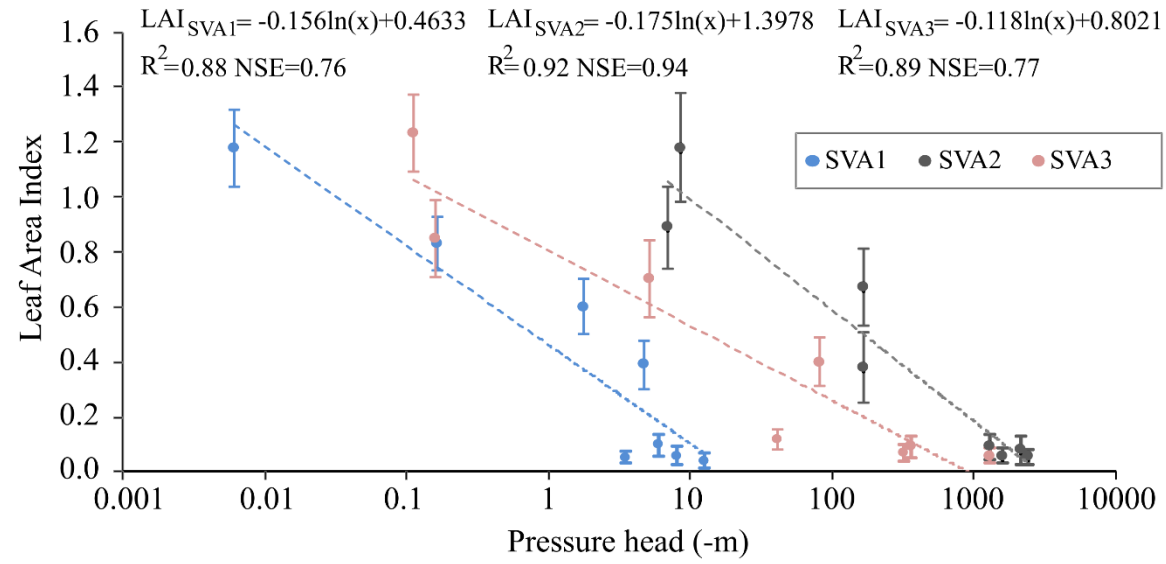

Figure 2.3 – Correlations between LAI obtained from SEBAL and the mean soil water pressure head in the 15-day period previous to satellite imaging. NSE (Nash-Sutcliffe efficiency)

For SVA_1, SVA_2 and SVA_3, the average values of LAI estimated from the above correlations during the rainy season were 0.97, 1.12 and 1.07, respectively. During the dry season when most of species shed leaves as survival behavior, mean LAI values were 0.15 for

SVA_1 and 0.11 for SVA_2 and SVA_3. The vegetation showed abrupt LAI changes which were highly correlated to mean soil water pressure head at 0.2 m depth in the 15-day period before satellite imaging. Maximum LAI was relatively stable over the years and occurred between March and April. The spatial behavior of LAI appeared to be independent of soil type and root depth, similar for the three SVAs. These LAI values are low when compared to many other forests, however, in a global synthesis of LAI observations representative of a wide range of geographical locations worldwide (ASNER; SCURLOCK; HICKE, 2003), deserts and shrublands registered the lowest values, 1.3 (± 0.9) and 2.1 (± 1.6), respectively. Although no measurement was recorded for the Caatinga biome in the aforementioned study, it indicates that biomes from arid and semi-arid lands with fragmented canopy, like Caatinga, tend to show a lower LAI, indicating that our correlations yielded representative results for canopy scale.

2.3.3 Simulations and validation results

Regarding the validation results, NSE values were well above zero, indicating good model performance. Values of RMSEP were around 0.04 $m^3\ m^{-3}$, similar to those obtained by de Jong van Lier et al. (2008) and achieved by the same physically based macroscopic uptake model incorporated in the SWAP (Table 2.2).

Table 2.2 – Values of the Nash-Sutcliffe (NSE) coefficient of efficiency and Root Mean Square Error of Prediction (RMSEP) for the water content at depth 0.2 m in the three SVAs

SVA	n	NSE	RMSEP ($m^3\ m^{-3}$)
1	2219	0.65	0.04
2	2064	0.34	0.04
3	1629	0.71	0.05

n - number of data of soil water content available to the validation procedure for each SVA

Cumulative probability curves of soil water content (Figure 2.4) and respective indices of agreement (*dr*) as proposed by Willmott et al. (2012), show the similarity between observed and simulated series.

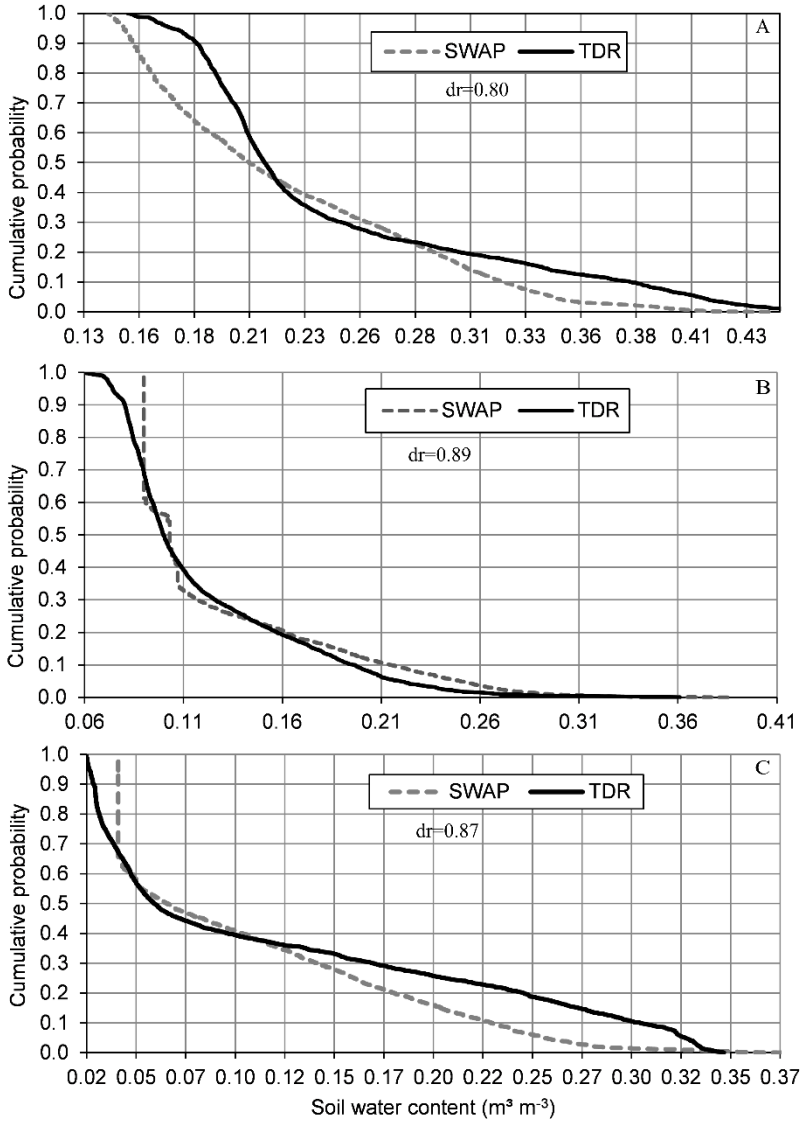

Figure 2.4 – Cumulative frequency of soil water content for SVA_1 (A), SVA_2 (B) and SVA_3 (C), for both simulated (SWAP) and measured (TDR) series

As satisfactory validation results were obtained with the site-specific parameterized model and without any further calibration, this may indicate that our modeling approach is transferable to other gauged and ungauged sites elsewhere. This methodology would then allow prediction of soil water balance components of complex ecosystems characterized with a relative scarcity of data.

Soil water content at 0.2 m depth indicates, both SVA_2 and SVA_3 become very dry during the rainless season, whereas in SVA_1 the surface layer remains at a higher water content (Figure 2.5 and Table 2.3). Both series, observed and predicted, show large variations in soil water content in the top layer, reflecting rainfall pattern and high evaporation rates.

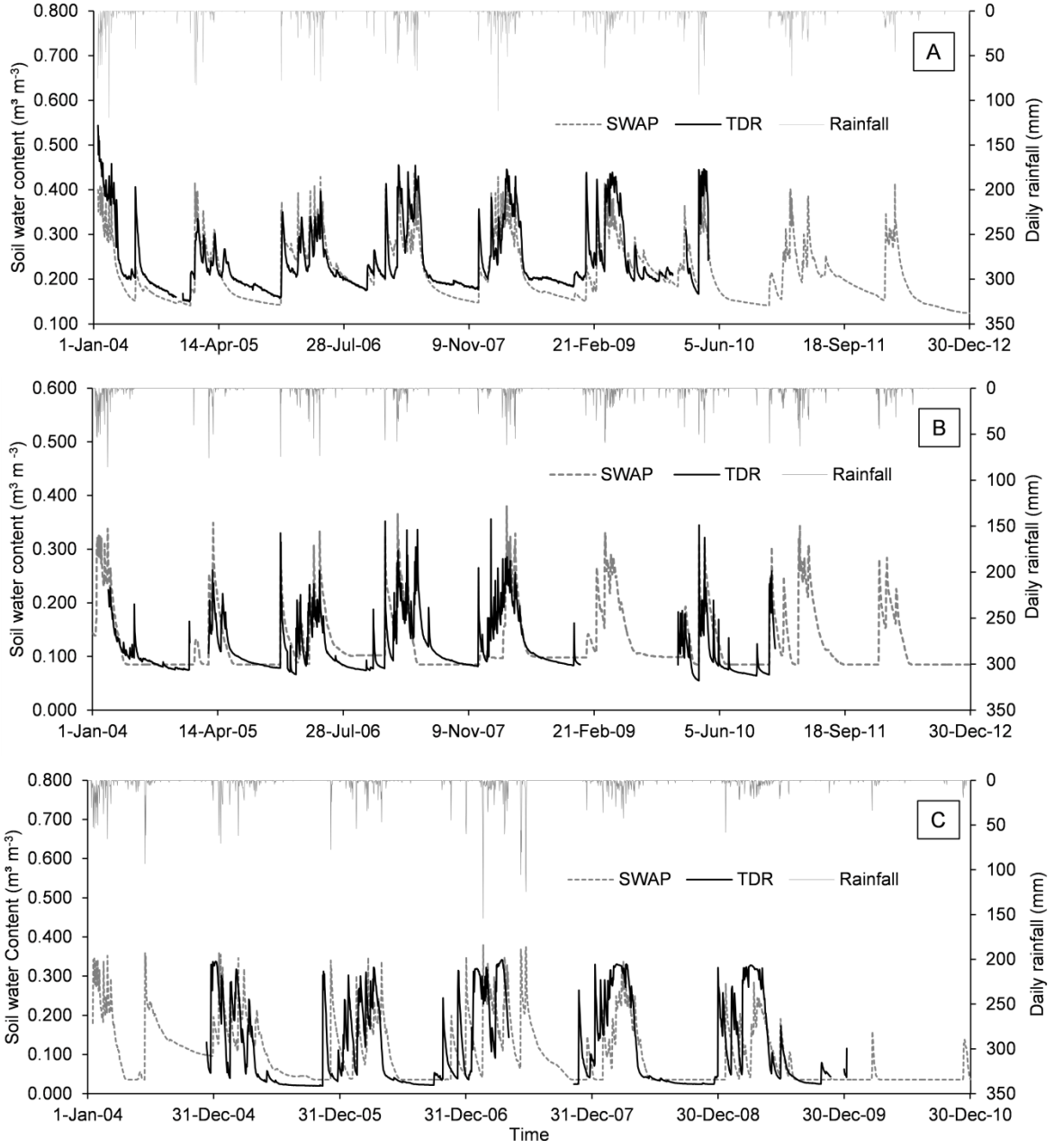

Figure 2.5 – Measured and simulated soil water content on a daily basis for 0.2 m depth together with rainfall for SVA_1 (A), SVA_2 (B) and SVA_3 (C)

Table 2.3 – Average pressure head (h) and soil water content (θ) in wet and dry seasons for each SVA (averages taken over the entire simulated period)

SVA	Wet season		Dry season	
	h (m)	θ (cm^3 cm^{-3})	h (m)	θ (cm^3 cm^{-3})
1	-0.8	0.285	-5.6	0.194
2	-10.0	0.196	<-150	0.125
3	-0.9	0.177	<-150	0.035

Water components (yearly precipitation, interception losses, actual transpiration, actual evaporation and deep drainage) do not differ statistically among the SVAs (Table 2.4),

regardless of difference in soil and vegetation parameterization. Despite limited experimental evidence, this may indicate a homogeneous spatial pattern of water use in the Caatinga biome, or, alternatively, more insight is needed to understand the dependency between hydrological components and soil-vegetation patterns in this ecosystem.

Table 2.4 – Yearly precipitation (P), interception losses (I_L), actual transpiration (T), actual evaporation (E) and deep drainage (D_d) for the three SVAs for the period 2004-2012

SVA	WBC[1]	Year									σ	$\overline{X}$	Statistical cluster
		2004	2005	2006	2007	2008	2009	2010	2011	2012			
		----------mm----------											
SVA_1	P	996	516	631	742	737	743	485	632	274	203	640	**a**
	I_L	118	62	80	86	98	102	60	84	44	23	81	**b**
	T	178	104	115	147	160	161	152	198	153	29	152	**c**
	E	210	129	214	173	206	263	158	191	99	49	182	**d**
	D_d	457	160	229	368	296	200	125	158	16	133	223	**e**
SVA_2	P	837	407	519	495	530	742	630	640	347	156	572	**a**
	I_L	100	50	73	68	72	103	83	83	52	18	76	**b**
	T	178	158	210	182	129	189	214	270	147	42	183	**c**
	E_{act}	224	122	201	168	161	297	249	217	146	45	198	**d**
	D_d	373	42	24	113	171	151	41	125	2	114	116	**e**
SVA_3	P	1033	684	551	1330	565	552	136	-	-	386	694	**a**
	I_L	126	89	78	145	85	89	24	-	-	39	91	**b**
	T	194	220	246	271	220	275	65	-	-	71	213	**c**
	E	194	156	150	165	150	173	46	-	-	48	148	**d**
	D_d	490	230	66	792	120	16	00	-	-	294	245	**e**

[1]WBC - Water Balance Components; σ – standard deviation; $\overline{X}$ - average; 'a, b, c, d, e' represent, each, a homogeneous cluster (Tukey at 0.05 significance)

Daily frequency of rainfall data is sufficient for most SWAP applications (KROES et al., 2008) and was used in our simulations. No runoff was predicted in the simulations, confirming experimental results of de Figueiredo et al. (2016) who evaluated runoff initiation in the AEB based on field measurements and found annual runoff coefficients smaller than 0.5% and no event with I_{60} (maximum 60-min rainfall intensity) below 12 mm h^{-1} to generate runoff. According to these authors, a possible explanation may be that initial abstractions change seasonably as a function of the dynamic behavior (expansion and contraction) of the root system in the Caatinga biome, enhancing macro-pore flow. The same authors seldom observed base flow at the catchment scale, because the water table was located several meters below the river bed in the downstream area. Measurable base flow were only observed during a long-lasting event (several days) in 2004. For the decade 2005-2014, the Aiuaba Experimental Basin had only five days with runoff per year, and river discharges lasted less than six hours after rainfall.

The amount of precipitation returned to the atmosphere (through T, E and I_L) by SVA_1, SVA_2 and SVA_3 was, on average, 69% (±16%); 82% (±11%) and 75% (±20%),

respectively. Considering the overall average for all SVAs, the Caatinga biome returns 75% (±17%) of annual precipitation back to the atmosphere. Moreover, for years with less precipitation, the percentage of rainfall returned to the atmosphere is close to 100%. For example, in the dry year of 2012 *ET* simulated for SVA_1 was slightly higher than precipitation (7%); this difference can be attributed to evapotranspiration of stored soil water. SVA_1 has a deeper root zone and soil water content in the rainless season is around 20% (Figure 2.5A and Table 2.3), which is possibly used in dry years. A similar observation was made by Raz-Yaseef et al. (2010) for a semiarid pine forest, in which both current forest density and canopy cover provided an optimal balance between *ET* components, storing some soil water content for forest transpiration in drier years as a survival strategy.

Ratios of actual transpiration, actual evaporation and interception losses to actual evapotranspiration (*T/ET, E/ET,* I_I/ET) on an annual basis for the Caatinga biome are 41% (±7%), 40% (±6%) and 19% (±3%), respectively (Table 2.5 and Figure 2.6).

Table 2.5 – Transpiration, evaporation and interception losses as a fraction of total water use over the analyzed period for each SVA

SVA	*T/ET*	*E/ET*	I_I/ET
1	0.37	0.43	0.19
2	0.41	0.43	0.17
3	0.47	0.33	0.20

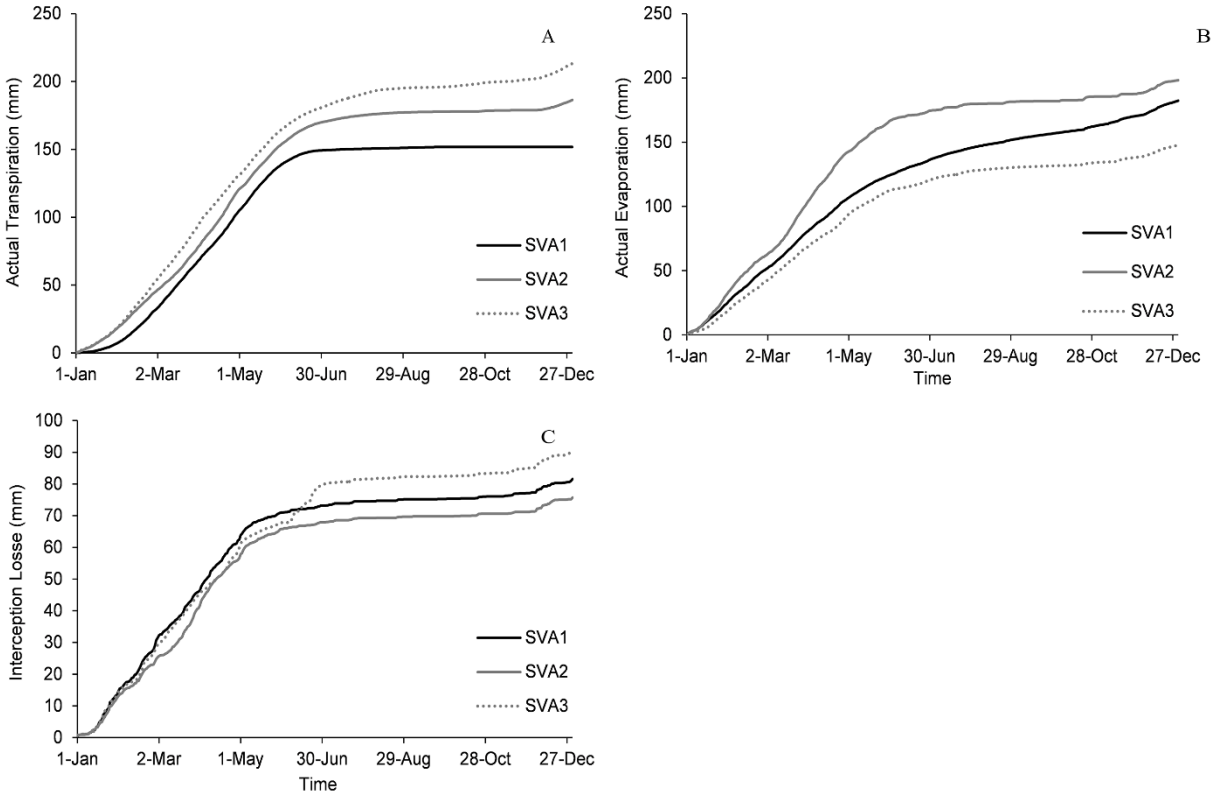

Figure 2.6 –Average cumulative transpiration (A), evaporation (B) and interception losses (C) for the three SVAs throughout the simulated period, from 2004 to 2012 for SVA_1 and SVA_2 and from 2004 to 2010 for SVA_3

In other studies carried out in several ecosystems around the world, including semi-arid environments, the *T/ET* ratio ranged from 40 to 70% on an annual basis (CAVANAUGH; KURC; SCOTT, 2010; MITCHELL et al., 2009; RAZ-YASEEF et al., 2012; STAUDT et al., 2011; ZHONGMIN et al., 2009). From a compilation of transpiration studies performed all over the globe, Schlesinger and Jasechko (2014) concluded that steppe and Mediterranean shrubland ecosystems with mean annual precipitation ranging from 440 to 480 mm (similar to the Caatinga biome) have a *T/ET* ratio of 47-48%. The *T/ET* ratio found for the Caatinga biome may indicate that it is the optimal value for the current rainfall regime, canopy cover and tree density, given that any increase of transpiration or soil evaporation would lead to a negative hydrological budget (RAZ-YASEEF et al., 2010).

Simulated interception losses account for 19% (±3%) of the *ET* and for 14% (±2%) of precipitation. According to Schlesinger and Jasechko (2014), interception losses for forest are typically in the range of 10-35%. In a study performed by Raz-Yaseef et al. (2012) in a semiarid forest, interception accounted for 12% of annual *ET*, however, it was larger than 20% during the rainy period. SWAP simulations suggest interception losses in the Caatinga biome are higher, especially when considering a low LAI. Nonetheless, measurements on an

event-based study carried out by Medeiros, de Araújo and Bronstert (2009) showed that interception losses in the Caatinga account for 13% of annual precipitation. This elevated interception value could be attributed to high evaporation turnover rate.

Root water uptake data demonstrated that in near-average years, the growing season starts shortly after the first rainfall events, by the end of December or beginning of January for all SVAs. For SVA_1, transpiration equaled potential rates in all simulated years, with water uptake ceasing in the second half of June. Meanwhile, for SVA_2 and SVA_3, potential transpiration never occurred during the simulated period, and water uptake ceased in the second half of July for SVA_2 and in the second half of September for SVA_3. It is worth noting that for the investigated period, 2012 was the only dry year, but in SVA_1 root water extraction continued at potential levels until September of that year with the fourth layer (0.60-0.80 m) contributing with 17% of water uptake (Figure 2.7). This illustrates the effects of drought are not linear, given the existence of, for example, discrete soil water content thresholds affecting vegetation and surface fluxes (KOSTER et al., 2004; SENEVIRATNE et al., 2010). This means that the same precipitation deficit will affect each region in a specific way, even within small areas like the Aiuaba Experimental Basin.

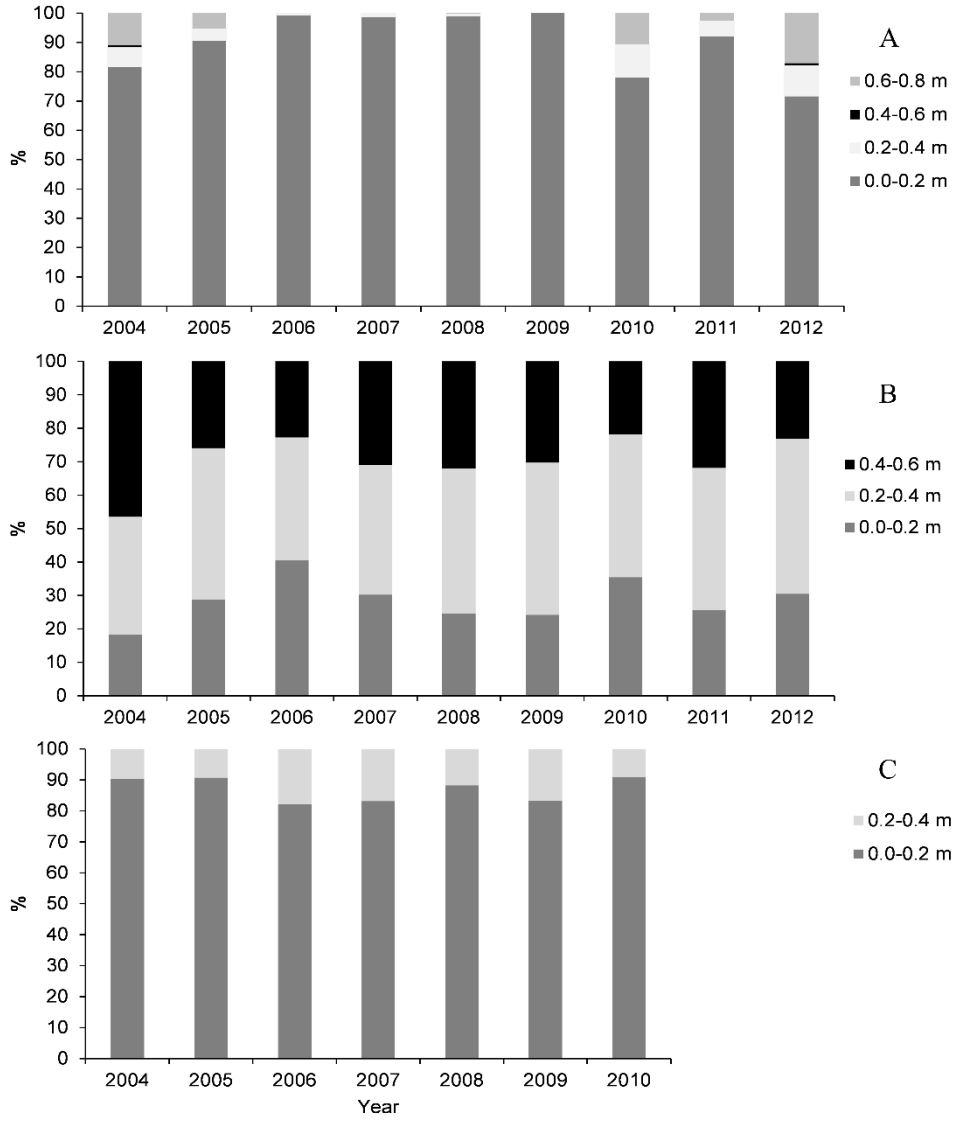

Figure 2.7 – Relative depth distribution of soil water uptake for SVA_1 (A), SVA_2 (B) and SVA_3 (C)

The surface layer (0.0-0.20 m) is the most important layer in the rooted profile regarding water availability for SVA_1 and SVA_3, providing more than 80% of all transpired water in normal years. These results are in agreement with Raz-Yaseef et al. (2012), who found transpiration to be controlled by soil water content in the 0.10-0.20 m layer in a semiarid pine forest in Southern Israel. They are also in agreement with findings by Liu et al. (2011) for a subalpine shrubland in China which, despite a very different climatic condition, also takes up soil water primarily from the top 0.3 m of the soil profile. For SVA_2, the three layers provided water in a more equal proportion, where the two first layers supplied on average 71% of the total demand (Figure 2.7). A previous analysis (PINHEIRO; COSTA; DE ARAÚJO, 2013) of profile images shows that the root length of the SVA_2 is on average four times higher than that of SVA_1 and double that of SVA_3. This difference could be the result of

denser vegetation covering the SVA_2 when compared to other areas. Another plausible reason for plants in SVA_2 to exploit the entire rooted profile may be a drier top layer. Soil water content is only equal or higher than field capacity (0.33 m^3 m^{-3}) in 3.2% of the studied period (Figure 2.4B).

Despite the high atmospheric demand experienced by the Caatinga biome, which could make the vegetation develop a deeper rooting system in order to balance *ET*, an earlier study about rooting characteristics of the Caatinga (PINHEIRO; COSTA; DE ARAÚJO, 2013) showed that its depth ranges from 0.60 m to 0.78 m when soil morphology is not restrictive. Schenk and Jackson (2002) concluded that, in water-limited environments, rooting depth is determined more by annual precipitation than by *ET*. This suggests that in such ecosystems water infiltration may limit rooting depth. Schenk (2008) cited several factors that favor shallow root distributions pointing out later that vertical root distributions in different biomes tend to approach the shallowest possible shape to fulfill evapotranspiration demands. An important advantage of a shallow root system is to maximize uptake of ephemeral water pulses in the upper soil layers. Additionally, shallow roots are more resistant to cavitation when compared to deeper roots, and less energy is spent for nutrient uptake, because nutrient concentrations are often higher in the upper soil layers, especially in environments with low biomass and turnover (ADIKU et al., 2000; JACKSON; SPERRY; DAWSON, 2000; BUCCI et al., 2009).

2.3.4 Climate change

Given the dependence of vegetation on the water availability in the top soil layers, the question is then how are these vegetation types influenced by climatic change. Many aspects of global change are highly uncertain, especially on a regional scale. From drought indices (e.g., consecutive dry days and soil water content anomalies) as well as from historical trends, some studies indicate that some large regions of the world, including Northeastern Brazil, will become drier due to the increase in duration and intensity of droughts and the frequency and magnitude of daily maximum air temperature extremes (DORE, 2005; SILVA, 2004; MARENGO et al., 2012; PESQUERO et al., 2010; SENEVIRATNE et al., 2012). In the case of available soil water, higher air temperature may lead to an increase of evapotranspiration, even without important changes in rainfall amount, resulting in reduction of soil water storage. This process could lead to the transition of present-day potential biomes by other

vegetation types, which may be more adapted to lower soil water availability (SALAZAR; NOBRE; OYAMA, 2007).

Investigating the processes that interact with coupling between soil water content and the main components driven by climate conditions (e.g., evapotranspiration and air temperature), periods in which these components are more sensitive to soil water content can be identified. A linear regression between daily soil water content at the depth of 0.2 m and daily *ET* for all SVAs identified periods with higher correlation in June-August and December-January (Figure 2.8A). This makes sense because both periods match the transitions between wet and dry soil conditions during which *ET* rates are naturally sensitive to soil water content.

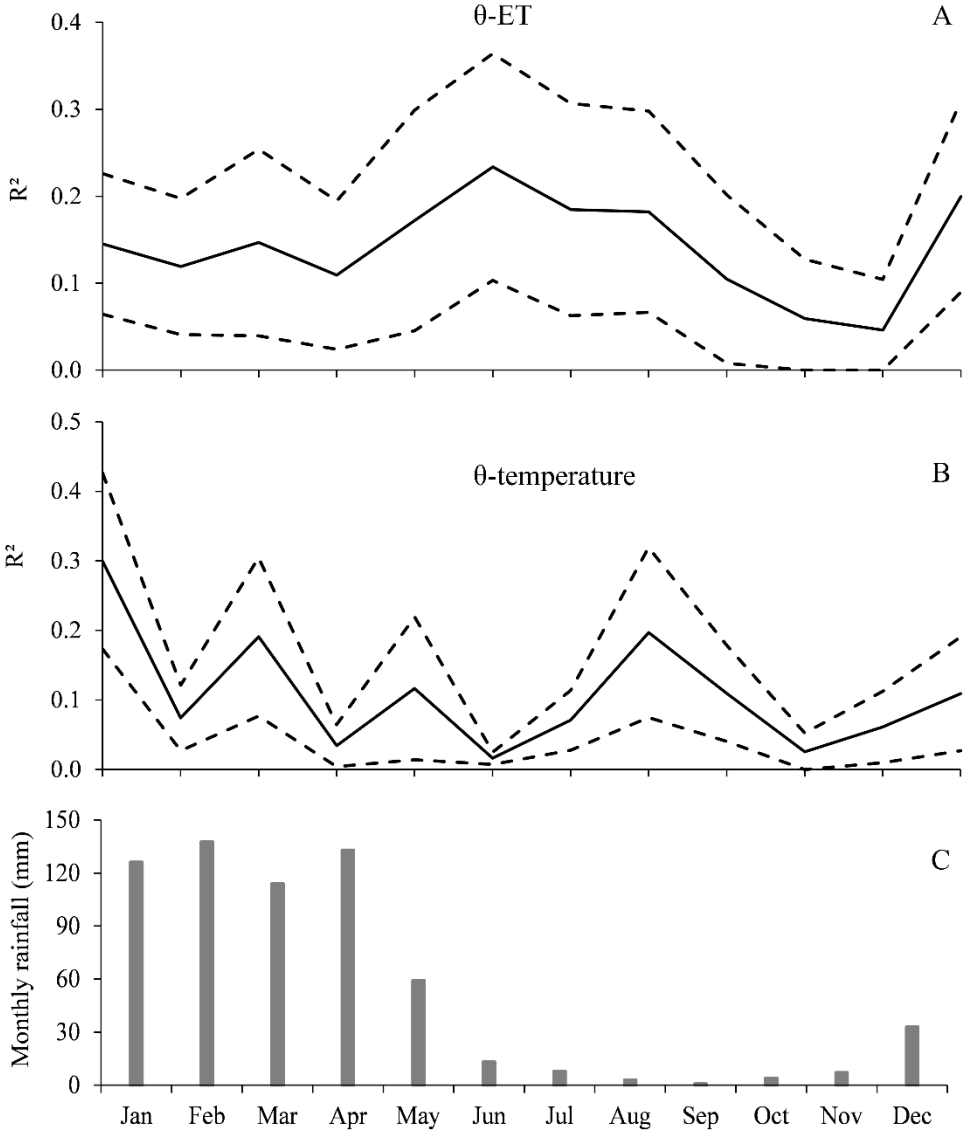

Figure 2.8 – R^2 of regression between daily soil water content and daily evapotranspiration (A) and air temperature (B) (solid lines refer to average values and dotted lines indicate the upper and lower limits with 95% of confidence), and average monthly rainfall (C) for the entire basin

The sensitivity observed for the months June-August agrees with the results from analyses based on Atmospheric General Circulation Models (KOSTER et al., 2004, 2006; SENEVIRATNE et al., 2010) and shows that despite the high temporal and spatial rainfall variability in the Brazilian semi-arid (MEDEIROS; DE ARAÚJO, 2014), soil water content is likely to have stronger influence on *ET* only in the very beginning (Dec-Jan) and at the end of the wet season. During the December-January period, a higher sensitivity between soil water content and *ET* is expected for the Caatinga biome because the rainy season usually starts in the second half of December. During this transitional period between dry and wet, instabilities may trigger additional precipitation from oceanic sources (SENEVIRATNE et al., 2010). Major global hot spots identified by AGCM occur in such transition conditions (KOSTER et al., 2004, 2006).

A similar argument holds for the relationship between air temperature and soil water content. Even in dry conditions, soil water content-air temperature sensitivity is likely to occur when increased temperature leads to a higher vapor pressure deficit and evaporative demand, and thus to a potential increase in *ET*, possibly leading to a further decrease in soil water content. As Seneviratne et al. (2010) pointed out, this feedback loop can go on until the soil is completely dry and temperature increases cannot be reduced by any further increase in *ET*, leading to extreme temperatures and heat waves. During the dry season, soil evaporation in the Caatinga biome is the main component of the feedback loop, driving soil water content to very low values, as shown by the fact that the vegetation shed leaves as a survival behavior to cope with limiting water availability. According to our simulations, soil evaporation accounted for 40% (±6%) of annual evapotranspiration, similar to the value (39%) reported by Raz-Yaseef et al. (2012) for a semiarid pine forest. Based on these system characteristics, analysis of the linear regression between soil water content and air temperature (Figure 2.8B) shows that the period of higher correlation between these components occurs in August-September and December-January, transitional periods between dry and wet seasons as discussed in the foregoing for soil water content-ET sensitivity.

The results from this study suggest that shallow root water uptake developed by the Caatinga biome likely ensures the vegetation can exploit ephemeral pulses of water in the upper soil layers, permitting a rapid start of the growing season following even small rain events. The concept of pulse water availability of short duration for arid and semi-arid regions has been widely recognized (SALA; LAUENROTH, 1982; REYNOLDS; KEMP; TENHUNEN, 2000; WILLIAMS et al., 2009; LAUENROTH; SCHLAEPFER; BRADFORD, 2014). This suggests that under a reduced rainfall climate change of up to 40%

(MARENGO et al., 2012), the Caatinga productivity could be maintained providing that storm intensity is increased. In terms of biomass productivity, temporal distribution of rainfall may be more important than the amount itself, since intensified storms may increase soil water storage (WANG et al., 2012). On the other hand, under a climate change scenario characterized by increasing *ET* driven by an increase in air temperature, water stress would be expected to increase and this would lead to a higher tree mortality, as observed by Raz-Yaseef et al. (2010). Many aspects still require research to analyse the influence of rainfall patterns on the capacity of the Caatinga biome to cope with climate change.

2.4 Conclusions

The hydrological modeling approach applied to a semi-arid Caatinga basin allows the following conclusions:

1. The satisfactory validation results of the simulations based on the parameterization with site-specific data indicates that our modeling approach may be transferable to other gauged or ungauged sites, opening the possibility to investigate interactions between soil-vegetation and environmental driving forces in sparsely studied ecosystem.
2. Soil water balance components do not differ statistically among the three soil and vegetation associations (SVA), suggesting a homogeneous spatial pattern of water use in the Caatinga biome.
3. Considering the overall average for all SVAs, the Caatinga biome returns 75% (±17%) of annual precipitation to the atmosphere, whereas partitioning of total evapotranspiration into its components (actual transpiration, actual evaporation and interception losses) on annual basis accounts for 41% (±7%), 40% (±6%), 19% (±3%), respectively.
4. Surface layer (0.0-0.2 m) is the most important layer in the rooted profile regarding water availability.
5. Higher sensitivity of soil water content-ET and soil water content-air temperature is expected to occur in the periods June-September and December-January. Despite the fact that our results were insufficient to produce robust conclusions about presence of coupling between the studied components in the Caatinga biome, they provide some preliminary indications of the period of the year during which *ET* and air temperature are more sensitive to hydrological processes, warranting further local investigation to assess more precisely the role of the soil water content on *ET*, air temperature and rainfall pattern.

References

ADIKU, S.G.K.; ROSE, C.W.; BRADDOCK, R.D.; OZIER-LAFONTAINE, H. On the simulation of root water extraction: examination of a minimum energy hypothesis. **Soil Science**, Philadelphia, v. 165, n. 3, p. 226-236, 2000.

ALLEN, R.G.; TREZZA, R.; TASUMI, M. **Surface energy balance algorithms for land:** advance training and users manual; version 1.0. Idaho, 2002. 98 p.

ALLEN, R.G.; PEREIRA, L.S.; RAES, D.; SMITH, M. **Crop evapotranspiration:** guidelines for computing crop water requirements. Rome: FAO, 1998. 333 p. (FAO. Irrigation and Drainage Paper, 56).

ASNER, G.P.; SCURLOCK, J.M.O.; HICKE, A. Global synthesis of leaf area index observations: implications for ecological and remote sensing studies. **Global Ecology and Biogeography**, Malden, v. 12, n. 3, p. 191–205, 2003.

BARBOSA, H.A.; HUETE, A.R.; BAETHGEN, W.E. A 20-year study of NDVI variability over the Northeast Region of Brazil. **Journal of Arid Environments**, London, v. 67, n. 2, p. 288-307, 2006.

BUCCI, S.J.; SCHOLZ, F.G.; GOLDSTEIN, G.; MEINZER, F.C.; ARCE, M.E. Soil water availability and rooting depth as determinants of hydraulic architecture of Patagonian woody species. **Oecologia**, New York, v. 160, n. 4, p. 631-641, 2009.

CAVANAUGH, M.L.; KURC, S.A.; SCOTT, R.L. 2010. Evapotranspiration partitioning in semiarid shrubland ecosystems: a two-site evaluation of soil moisture control on transpiration. **Ecohydrology**, Hoboken, v. 4, n. 5, p. 671-681, 2010.

CHOW, V.T.; MAIDMENT, D.R.; MAYS, L.W. **Applied hydrology**. New York: McGraw-Hill, 1988. 588 p.

COSTA, A.C.; BRONSTERT, A.; DE ARÚJO, J.C. A channel transmission losses model for different dryland rivers. **Hydrology and Earth System Sciences**, Gottingen, v. 16, n. 4, p. 1111–1135, 2012.

COSTA, A.C.; FOERSTER, S.; DE ARAÚJO, J.C.; BRONSTERT, A. Analysis of channel transmission losses in a dryland river reach in north-eastern Brazil using streamflow series, groundwater level series and multi-temporal satellite data. **Hydrological Processes**, Chichester, v. 27, n. 7, p. 1046-1060, 2013.

COSTA, C.A.G.; LOPES, J.W.B.; PINHEIRO, E.A.R.; DE ARAÚJO, J.C.; GOMES FILHO, R.R. Spatial behaviour of soil moisture in the root zone of the Caatinga biome. **Revista Ciência Agronômica**, Fortaleza, v. 44, n. 4, p. 685-694, 2013.

DE ARAÚJO, J.C.; PIEDRA, J.I.G. Comparative hydrology: analysis of a semiarid and a humid tropical watershed. **Hydrological Processes**, Chichester, v. 23, n.8, p. 1169-1178, 2009.

DE ARAÚJO, J.C.; GÜNTNER, A.; BRONSTERT, A. Loss of reservoir volume by sediment deposition and its impact on water availability in semiarid Brazil. **Hydrological Sciences Journal**, Wallingford, v. 51, n.1, p.157-170, 2006.

DE FIGUEIREDO, J.V.; DE ARAÚJO, J.C.; MEDEIROS, P.H.A.; COSTA, A.C. Runoff initiation in a preserved semiarid Caatinga small watershed, Northeastern Brazil. **Hydrological Processes**, Chichester, 2016. In press.

DE JONG VAN LIER, Q.; VAN DAM, J.C.; DURIGON, A.; DOS SANTOS, M.A.; METSELAAR, K. Modeling water potentials and flows in the soil-plant system comparing hydraulic resistances and transpiration reduction functions. **Vadose Zone Journal**, Madison, v. 12, n. 3, p. 1-20, 2013.

DE JONG VAN LIER, Q.; VAN DAM, J.C.; METSELAAR, K.; DE JONG, R.; DUIJNISVELD, W.H.M. Macroscopic Root Water Uptake Distribution Using a Matric Flux Potential Approach. **Vadose Zone Journal**, Madison, v. 7, n. 3, p. 1065-1078, 2008.

DORE, M.H.I. Climate change and changes in global precipitation patterns: what do we know? **Environment International**, Kidlington, v. 31, n. 8, p. 1167-1181, 2005.

FISCHER, E.M.; SENEVIRATNE, S.I.; VIDALE, P.L.; LÜTHI, D.; SCHÄR, C. Soil moisture: atmosphere interactions during the 2003 European summer heat wave. **Journal of Climate**, Boston, v. 20, p. 5081–5099, 2007.

GASH, J.H.C. An analytical model of rainfall interception by forests. **Quarterly Journal of the Royal Meteorological Society,** Chichester, v. 105, n. 443, p. 43-55, 1979.

MITTERMEIER, R.A.M.; PILGRIM, C.G.; FONSECA, J.; KONSTANT, G.; WILLIAM, R. **Wilderness:** earth's last wild places. Mexico City: CEMEX, 2002. 576 p.

GÜNTNER, A.; KROL, M.; DE ARAÚJO, J.C.; BRONSTERT, A. Simple water balance modeling of surface reservoir systems in a large data-scarce semiarid region. **Hydrological Sciences Journal**, Wallingford, v. 49, n. 5, p. 901-918, 2004.

JACKSON, R.B.; SPERRY, J.S.; DAWSON, T.E. Root water uptake and transport: using physiological processes in global predictions. **Trends in plant science**, London, v. 5, n. 11, p. 482-488, 2000.

KOSTER, R.D.; DIRMEYER, P.A.; GUO, Z.; BONAN, G.; CHAN, E.; COX, P.; GORDON, C.T.; KANAE, S.; KOWALCZYK, E.; LAWRENCE, D.; LIU, P.; LU, C.; MALYSHEV, S.; MCAVANEY, B.; MITCHELL, K.; MOCKO, D.; OKI T.; OLESON, K.; PITMAN, A.; SUD, Y.C.; TAYLOR, C.M.; VERSEGHY, D.; VASIC, R.; XUE, Y.;, YAMADA, T. Regions of strong coupling between soil moisture and precipitation. **Science**, Washington, v. 305, n. 5687, p. 1138–1140, 2004.

KOSTER, R.D.; SUD, Y.C.; GUO, Z.; DIRMEYER, P.A.; BONAN, G.; OLESON, W.K.; CHAN, E.; VERSEGHY, D.; COX, P.; DAVIES, H.; KOWALCZYK, E.; GORDON, C.T.; KANAE, S.; LAWRENCE, D.; LIU, P.; MOCKO, D.; LU, C.; MITCHELL, K.; MALYSHEV, S.; MCAVANEY, B.; OKI, T.; YAMADA, T.; PITMAN, A.; TAYLOR, C.M.; VASIC, R.; XUE, Y. GLACE: the global land– atmosphere coupling experiment. Part I: overview. **Journal of Hydrometeorology**, Boston, v. 7, p. 590–610, 2006.

KROES, J.G; VAN DAM, J.C.; GROENENDIJK, P.; HENDRIKS, R.F.A.; JACOBS, C.M.J. **SWAP version 3.2:** theory description and user manual. Wageningen: Alterra, 2008. 262p. (Alterra Report, 1649).

LAUENROTH, W.K.; SCHLAEPFER, D.R.; BRADFORD, J.B. Ecohydrology of dry regions: storage versus pulse soil water dynamics. **Ecosystems**, New York, v. 17, n.8, p. 1469–1479, 2014.

LEAL, I.R.; DA SILVA, J.M.C.; TABARELLI, M.; LACHER JR, T.E. Changing the course of biodiversity conservation in the Caatinga of Northeastern Brazil. **Conservation Biology**, Malden, v. 19, n.3, p. 701-706, 2005.

LEGATES, D.R.; MCCABE, G.J. Evaluating the use of "goodness-of-fit" measures in hydrologic and hydroclimatic model validation. **Water Resources Research**, Washington, v. 35, n.1, p. 233-241, 1999.

LIU, Y.; XU, Z.; DUFFY, R.; CHEN, W.; AN, S.; LIU, S.; LIU, F. Analyzing relationships among water uptake patterns, rootlet biomass distribution and soil water content profile in a subalpine shrubland using water isotopes. **European Journal of Soil Biology**, Paris, v. 47, n. 6, p. 380-386, 2011.

MARENGO, J.A.; CHOU, S.C.; KAY, G.; ALVES, L.M.; PESQUERO, J.F.; SOARES, W.R.; SANTOS, D.C.; LYRA, A.A.; SUEIRO, G.; BETTS, R.; CHAGAS, D.J.; GOMES, J.L.; BUSTAMENTE, J.F.; TAVARES, P. Development of regional future climate change scenarios in South America using the Eta CPTEC/HadCM3 climate change projections: climatology and regional analyses for the Amazon, São Francisco and the Paraná River basins. **Climate Dynamics**, New York, v. 38, n. 9, p. 1829–1848, 2012.

MEDEIROS, P.H.A.; DE ARAÚJO, J.C.; BRONSTERT, A. Interception measurements and assessment of Gash model performance for a tropical semi-arid region. **Revista Ciência Agronômica**, Fortaleza, v. 40, n. 2, p. 165-174, 2009.

MEDEIROS, P.H.A.; DE ARAÚJO J.C. Temporal variability of rainfall in a semiarid environment in Brazil and its effect on sediment transport processes. **Journal of Soils and Sediments**, Heidelberg, v. 14, n.7, p. 1216-1223, 2014.

MITCHELL, P.J.; VENEKLAAS, E.; LAMBERS, H.; BURGESS, S.S.O. Partitioning of evapotranspiration in a semi-arid eucalypt woodland in South-Western Australia. **Agricultural and Forest Meteorology**, Amsterdam, v. 149, n. 1, p. 25–37, 2009.

MUALEM, Y. A New model for predicting the hydraulic conductivity of unsaturated porous media. **Water Resources Research**, Washington, v. 12, n. 3, p. 513-522, 1976.

NASH, J.E.; SUTCLIFFE, J.V. River flow forecasting through conceptual models. Part I: A discussion of principles. **Journal of Hydrology**, Amsterdam, v. 10, n. 3, p. 282-290, 1970.

PESQUERO, J.F.; CHOU, S.C.; NOBRE, C.A.; MARENGO, J.A. Climate downscaling over South America for 1961–1970 using the Eta Model. **Theoretical and Applied Climatology**, Wien, v. 99, n.1, p. 75–93, 2010.

PINHEIRO, E.A.R.; COSTA, C.A.G.; DE ARAÚJO, J.C. Effective root depth of the Caatinga biome. **Journal of Arid Environments**, London, v. 89, p. 1-4, 2013.

PINHEIRO, E.A.R.; DE JONG VAN LIER, Q.; METSELAAR, K. Spatial and temporal dynamics of the leaf area index of the Caatinga biome. **Geophysical Research Abstracts**, Vienna, v. 17, EGU2015-1413, 2015.

RAZ-YASEEF, N.; ROTENBERG, E.; YAKIR ,D. Effects of spatial variations in soil evaporation caused by tree shading on water flux partitioning in a semi-arid pine forest. **Agricultural and Forest Meteorology**, Amsterdam, v. 150, n. 3, p. 454–462, 2010.

RAZ-YASEEF, N.; YAKIR, D.; SCHILLER, G.; COHEN, S. Dynamics of evapotranspiration partitioning in a semi-arid forest as affected by temporal rainfall patterns. **Agricultural and Forest Meteorology**, Amsterdam, v. 157, p. 77-85, 2012.

RAZ-YASEEF, N.; YAKIR, D.; ROTENBERG, E.; SCHILLER, G.; COHEN, S. Ecohydrology of a semi-arid forest: partitioning among water balance and its components implications for predicted precipitation changes. **Ecohydrology**, Hoboken, v. 3, n.2, p.1 43–154, 2010.

REYNOLDS, J.F.; KEMP, P.R.; TENHUNEN, J.D. Effects of long-term rainfall variability on evapotranspiration and soil water distribution in the Chihuahuan Desert: a modeling analysis. **Plant Ecology**, Dordrecht, v. 150, n. 1, 145–59, 2000.

SALA, O.E.; LAUENROTH, W.K. Small rainfall events: an ecological role in semiarid regions. **Oecologia**, New York, v. 53, n. 3, p. 301–304, 1982.

SALAZAR, L.F.; NOBRE, C.A.; OYAMA, M.D. Climate change consequences on the biome distribution in tropical South America. **Geophysical research letters**, Washington, v. 34, n. 9, p. 1-6, 2007.

SANTOS, J.C.; LEAL, I.R.; ALMEIDA-CORTEZ, J.S.; FERNANDES, G.W.; TABARELLI, M. Caatinga: the scientific negligence experienced by a dry tropical forest. **Tropical Conservation Science**, Washington, v. 4, n. 3, p**.** 276-286, 2011.

SCHENK, H.J. The shallowest possible water extraction profile: a null model for global root distributions. **Vadose Zone Journal,** Madison, v. 7, n. 3, p. 1119-1124, 2008.

SCHENK, H.J.; JACKSON, R.B. Rooting depths, lateral root spreads and below-ground/above-ground allometries of plants in water-limited ecosystems. **Journal of Ecology**, Malden, v. 90, n. 3, p. 480-494, 2002.

SCHLESINGER, W.H.; JASECKO, S. Transpiration in the global water cycle. **Agricultural and Forest Meteorology**, Amsterdam, v. 189/190, p. 115-117, 2014.

SENEVIRATNE, S.I.; LÜTHI, D.; LITSCHI, M.; SCHÄR, C. Land–atmosphere coupling and climate change in Europe. **Nature**, London, v. 443, p. 205–209, 2006.

SENEVIRATNE, S.L.; CORTI, T.; DAVIN, E.L.; HIRSCHI, M.; JAEGER, E.B.; LEHNER, I.; ORLOWSKY, B.; TEULING, A.J. Investigating soil moisture–climate interactions in a changing climate: a review. **Earth-Science Reviews**, Amsterdam, v. 99, n. 3/4, p. 125–161, 2010.

SENEVIRATNE, S.I.; NICHOLLS, N.; EASTERLING, D.; , GOODESS, C.M.; KANAE, S.; KOSSIN, J.; LUO, Y.; MARENGO, J.; MCINNES, K.; RAHIMI, M.; REICHSTEIN, M.; SORTEBERG, A.; VERA, C.; ZHANG, X. Changes in climate extremes and their impacts on the natural physical environment. In: FIELD, C.B., BARROS, V.; STOCKER, T.F.; QIN, D.; DOKKEN, D.J.; EBI, K.L.; MASTRANDREA, M.D.; MACH, K.J.; PLANTTNER, G.-K, ALLEN, S.K.; TIGNOR, M.; MIDGLEY, P.M. (Ed.). **Managing the risks of extreme events and disasters to advance climate change adaptation:** a special report of Working Groups I and II of the Intergovernmental Panel on Climate Change (IPCC). Cambridge; New York: Cambridge University Press, 2012. p. 109-230.

SILVA, V.P.R. On climate variability in Northeast of Brazil. **Journal of Arid Environments**, London, v. 58, n. 4, 575-596, 2004.

STAUDT, K.; SERAFIMOVICH, A.; SIEBICKE, L.; PYLES, R.D.; FALGE, E. Vertical structure of evapotranspiration at a forest site (a case study). **Agricultural and Forest Meteorology**, Amsterdam, v. 151, n. 6, p. 709–729, 2011.

TRENBERTH, K.E.; FASULLO, J.; KIEHL, J. Earth's global energy budget. **Bulletin of the American Meteorological Society**, Boston, v. 90, p. 311–323, 2009.

VAN DER WERF, W.; KEESMAN, K.; BURGESS, P.; GRAVES, A.; PILBEAM, D.; INCOLL, L.D.; METSELAAR, K.; MAYUS, M.; STAPPERS, R.; VAN KEULEN, H.; PALMA, J.; DUPRAZ, C. Yield-SAFE: a parameter-sparse, process-based dynamic model for predicting resource capture, growth, and production in agroforestry systems. **Ecological Engineering**, Amsterdam, v. 29, n. 4, p. 419-433, 2007.

VAN GENUCHTEN, MT. A closed-form equation for predicting the hydraulic conductivity of unsaturated soils. **Soil Science Society of America Journal**, Madison, v. 44, n. 5, p. 892-898, 1980.

WANG, L.; D'ODORICO, P.; EVANS, J.P.; ELDRIDGE, D.J.; MCCABE, M.F.; CAYLOR, K.K.; KING, E.G. Dryland ecohydrology and climate change: critical issues and technical advances. **Hydrolpgical Earth Systematic Science**, Gottingen, v. 16, p. 2585–2603, 2012.

WANG, X.; AULER, A.S.; EDWARDS, R.L.; CHENG, H.; CRISTALLI, P.S.; SMART, P.L.; RICHARDS, D.A.; SHEN, C. Wet periods in northeastern Brazil over the past 210 kyr linked to distant climate anomalies. **Nature**, London, v. 432, p. 740-743, 2004.

WILLIAMS, C.A.; HANAN, N.; SCHOLES, R.J.; KUTSCH, W. Complexity in water and carbon dioxide fluxes following rain pulses in an African savanna. **Oecologia**, New York, v. 161, n. 3, p. 469–480, 2009.

WILLMOTT, C.J.; ROBESON, S.M.; MATSUURA, K. A refined index of model performance. **International Journal of Climatology**, Chichester, v. 32, n. 13, p. 2088–2094, 2012.

ZHONGMIN, H.; GUIRUI, Y.; YANLIAN, Z.; XIAOMIN, S.; YINGNIAN, L.; PEILI, S.; YANFEN, W.; XIA, S.; ZEMEI, Z.; LI, Z.; SHENGGONG, L. Partitioning of evapotranspiration and its controls in four grassland ecosystems: application of a two-source model. **Agricultural and Forest Meteorology**, Amsterdam, v. 149, n. 9, p. 1410–1420, 2009.

3 CAATINGA HYDROLOGY UNDER A CLIMATE CHANGE SCENARIO

Abstract

Given the strong interactions between climate and vegetation, climate change effects on natural and agricultural ecosystems are a common object of research. Reduced water availability is predicted to take place in large regions of the globe, including Northeastern Brazil, a region already vulnerable to droughts. The Caatinga biome, a complex tropical and water-limited ecosystem, prevails as the main natural forest of this region. The aim of this study was to examine the soil-water balance for the Caatinga biome in a climate-warming scenario with reduced rainfall. Climate change projections for the period between 2011 and 2040 were assessed from regional circulation models earlier applied to the Brazilian territory. A statistical climate data generator was used to compose a synthetic weather dataset in which rainfall reduction and air temperature increase were linearly incorporated, such that the maximum changes were reached by the year 2040. The synthetic weather dataset was then integrated into a hydrological model to assess soil-water balance. Compared to simulations with current climate for the same Caatinga site, in the scenario with climate change transpiration was enhanced by 36%, soil evaporation and interception losses reduced by 16% and 34%, respectively. The amount of precipitation returned to the atmosphere as evapotranspiration was, on average, 98%. The greatest change in soil water balance components was observed for deep drainage, accounting only for 2% of the annual rainfall, followed by top soil water reduction of 38%. Regarding soil water availability, the soil-plant-atmosphere fluxes seem to be controlled by the top layer (0.0-0.2 m), which provides, on average, 80% of the total transpiration, suggesting that the Caatinga biome may become completely soil-water pulse dominated under scenarios of reduced water availability.

Keywords: Semiarid environment; Soil-water; Evapotranspiration; Rainfall reduction

3.1 Introduction

Climate and vegetation interact on temporal and spatial scales and climate is considered as the main factor determining vegetation distribution (SALAZAR; NOBRE; OYAMA, 2007). On the other hand, vegetation plays a role in climate as well, mainly on the regional scale, and replacement of a vegetation type by another will affect evapotranspiration and other climate factors simultaneously. This process may result directly in land-atmosphere feedbacks, suggesting that a land-cover change may modify precipitation cycle dynamics, and thus, play an important role in the water balance of a land surface (JASECHKO et al., 2013; STERLING; DUCHARNE; POLCHER, 2012).

When predicted climate change scenarios include rainfall reduction and air temperature increase, soil water content is expected to decrease, thus affecting evapotranspiration rates. According to Seneviratne et al. (2010), effects of land cover changes or vegetation dynamics are often associated with modification in the soil moisture regime. If frequency, duration and severity of droughts increase, as is the case for predicted climatic

change scenarios (MARENGO et al., 2012; SENEVIRATNE et al., 2012), this could alter composition, structure and biogeography of forests in many global regions (ALLEN et al., 2010).

Drylands cover about 40% of the land surface of the earth. They are characterized by a low precipitation and a high incidence of drought. Vegetation and atmosphere feedbacks are especially critical in drylands, mainly due to the tight coupling that exists between water, energy and biogeochemical budgets (WANG et al., 2012). Therefore, to improve our understanding of forest-climate interactions in arid and semi-arid zones, an ecosystem approach might be necessary to assess forest water-use and hydrological limitations in a warmer and drier climate (KLEIN et al., 2014).

The northeastern part of Brazil contains a large semiarid region, the Caatinga, representing 12% of the total Brazilian territory. The Caatinga biome prevails as the main natural forest of this region, a complex tropical and water-limited ecosystem with a wide variety of both herbaceous and arborescent vegetation, characterized by its ability to cope with low soil water content ranges (PINHEIRO et al., 2016; PINHEIRO; COSTA; DE ARAÚJO, 2013). Recently predicted climate changes, assessed by indices from global and regional climate models like consecutive dry days and soil moisture anomalies, have projected an increase in air temperature and in duration and intensity of drought in some large regions of the world. For the semiarid region of Northeastern Brazil, rainfall reductions of up to 40% and air temperature increase up to 4.0 ºC are predicted by the year 2100 (MARENGO et al., 2012; SENEVIRATNE et al., 2012).

The Caatinga biome is important to the Brazilian semi-arid region as a whole for its rich and diverse biota (LEAL et al., 2005). Beyond the role of being a shelter for several endemic species, the Caatinga biome provides essential services to society such as timber, forage and watershed protection. Regarding the latter, as the population from the northeastern part of Brazil is highly dependent on surface water reservoirs, the biome is a key component for water security. A severe water depletion of the biome is likely when the natural protection of the watersheds by vegetation would be damaged (PETER et al., 2014). Some specific issues remain uncertain regarding climate change and its effects on the Caatinga biome water cycle, such as the fact that the desertification processes may be enhanced as the vegetation faces higher atmospheric demand in a drier soil (D'ODORICO et al., 2013). With the objective to study the effects on the hydrology of the Caatinga biome triggered by a climate change characterized by an increase in air temperature and a reduction of rainfall, we

performed a hydrological simulation study focusing on the soil-water balance components of a representative Caatinga site under possible future scenarios.

3.2 Material and Methods

3.2.1 Study area

The study was conducted for the Aiuaba Experimental Basin (AEB), a 12 km^2 integrally-preserved Caatinga watershed (6º42'S; 40º17'W). The AEB is completely located inside the ecological station of Aiuaba, state of Ceará, Brazil, which is under jurisdiction of the Brazilian Federal Environmental Institute (IBAMA). Following the Köppen classification system, the climate is of the BSh type (semi-arid, low latitude and altitude) with an average annual class-A pan evaporation of 2500 mm. Average annual rainfall is 549 mm, concentrated in the rainy season between January and May. The monthly average temperatures range from 24ºC to 28ºC. The watershed is covered by dense native vegetation characterized by tree heights typically between 5 and 12 m. More detailed information can be found in de Figuereido et al. (2016), Medeiros and de Araújo (2014) and Pinheiro et al. (2016).

Based on previous studies (COSTA et al., 2013; GÜNTNER; BRONSTERT, 2004; PINHEIRO et al., 2016), the Aiuaba Experimental Basin (AEB) was subdivided in three parts, each of them characterized by a specific "soil and vegetation association" or SVA (Figure 3.1). The first association (SVA1), developed in a Lixisol and occupies 20% of the AEB area. The rooting depth of the vegetation is around 0.8 m. In the second system (SVA2, 34% of the experimental area) the soils are classified as Luvisol and the average rooting depth is 0.6 m. SVA3 contains a shallow soil (Leptosol) with average rooting depth of 0.4 m, occupying 46% of the AEB (Figure 3.1).

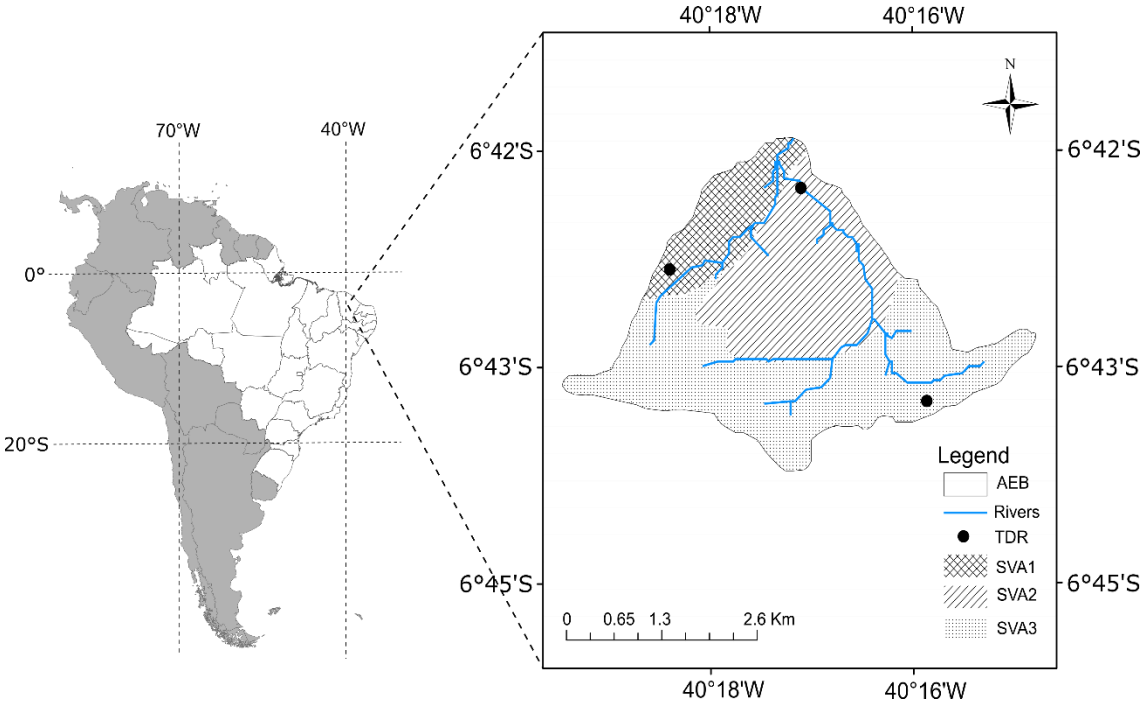

Figure 3.1 – Geographical location of the Aiuaba Experimental Basin (AEB) and subdivision into three Soil and Vegetation Associations – SVA1, 2 and 3, showing the position of rivers and soil water content observation locations (TDR)

3.2.2 Climatic data generator – *ClimGen*

Statistical weather generator software uses existing weather records (baseline data) to produce long series of synthetic daily climatic data. The statistical properties of the generated series are expected to be similar to those of the baseline data. We used the Climatic data generator (*ClimGen*) developed by Stöckle, Campbell and Nelson (1999). *ClimGen* does not use any fixed coefficients optimized from specific weather database, therefore it can be applied to any location as long as enough information exists to parameterize its code, i.e., 25 years of daily rainfall, 10 years of temperature data, two years of solar radiation data, wind speed and relative humidity, without missing values. For our simulations, weather data was reproduced stochastically for the period from 2016 to 2040 for the Aiuaba Experimental Basin, with baseline data from the period 1990-2015. The synthetically generated daily weather data consist of rainfall, daily maximum and minimum temperature, solar radiation, air humidity, and wind speed.

The meteorological baseline data used in the parameterization of *ClimGen* software were provided by the Ceará State Foundation of Meteorology and Water Resources (FUNCEME, www.funceme.br), comprising daily records from the AEB dataset as well as from a neighboring weather station. According to earlier soil-water balance simulations (PINHEIRO et al., 2016), the hydrological components do not differ statistically among the

three SVA. Nevertheless, SVA1 was chosen for the simulation of climate change scenarios, as its soil does not contain a shallow stony layer as occurs in SVA2 and SVA3, and it may therefore provide a more representative picture of the Caatinga hydrology adaptation under climate change scenarios.

3.2.3 Climate change scenario

Marengo et al. (2012) have assessed the impact of climate change on rainfall and temperature for different Brazilian regions and periods based on the Eta-CPTEC regional model driven by four members of an ensemble of the Met Office Hadley Centre Global Coupled climate model HadCM3. The model ensemble was run according to the SRES A1B emissions. According to these authors, for mesoscale processes, climate change projections derived from Regional Climate Models may be considered more representative than projections derived from Global Climate Models (GCMs), mainly due to the better resolution which allows improvements in the representation of topography, land use and land-sea distribution.

Based on that, a climate change projection was selected from the simulations performed by Marengo et al. (2012) over Brazil. For our purpose, we selected the predicted changes corresponding to an atmospheric CO_2 concentration of 418 ppm by the period 2011-2040, projected for the São Francisco River Basin. The São Francisco River Basin is predominantly located in Northeastern Brazil with its middle and lower parts covered mainly by the Caatinga biome, therefore, representative of the here analyzed site. Under this scenario and during this period, rainfall is predicted to be reduce by 15% and air temperature is predicted to increase by 1.5 ºC.

Rainfall reduction and temperature increase were linearly incorporated into a stochastic weather generator model such that the maximum changes were reached by the year 2040. As the simulation of the synthetic climatic data started in the year 2016, the projected changes of rainfall and air temperature for the first five years (2011-2015) were considered in the period 2016-2040. As the stochastic weather generator relies on random numbers, one hundred stochastic realizations were performed in order to obtain scenarios with more representativeness. The 100 generated weather datasets were integrated into the hydrological model SWAP, resulting in 100 water balance simulations for the period.

3.2.4 Modeling

Hydrological modeling was performed with the 1-D SWAP model (KROES et al., 2008). The model simulates water flow and plant growth in a soil-plant-atmosphere environment. To calculate the water balance terms, the model employs the Richards equation with a root water extraction sink term:

$$\frac{\partial \theta}{\partial t} = \frac{\partial}{\partial z}\left[K(h)\left(\frac{\partial h}{\partial z} + 1 \right) \right] - S(h) \tag{3.1}$$

In this equation, *t* is time *(d)*, *z* is the vertical coordinate (cm, positive upwards), *K(h)* is the hydraulic conductivity (cm d^{-1}) and *S(h)* represents the water uptake by plant roots (d^{-1}). Equation (3.1) is solved numerically describing the *θ-h-K* relation by the Mualem–van Genuchten equations (MUALEM, 1976; VAN GENUCHTEN, 1980). To estimate the sink term S*(h)*, the reduction function proposed by de Jong van Lier et al. (2008; 2013) was used. This reduction function includes an implicit compensation mechanism such that uptake restrictions in drier layers is compensated by increased uptake from wetter parts of the rooted soil profile.

Simulations with SWAP were based on a parameterization of vegetation (leaf area index, crop factor, root length density and interception losses) and soil hydraulic properties performed by Pinheiro et al. (2016) for the Aiuaba Experimental Basin. Regarding the crop factor (K_c), Pinheiro et al. (2016) developed equation (3.2) based on the modeling of plant growth:

$$K_c = \frac{1 - \alpha_v - (\alpha_s - \alpha_v) e^{-kLAI}}{1 - 0.23} \tag{3.2}$$

where α_v is the vegetation albedo; α_s is the surface soil albedo; *k* is the light extinction coefficient and LAI is the leaf area index. Values of α_v, α_s were assumed constant over time and estimated using satellite images. The light extinction coefficient (*k*) was assumed constant as well and fixed to the value of 0.75 (GOURDIAAN; VAN LAAR, 1994).

For a seasonal forest like Caatinga, LAI values are not constant over time. Pinheiro et al. (2016) found a strong correlation between LAI estimated from satellite images and the mean soil water pressure head in the 15-day period before the satellite imaging. However, for future scenarios no soil water content dataset is available and forecasting the Caatinga leaf area index would be cumbersome.

We opted to establish a correlation between LAI measurements obtained from satellite images and the rainfall in a period of p days before the satellite imaging. Daily rainfall (R) was weighed by a factor η defined according to a sine function, making rainfall amounts in the middle of the period (at $d = p/2$) of highest weight and at the beginning and end (at $d = 0$ and $d = p$) of zero weight:

$$\eta = \frac{\sum_{d=1}^{p} R\left(1+\sin\left[\frac{2\pi}{p}\left(d-\frac{p}{4}\right)\right]\right)}{\sum_{d=1}^{p}\left(1+\sin\left[\frac{2\pi}{p}\left(d-\frac{p}{4}\right)\right]\right)} \tag{3.3}$$

The highest correlation between LAI and η was found for $p = 31$ days, and resulted in the equation (3.4) with coefficient of determination of 0.95:

$$LAI = 0.4188\eta^{0.4252} \tag{3.4}$$

The LAI estimated by equation (3.4) has the same order of magnitude as the estimates carried out by Pinheiro et al. (2016) using soil pressure head.

SWAP simulated the following water balance components: actual transpiration (T), actual soil evaporation (E), interception losses (IL) and deep drainage (D). T+E+IL will be referred to as ET.

3.3 Results and Discussion

3.3.1 *ClimGen* outputs

The 100 stochastic daily rainfall series simulated by *ClimGen* for each year for the period 2016-2040 resulted in total annual rainfall ranging from 133-1142 mm with an annual average of 473 mm and an average standard deviation of 129 mm (Figure 3.2). This figure shows the simulated trend of rainfall reduction as well. For the baseline climate period (1990-2015), annual rainfall ranged from 221-1266 mm with an average of 518 mm.

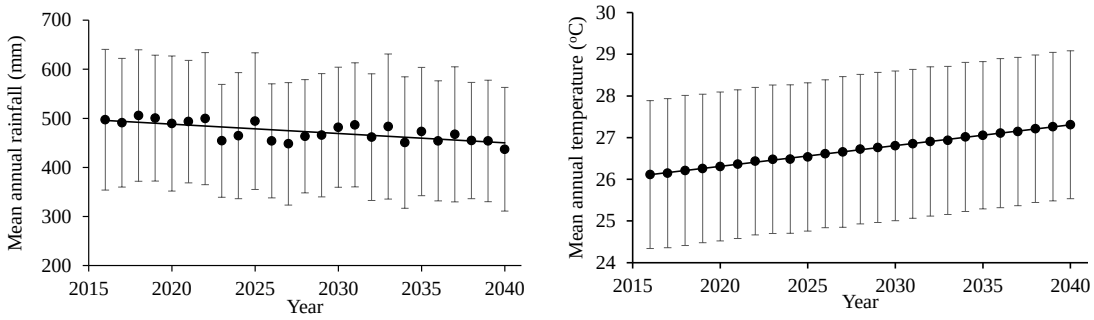

Figure 3.2 – Mean annual rainfall and air temperature together with trendlines ± standard deviations of 100 stochastic daily data series simulated by 2016-2040 relative to 1990-2015 associated with rainfall reduction and air temperature increase

Regarding temperature increase, the annual average of the 100 stochastic realizations for the simulated period ranged from 19-34 ºC with an average of 26.7ºC and a standard deviation of 1.8 ºC (Figure 3.2). The baseline climate dataset had a mean annual temperature of 25.8ºC (±1.7ºC) with minimum and maximum values ranging from 18-31ºC.

3.3.2 SWAP simulations

Actual transpiration, actual evaporation and interception losses showed normality according to the Kolmogorov–Smirnov test ($p>0.05$); 95% levels of confidence were calculated and are shown in Figure 3.3 together with their mean annual values.

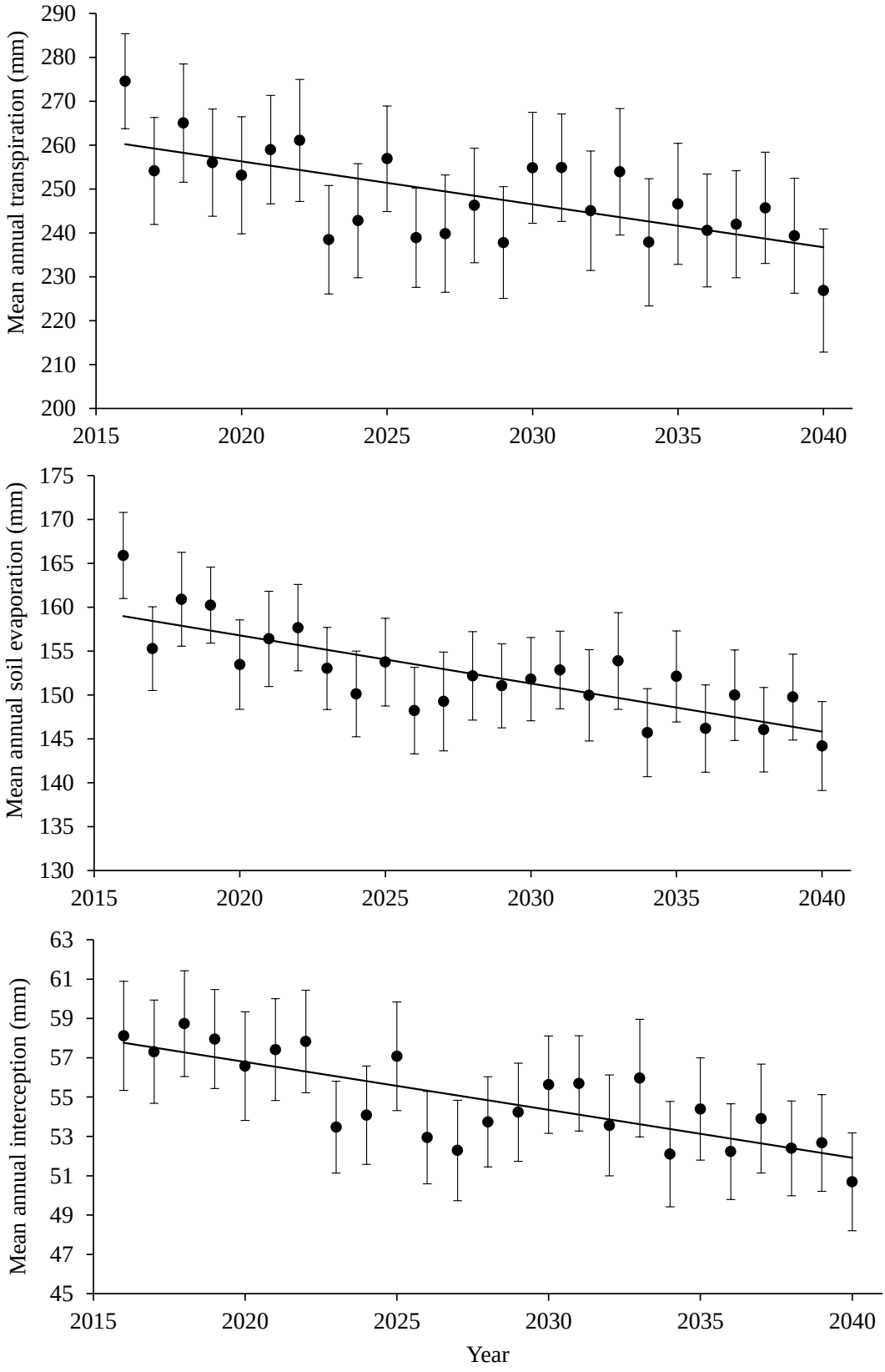

Figure 3.3 – Mean annual actual transpiration, actual soil evaporation and interception losses with their 95% confidence levels and trendlines

Based on the 95% levels of confidence, *T*, *E* and *IL* for the year 2040 are predicted to be between the interval of 212-241 mm, 139-149 mm and 48-53 mm, respectively. Therefore, in order to obtain a positive year-based water budget, annual rainfall should be higher than 443 mm. A lower amount of rainfall would make the vegetation either to increase stomatal resistance, to reduce transpiration or to further deplete soil-water stocks from previous years, enhancing soil drought and possibly leading to mortality of certain species as suggested by Choat et al. (2012) and Raz-Yaseef et al. (2010). Comparing the future predictions to the simulations carried out by Pinheiro et al. (2016) with measured weather data for the Caatinga biome, on average actual transpiration increased by 36%, actual soil evaporation and interception losses decreased by 16% and 34%, respectively. As pointed out by Jasechko et al. (2013), biological fluxes (transpiration) play a bigger role in water fluxes than physical fluxes (evaporation). This is expected because plant roots are able to take up stored soil-water and moving deeper sources of water to the atmosphere, whereas evaporation is only effective for water at or near the soil surface.

According to Ohmura and Wild (2002), the trend of evaporation rates under a warming climate scenario is unclear. Class A Pan measurements (PETERSON; GOLUBEV; GROISMAN, 1995) and simulations by global circulation models (WILD; OHMURA; CUBASCH, 1997) have revealed a reducing tendency, which would be related to an increase in the terrestrial water flux correlating to an increasing air humidity, or due to changes in radiation intensity or in strength of air circulations.

The amount of precipitation that returns to the atmosphere as actual evapotranspiration, *ET*, (through *T*, *E* and *IL*) for the whole simulated period at the studied site was, on average, 98% (± 8.3%), which is 23% higher than the values simulated by Pinheiro et al. (2016) in the period 2004-2012 for the same site. Lauenroth et al. (2014) investigated the water balance of dry regions and found that 96 to 98% of total precipitation returned to atmosphere as *ET* for shallow-rooted sites, which are dependent on water-pulse dynamics. For the Caatinga biome, an *ET* greater than the annual rainfall corresponded to years with a rainfall amount below the long-term average preceded by years with rainfall above the long-term average. This can be explained by the depletion of soil-water stored from the year before. For the analyzed period, the average fraction ± standard deviation of total water use by *T* was 54% (±4%), *E* 34% (±4%) and *IL* 12% (±1%).

The observed behavior of the actual transpiration over the simulated period can be explained by the simulated changes in air temperature and rainfall. However, due to the diversity of plant species in the Caatinga biome, different plant responses to drought stress are

expected. For instance, transpiration will probably reduce when atmospheric CO_2 concentration increases (GEDNEY et al., 2006), enforced by stomatal adjustments to atmospheric variables and soil moisture (CHOAT et al., 2012). Laboratory experiments have shown that the stomatal openings of many plants species reduce under elevated CO_2 concentrations (FIELD; JACKSON; MOONEY, 1995), which would impact the global water cycle (GEDNEY et al., 2006). It is unclear whether this process would have a significant effect on the regional water cycle, especially in water-limited ecosystems, which are typically constrained by water and nutrient availability. Therefore, most predictions of future water availability ignore stomatal-closure effects.

Pinheiro et al. (2016) found that the surface soil layer (0.0-0.2 m) is the most important one regarding water availability in the Caatinga biome, providing more than 80% of total transpired water for years with annual rainfall slightly above the long-term average. Regarding the hydrological simulations with climate change scenarios, the average values of root water uptake at depth 0.0-0.2 m remained close to 80% (±7%) with a slight increasing trend (Figure 3.4).

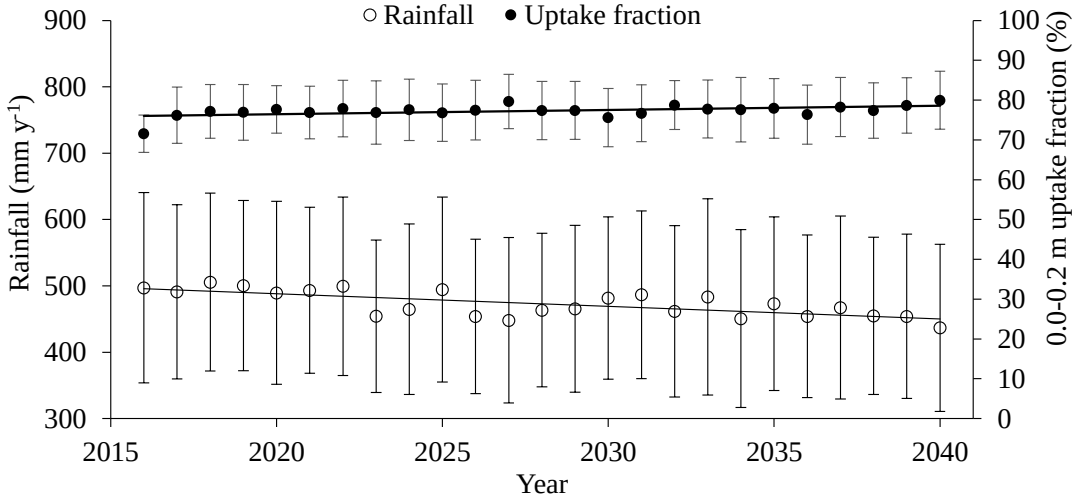

Figure 3.4 – Annual rainfall and fraction of total transpired water taken up from the 0.0-0.2 m soil layer, together with respective standard deviations. Results obtained from stochastic simulations. Trendlines obtained by linear fitting to average values

Considering all stochastic realizations, the contribution of the soil top layer to actual transpiration ranged from 60 to 95%. As discussed by Pinheiro et al. (2016), other authors have found the soil-water fluxes to be controlled by top layers as well, for instance, Liu et al. (2011), Raz-Yaseef et al. (2012) and Gaines et al. (2015). The importance of top layers for dryland forests is based on maximizing the uptake of ephemeral water pulses from rainfall,

together with an optimization of nutrient cycling (ADIKU et al., 2000; JACKSON et al., 2000; BUCCI et al., 2009). Under drier conditions, however, an increase in water extraction from deeper layers may be expected rather than maintenance of the predominance of shallow root water uptake. However, apparently the Caatinga water balance not only depends on rainfall amount, but also on temporal rainfall distribution. The Caatinga vegetation has a shallow and laterally spread root system (PINHEIRO; COSTA; DE ARAÚJO, 2013) enhancing the importance of the top layer and indicating that the water regime of this ecosystem is water pulse rather than storage dominated. According to Lauenroth et al. (2014), ecosystems dominated by soil-water storage are likely to be more harmed by water shortage enhanced by increased temperature, higher evapotranspiration demand, and decreased rainfall, than ecosystems with soil water dynamics that depend on pulsed soil-water patterns.

The temporal pattern of the monthly soil water content for the surface layer (0.0-0.2 m) shows a high correlation to the monthly rainfall pattern, with a large temporal variability on the yearly scale grouped into periods (Figure 3.5). The highest monthly soil water contents were observed between February and April (rainy season) and the lowest values between July and December (dry season). The average value for the whole simulated period was 0.15 m^3 m^{-3} (±0.039), while the average measured soil water content during the analyzed period 2004-2012 at depth 0-0.2 m was 0.24 m^3 m^{-3} (see details in PINHEIRO et al., 2016).

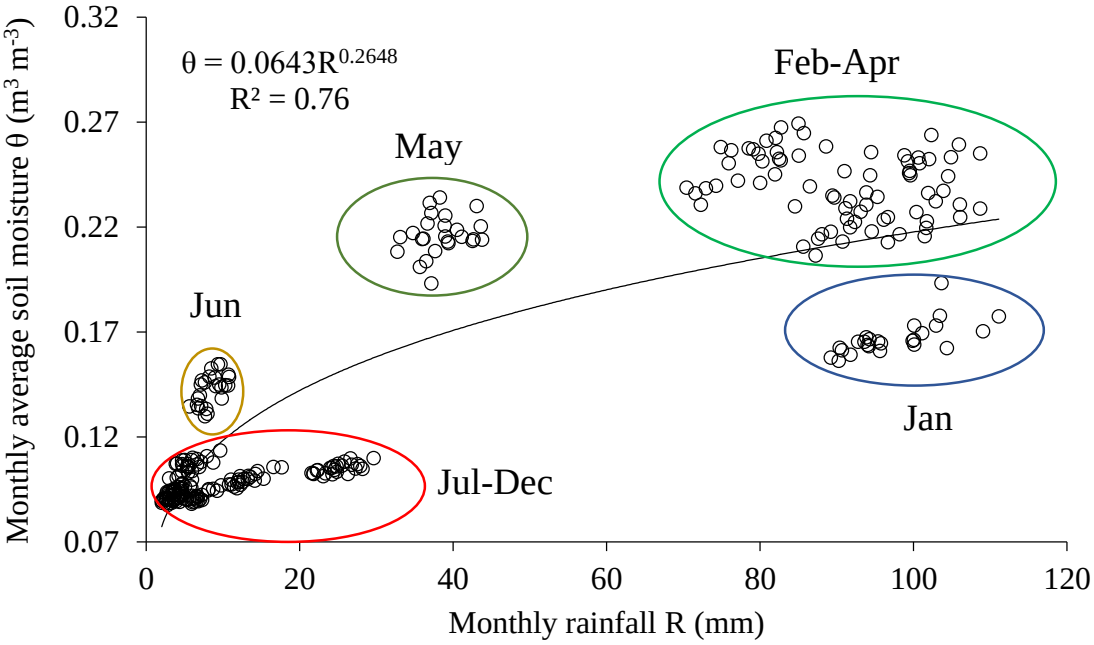

Figure 3.5 - Monthly average soil water content at depth 0-0.2 m, together with monthly rainfall

Monthly average soil water pressure head (*h*) over depth is displayed in Figure (3.6). The values of *h* at 0.1 m and 0.3 m depth show larger variations when compared to deeper layers, reflecting rainfall pattern and shallow root water uptake associated with high evaporation rates. Figure (3.6B) shows the soil water pressure head at 0.1 m depth along the year averaged for the simulated period and for the first (2016) and last (2040) simulated year. Comparing the year 2040 to the overall average, one can observe that there is a tendency of more negative *h* values during the rainless season (Jun-Dec) with pressure head values reaching -110 m by the end of the rainy season (period Jun-Jul), 37% higher than registered for the first simulated year (2016). June and July normally represent the onset of leaf shedding in the biome and a drier soil may speed up this phenological behavior.

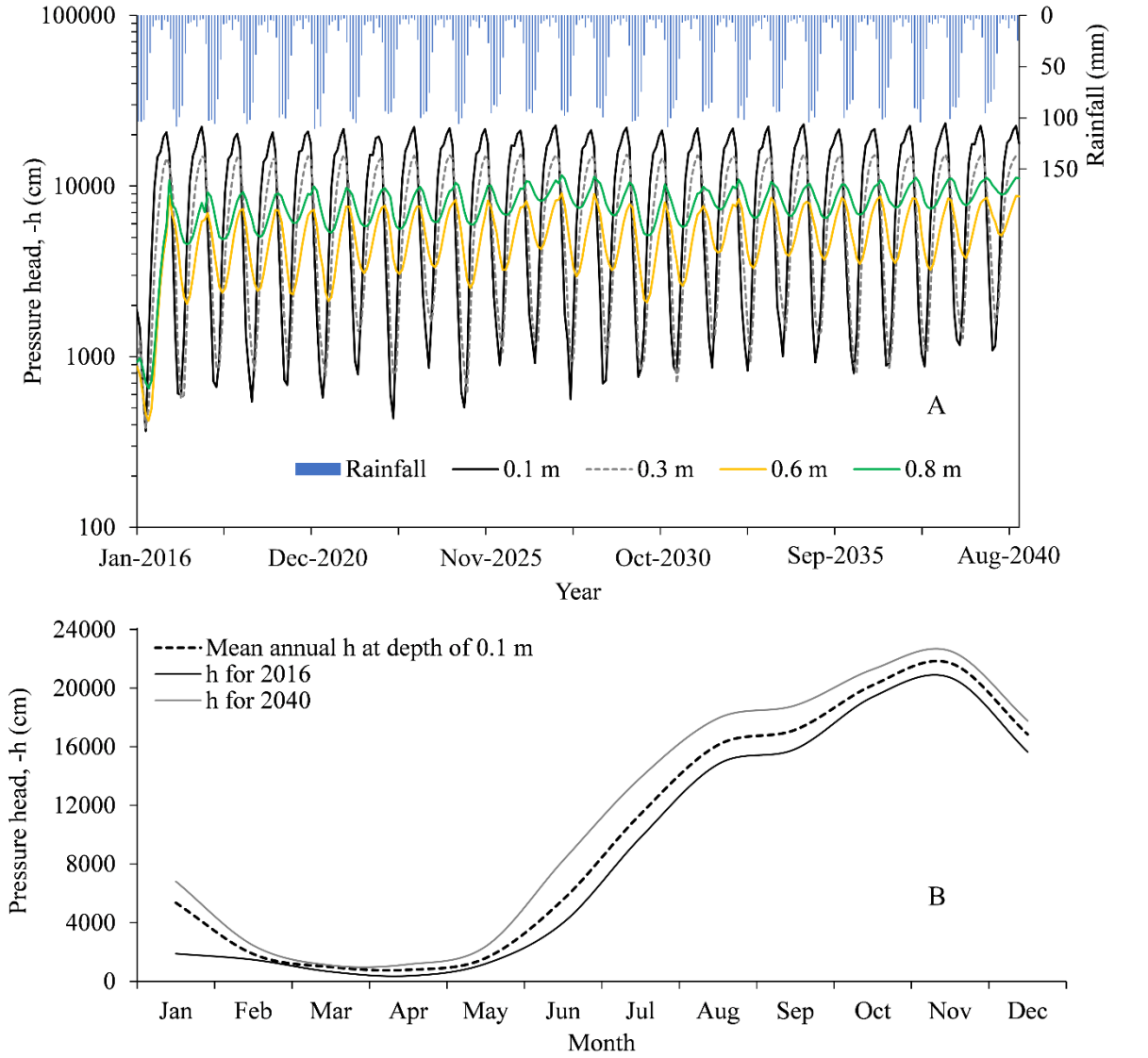

Figure 3.6 – Average monthly soil water pressure head (*h*) of 100 realizations at four depths (0.1; 0.3; 0.6 and 0.8 m) together with monthly rainfall (A). Soil water pressure head at 0.1 m depth along the year, average for the simulated period and first (2016) and last (2040) simulated year (B)

The canopy of the Caatinga biome and soil moisture dynamics allow the development of understory vegetation. Such understory composed of very shallow-rooted herbaceous plants quickly dries at the end of rainy season and together with the leaf shedding behavior of overstory vegetation and coarse woody debris yields a thick layer of potential ground fuel. The depletion of soil water content in the root zone due to higher evapotranspiration demands may increase the risk of forest fires (WARING; COOPS, 2016). Krueger et al. (2015) found that low soil moisture strongly affects wildfires across the Southern Great Plains of United States. Projections of a warming climate and rainfall reduction would reduce the soil water content of the Caatinga biome and increase wildfire occurrence.

Comparing the simulated period 2016-2040 to the period (2004-2012) studied by Pinheiro et al. (2016), the greatest change in water balance components was observed for the annual amount of deep drainage below the root zone. For 2004-2012, deep drainage averaged 34% of total annual rainfall, whereas for the period 2016-2040 deep drainage accounted for only about 2%. The highest annual value of deep drainage was 427 mm for one of the 2016 realizations. For this specific simulation, total rainfall was 1000 mm; Pinheiro et al. (2016) obtained a similar value with measured weather data for the year 2004 for the same site. Taking into account only annual averages, deep drainage ranged from 11-42 mm with a high mean standard deviation of 41.5 mm (Figure 3.7).

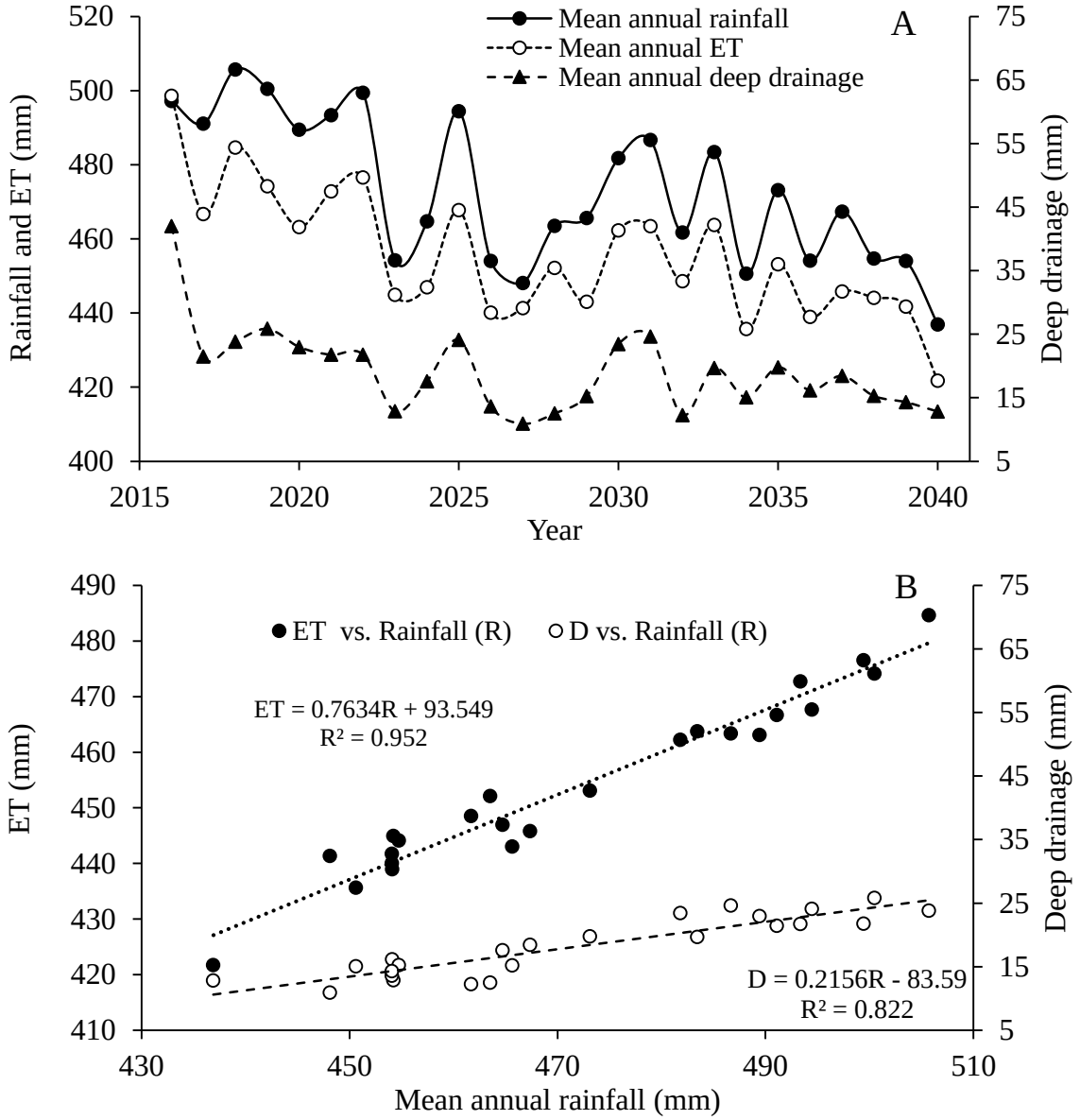

Figure 3.7 - Mean annual actual evapotranspiration (*ET*), deep drainage (*D*) and rainfall (R) over time (A) together with relationships between *ET* and *D* with mean annual rainfall (B)

A reduction of the amount of deep drainage, as predicted, would represent an increase in problems related to soil salinity. This would be especially impacting for the Caatinga biome, a naturally salinization prone ecosystem due to its geological formation (shallow soils on crystalline basement) together with water scarcity. In a drier soil, the vegetation will experience higher salt concentration than in a wet soil. With a higher atmospheric water demand and a 98% fraction of precipitation being used for *ET*, there will be insufficient downward water flow to leach salts out of the soil profile. The combination of salt and water stress could be very damaging to the biome, provoking modifications in vegetation composition and, perilously, desertification. Although the water table is located several meters below the river bed (DE FIGUEIREDO et al., 2016) making capillary rise irrelevant, salts can be introduced in the root zone by rain itself and by weathering of rocks (D'ODORICO et al., 2013). Even at low rates, the increase of salt concentrations in the surface layer could impact the ecosystem, which currently depends on shallow soil water. A shift in plant community composition (e.g., encroachment and decrease in vegetation cover) and a loss of ecosystem productivity would be a natural consequence.

Our modeling approach pinpointed important features concerning reduction in water availability for the Caatinga biome, taking into account the water balance at ecosystem scale; therefore, our results may provide a big picture of the likelihood of threats to the ecosystem brought about by climate change. Nonetheless, predictions about the response of individual species in the Caatinga to future climate change rely on details at species level. To improve predictions of drought related vulnerability of forests, according to Choat et al. (2012), a better understanding of quantitative physiological mechanisms governing drought stress together with hydrological modeling is needed. The Caatinga biome shows a remarkable capacity to cope with low soil-water ranges, with matric potentials dropping below -150 m during dry seasons that last up to nine months (PINHEIRO et al., 2016). A further decrease in water availability, however, would trigger the replacement of prevailing species by pre-adapted individuals already present within the population (KELLY et al., 2003). Biomes with substantial variability for the traits that regulate the species responses to climate are likely to show greater tolerance to climate changes. Although genetic response of vegetation to climate change may play an important role in selection pressure of individuals, when environmental variation occurs on a timescale shorter than the life of the plant, any response must be in terms of a plastic phenotype (JUMP; PEÑUELAS, 2005, and references cited therein). These responses alter plants productivity through both growth (photosynthesis and biomass

accumulation) and development (phenological and morphological responses) (CHALLINOR et al., 2016).

3.4 Conclusions

From the soil-water balance simulations applied to the Caatinga biome, including a climatic change over the period 2016-2040, we conclude that:

1. Based on 95% levels of confidence, in order to obtain a positive year-based water budget, annual rainfall should be higher than 443 mm.
2. Compared to simulations with current climate, climate change will lead to an increase of actual transpiration of 36%, and a decrease of 16% and 34% for soil evaporation and interception losses, respectively, whereas the amount of precipitation returned to the atmosphere as evapotranspiration was predicted to reach, on average, 98%.
3. The greatest change in water balance components under the simulated climate change was predicted for deep drainage, accounting only for 2% of the annual rainfall, followed by top soil water reduction of 38%.
4. Regarding soil water availability, the soil-plant-atmosphere fluxes seem to be controlled by the top layer (0.0-0.2 m), which provides, on average, 80% of the total transpiration, suggesting that the Caatinga biome may become completely soil-water pulse dominated under scenarios of reduced water availability.

References

ADIKU, S.G.K.; ROSE, C.W.; BRADDOCK, R.D.; OZIER-LAFONTAINE, H. On the simulation of root water extraction: examination of a minimum energy hypothesis. **Soil Science**, Philadelphia, v. 165, n. 3, p. 226-236, 2000.

ALLEN, C.D.; MACALADY, A.K.; CHENCHOUNI, H.; BACHELET, B.; MCDOWELL, N.; VENNETIER, M.; KITZBERGER, T.; RIGLING, A.; BRESHEARS, D.D.; HOGG, E.H.; GONZALEZ, P.; FENSHAM, R.; ZHANGM, Z.; CASTRO, J.; DEMIDOVA, N.; LIM, J.H.; ALLARD, G.; RUNNING, S.W.; SEMERCI, A.; COBB, N. A global overview of drought and heat-induced tree mortality reveals emerging climate change risks for forests. **Forest ecology and management**, Amsterdam, v. 259, n. 4, p. 660-684, 2010.

BUCCI, S.J.; SCHOLZ, F.G.; GOLDSTEIN, G.; MEINZER, F.C.; ARCE, M.E. Soil water availability and rooting depth as determinants of hydraulic architecture of Patagonian woody species. **Oecologia**, New York, v. 160, n. 4, p. 631-641, 2009.

CHALLINOR, A.J.; KOEHLER, A.K.; RAMIREZ-VILLEGAS, J.; WHITFIELD, S.; DAS, B. Current warming will reduce yields unless maize breeding and seed systems adapt immediately. **Nature Climate Change**, London, 2016. In press.

CHOAT, B.; JANSEN, S.; BRODRIBB, T.J.; COCHARD, H.; DELZON, S.; BHASKAR, R.; BUCCI, S.J.; FEILD, T.S.; GLEASON, S.M.; HACKE, U.G.; JACOBSEN, A.L.; LENS, F.; MAHERALI, H.; MARTÍNEZ-VILALTA, J.; MAYR, S.; MENCUCCINI, M.; MITCHELL, P.J.; NARDINI, A.; PITTERMANN, J.; PRATT, R.B.; SPERRY, J.S.; WESTOBY, M.; WRIGHT, I.J.; ZANNE, A.E. Global convergence in the vulnerability of forests to drought. **Nature**, London, v. 491, p. 752–755, 2012.

COSTA, C.A.G.; LOPES, J.W.B.; PINHEIRO, E.A.R.; DE ARAÚJO, J.C.; GOMES FILHO, R.R. Spatial behaviour of soil moisture in the root zone of the Caatinga biome. **Revista Ciência Agronômica**, Fortaleza, v. 44, n. 4, p. 685-694, 2013.

D'ODORICO, P.; BHATTACHAN, A.; DAVIS, K.F.; RAVI, S.; RUNYAN, C.W. Global desertification: drivers and feedbacks. **Advances in Water Resources**, Kidlington, v. 51, p. 326-344, 2013.

DE FIGUEIREDO, J.V.; DE ARAÚJO, J.C.; MEDEIROS, P.H.A.; COSTA, A.C. Runoff initiation in a preserved semiarid Caatinga small watershed, Northeastern Brazil. **Hydrological Processes**, Chichester, 2016. In press.

DE JONG VAN LIER, Q.; VAN DAM, J.C.; DURIGON, A.; DOS SANTOS, M.A.; METSELAAR, K. Modeling water potentials and flows in the soil-plant system comparing hydraulic resistances and transpiration reduction functions. **Vadose Zone Journal**, Madison, v. 12, n. 3, p. 1-20, 2013.

DE JONG VAN LIER, Q.; VAN DAM, J.C.; METSELAAR, K.; DE JONG, R.; DUIJNISVELD, W.H.M. Macroscopic root water uptake distribution using a matric flux potential approach. **Vadose Zone Journal**, Madison, v. 7, n. 3, p. 1065-1078, 2008.

FIELD C.B.; JACKSON, R.B.; MOONEY, H.A Stomatal responses to increased CO2: implications from the plant to the global-scale. **Plant, Cell and Environment**, Malden, v. 18, n. 10, p. 1214-1225, 1995.

GAINES, K.P.; STANLEY, J.W.; MEINZER, F.C.; MCCULLOH, K.A.; WOODRUFF, D.R.; CHEN, W.; ADAMS, T.S.; LIN, H.; EISSENSTAT, D.M. Reliance on shallow soil water in a mixed-hardwood forest in central Pennsylvania. **Tree Physiology**, Oxford, v. 00, p. 1-15, 2015.

GEDNEY, N.; COX, .PM.; BETTS, R.A.; BOUCHER, O.; HUNTINGFORD, C.; STOTT, A. Detection of a direct carbon dioxide effect in continental river runoff records. **Nature**, London, v. 439, p. 835-838, 2006.

GOURDIAAN, J.; VAN LAAR, H.H. **Modelling potential crop growth processes**. 2nd ed. Wageningen: Kluwer Academic, 1994. 238 p.

GÜNTNER, A.; KROL, M.; DE ARAÚJO, J.C.; BRONSTERT, A. Simple water balance modeling of surface reservoir systems in a large data-scarce semiarid region. **Hydrological Sciences Journal**, Wallingford, v. 49, n. 5, p. 901-918, 2004.

JACKSON, R.B.; SPERRY, J.S.; DAWSON, T.E. Root water uptake and transport: using physiological processes in global predictions. **Trends in Plant Science**, London, v. 5, n. 11, p. 482-488, 2000.

JASECHKO, S.; SHARP, Z.D.; GIBSON, J.J.; BIRKS, S.J.; YI ,Y.; FAWCETT, P.J. Terrestrial water fluxes dominated by transpiration. **Nature**, London, v. 496, p. 347-350, 2013.

JUMP, A.; PEÑUELAS, J. Running to stand still: adaptation and response of plants to rapid climate change. **Ecology Letters**, Malden, v. 8, n. 9, p. 1010-1020, 2005.

KELLY, C.K.; CHASE, M.W.; DE BRUIJN, A.; FAY, M.F.; WOODWARD, F.I. Temperature-based population segregation in birch. **Ecology Letters**, Malden, v. 6, n. 2, p. 1–3, 2003.

KLEIN, T.; YAKIR, D.; BUCHMANN, N.; GRÜNZWEIG, J.M. Towards an advanced assessment of the hydrological vulnerability of forests to climate change-induced drought. **New Phytologist**, Malden, v. 201, n. 3, p. 712-716, 2014.

KROES, J.G; VAN DAM, J.C.; GROENENDIJK, P.; HENDRIKS, R.F.A.; JACOBS, C.M.J. **SWAP version 3.2:** theory description and user manual. Wageningen: Alterra, 2008. 262 p. (Alterra Report, 1649).

KRUEGER, E.S, OCHSNER TE, ENGLE DM, CARLSON JD, TWIDWELL D, FUHLENDORF SD. Soil moisture affects growing-season wildfire size in the Southern great plains. **Soil Science Society of America Journal**, Madison, v. 79, p. 1567-1576, 2015.

LAUENROTH, W.K.; SCHLAEPFER, D.R.; BRADFORD, J.B. Ecohydrology of dry regions: storage versus pulse soil water dynamics. **Ecosystems**, New York, v. 17, n. 8, p. 1469–1479, 2014.

LEAL, I.R; DA SILVA, J.M.C.; TABARELLI, M.; LACHER JR, T.E. Changing the course of biodiversity conservation in the Caatinga of Northeastern Brazil. **Conservation Biology**, Malden, v. 19, n. 3, p. 701-706, 2005.

MARENGO, J.A.; CHOU, S.C.; KAY, G.; ALVES, L.M.; PESQUERO, J.F.; SOARES, W.R.; SANTOS, D.C.; LYRA, A.A.; SUEIRO, G.; BETTS, R.; CHAGAS, D.J.; GOMES, J.L.; BUSTAMENTE, J.F.; TAVARES, P. Development of regional future climate change scenarios in South America using the Eta CPTEC/HadCM3 climate change projections: climatology and regional analyses for the Amazon, São Francisco and the Paraná River basins. **Climate Dynamics**, New York, v. 38, n. 9, p. 1829–1848, 2012.

MEDEIROS, P.H.A.; DE ARAÚJO J.C. Temporal variability of rainfall in a semiarid environment in Brazil and its effect on sediment transport processes. **Journal of Soils and Sediments**, Heidelberg, v. 14, n.7, p. 1216-1223, 2014.

MUALEM, Y. A New model for predicting the hydraulic conductivity of unsaturated porous media. **Water Resources Research**, Washington, v. 12, n. 3, p. 513-522, 1976.

OHMURA, A.; WILD, M. Is the hydrological cycle accelerating? **Science**, Washington, v. 298, p. 1345-1346, 2002.

PETER, A.J.; DE ARAÚJO, J.C.; ARAÚJO, N.A.M.; HERMANN, H.J. Flood avalanches in a semiarid basin with a dense reservoir network. **Journal of Hydrology**, Amsterdam, v. 512, p. 408-420, 2014.

PETERSON, T.C.; GOLUBEV, V.S.; GROISMAN, P.Y. Evaporation losing its strength. **Nature**, London, v. 377, p. 687-688, 1995.

PINHEIRO, E.A.R.; COSTA, C.A.G.; DE ARAÚJO, J.C. Effective root depth of the Caatinga biome. **Journal of Arid Environments**, London, v. 89, p. 1-4, 2013.

PINHEIRO, E.A.R.; METSELAAR, K.; DE JONG VAN LIER, Q.; DE ARAÚJO, J.C. Importance of soil water to the Caatinga biome, Brazil. **Ecohydrology**, Hoboken, 2016. In press.

RAZ-YASEEF, N.; YAKIR, D.; ROTENBERG, E.; SCHILLER, G.; COHEN, S. Ecohydrology of a semi-arid forest: partitioning among water balance and its components implications for predicted precipitation changes. **Ecohydrology**, Hoboken, v. 3, n.2, p. 143–154, 2010.

RAZ-YASEEF, N.; YAKIR, D.; SCHILLER, G.; COHEN, S. Dynamics of evapotranspiration partitioning in a semi-arid forest as affected by temporal rainfall patterns. **Agricultural and Forest Meteorology**, Amsterdam, v. 157, p. 77-85, 2012.

SALAZAR, L.F.; NOBRE, C.A.; OYAMA, M.D. Climate change consequences on the biome distribution in tropical South America. **Geophysical Research Letters**, Washington, v. 34, n. 9, p. 1-6, 2007.

SENEVIRATNE, S.I.; NICHOLLS, N.; EASTERLING, D.; , GOODESS, C.M.; KANAE, S.; KOSSIN, J.; LUO, Y.; MARENGO, J.; MCINNES, K.; RAHIMI, M.; REICHSTEIN, M.; SORTEBERG, A.; VERA, C.; ZHANG, X. Changes in climate extremes and their impacts on the natural physical environment. In: FIELD, C.B., BARROS, V.; STOCKER, T.F.; QIN, D.; DOKKEN, D.J.; EBI, K.L.; MASTRANDREA, M.D.; MACH, K.J.; PLANTTNER, G.-K, ALLEN, S.K.; TIGNOR, M.; MIDGLEY, P.M. (Ed.). **Managing the risks of extreme events and disasters to advance climate change adaptation:** a special report of Working Groups I and II of the Intergovernmental Panel on Climate Change (IPCC). Cambridge; New York: Cambridge University Press, 2012. p. 109-230.

SENEVIRATNE, S.L.; CORTI, T.; DAVIN, E.L.; HIRSCHI, M.; JAEGER, E.B.; LEHNER, I.; ORLOWSKY, B.; TEULING, A.J. Investigating soil moisture–climate interactions in a changing climate: a review. **Earth-Science Reviews**, Amsterdam, v. 99, n. 3/4, p. 125–161, 2010.

STERLING, S.M.; DUCHARNE, A.; POLCHER, J. The impact of global land-cover change on the terrestrial water cycle**. Nature Climate Change**, London, v. 3, p. 385-390, 2013.

STÖCKLE, C.O., G.S. CAMPBELL, R. NELSON. **ClimGen manual**. Washington: Pullman, 1999. 28 p. (Washington State University, Biological Systems Engineering Department).

VAN GENUCHTEN, MT. A closed-form equation for predicting the hydraulic conductivity of unsaturated soils. **Soil Science Society of America Journal**, Madison, v. 44, n. 5, p. 892-898, 1980.

WANG, L.; D'ODORICO, P.; EVANS, J.P.; ELDRIDGE, D.J.; MCCABE, M.F.; CAYLOR, K.K.; KING, E.G. Dryland ecohydrology and climate change: critical issues and technical advances. **Hydrology and Earth System Sciences**, Gottingen, v. 16, p. 2585–2603, 2012.

WARING, R.H.; COOPS, N.C. Predicting large wildfires across western North America by modeling seasonal variation in soil water balance. **Climatic Change**, Dordrecht, v. 135, n. 2, p. 325-339, 2016.

WILD, M.; OHMURA, A.; CUBASCH, U. GCM simulated surface energy fluxes in climate change experiments. **Journal of Climate**, Boston, v. 10, p. 3093-3110, 1997.

4 A MATRIC FLUX POTENTIAL APPROACH TO ASSESS WATER AVAILABILITY APPLIED TO SOME BRAZILIAN SOILS

Abstract

Predicting soil water availability to plants is important for agricultural and ecological models. Models that explicitly take into account root water uptake and transpiration reduction describe the ability of soil to supply water to plants based on soil hydraulic properties that depend on soil water content. The objective of this study was to evolve an existing single-layer root water uptake model based on matric flux potential to allow for multi-layer scenarios; and to illustrate its functionality using soil hydraulic properties from layered soils from two agro-ecological zones in Brazil: a semiarid zone and a sub-humid zone. For each soil layer, the hydraulic properties were determined by inverse modeling of laboratory evaporation experiment data for the pressure head range between -1.5 and -165 m. The water supplying capacities were evaluated using the multi-layer root water uptake model. Soils from the semiarid zone were able to deliver water to plants at potential rates over a wide range of bulk soil pressure head (-36 to -148 m). On the other hand, the soils from the sub-humid zone showed more hydraulic limitations. Their limiting soil water condition was wetter than the range of pressure heads for which parameters were determined. For the analyzed soils, a negligible increase in available water results from decreasing the root water potential below -150 m. It is therefore reasonable to expect that, in order to adapt to water-limited conditions, plant species will invest in other adaptive strategies, rather than spend energy in structures that allow a reduction of the lower suction limit in their root tissues.

Keywords: Climatic zone; Pressure head; Caatinga biome; Hydraulic conductivity

4.1 Introduction

Hydraulic properties determine the ability of soils to supply water to plants. The ability of a soil to provide transpirable water to plants under dry conditions is crucial in the establishment and maintenance of natural vegetation, especially when dealing with drought-prone ecosystems. In agricultural areas, a less negative limiting pressure head results in higher rainfed yields, whereas in irrigated agriculture it implies a lower cost to obtain optimized yields. Assessment of soil-water dynamic availability to plants over depth, especially in dry regions, is necessary to evaluate strengths and restrictions of ecosystems given the expected increase in water limitation due to environmental changes projected to occur on some large regions of the globe (KLEIN et al., 2014b; SENEVIRATNE et al., 2012). According to Marengo et al. (2012), the whole Brazilian territory is likely to face rainfall reductions and higher temperatures in the coming years. Hence, it may pose a threat to natural ecosystems productivity and to rainfed crops grown in soils with limited water supplying capacity.

Soil hydraulic properties together with limiting crop water potentials allow to characterize crop water stress by predicting the threshold value of water content or pressure

head that delimits the constant and falling water uptake rate phase (DE JONG VAN LIER et al., 2013; RAATS, 2007). Therefore, the assessment of soil water availability combines a theoretical root water uptake model with soil hydraulic properties (DE JONG VAN LIER et al., 2013; DURIGON et al., 2011; IDEN et al., 2015; ŠIMUNEK et al., 1998). One such model was developed by De Jong van Lier et al. (2006), who proposed an equation to calculate the limiting matric flux potential M_{lim} (threshold value between constant and falling rate phase) for a given transpiration rate and root length density in a single-layer soil.

Matric flux potential is a composite quantity combining hydraulic conductivity and pressure head. The relation between these hydraulic properties can be determined from field and laboratory experiments using direct methods or inverse modeling techniques. Gardner and Miklich (1962) developed a laboratory method for the simultaneous measurement of retention and unsaturated hydraulic conductivity. Their method was modified by Wind (1968) who proposed an iterative graphical procedure to decrease deviations in readings. Wendroth et al. (1993) proposed the use of different evaporation rates to overcome problems of small hydraulic gradients near saturation. The implementation of any of these methods usually relies on water-filled tensiometers with a limited range of operation. For the determination of hydraulic conductivity in the dry soil, at pressure heads below -10 m, special measurement devices like the polymer tensiometer (BAKKER et al., 2007; DURIGON et al., 2011) are needed.

Soil water hydraulic properties usually vary with depth (DOMEC et al., 2010; KLEIN et al., 2014b), therefore, the amount of transpirable water is not necessarily distributed homogenously over the rooting zone. In this context, we aimed to further develop the single-layer M_{lim} equation proposed by De Jong van Lier et al. (2006), making it applicable to multi-layer scenarios. To illustrate the theory, soil hydraulic properties were assessed for soils from two important ecological zones in Brazil: the northeast Brazilian semiarid zone, an ecosystem representing 12% of the total national territory, and the southeast Brazilian sub-humid tropical/subtropical zone covering great parts of Brazil´s southern and southeastern states, including high intensity agricultural areas.

4.2 Material and Methods

4.2.1 Development of an expression to calculate limiting hydraulic conditions

A convenient soil hydraulic property that is often used in soil water movement studies is the matric flux potential M (GRANT and GROENEVELT, 2015; PULLAN, 1990; RAATS,

1977). M ($m^2\ d^{-1}$) is defined as the integral of hydraulic conductivity K ($m\ d^{-1}$) over pressure head h (m) starting at an arbitrary reference pressure head h_{ref}:

$$M = \int_{h_{ref}}^{h} K(h)dh \tag{4.1}$$

Using h_{ref} equal to h_w (the pressure head at permanent wilting point), De Jong van Lier et al. (2006) proposed a linear relation between M and transpiration rate (T_p, $m\ d^{-1}$) with intercept equal to zero and a slope depending on the half-distance between roots (r_m, m):

$$M_{\lim} = p r_m^{\ q} T_p \tag{4.2}$$

where $M_{\lim}$ ($m^2\ d^{-1}$), the limiting matric flux potential, is bulk soil M at the onset of limiting hydraulic conditions, when $h = h_w$ at the root surface.

Half-distance between roots r_m is related to root length density R ($m\ m^{-3}$) according to

$$r_m = \sqrt{\frac{1}{\pi R}} \tag{4.3}$$

and eq. (4.2) can be written in terms of root length density as

$$M_{\lim} = p\left(\frac{1}{\pi R}\right)^{\frac{q}{2}} T_p \tag{4.4}$$

After performing a series of simulations with rooting depth z = 0.5 m (DE JONG VAN LIER et al., 2006, their table 2), values for p and q were obtained by linear regression: p = 23.5 (m^{1-q}) and q = 2.367. It should be noted that these values are only valid for z = 0.5 m. In a more general form for any rooting depth, eq. (4.2) is written as

$$M_{lim} = p^* r_m^{\ q} \frac{T_p}{z} \tag{4.5}$$

with p^* (m^{2-q}) equal to

$$p^* = \left(23.5\,\mathrm{m}^{1-q}\right)\left(0.5\,\mathrm{m}\right) = 11.75\,\mathrm{m}^{2-q} \tag{4.6}$$

Equation (4.5) refers to a single-layer rooted soil of depth z. To adapt this equation for a scenario in which the root zone expands over n soil layers, T_p is substituted by the share of water extraction per soil layer (S_j, $m\ d^{-1}$):

$$M_{lim,j} = p^* r_{m,j}^{\ q} \frac{S_j}{L_j} \tag{4.7}$$

where indices j refer to the soil layer and L_j (m) is the layer thickness. A reasonable way to estimate S_j, in non-limiting conditions is by weighing potential transpiration according to L_j and root length density R_j:

$$S_j = T_p \frac{L_j R_j}{\sum_{i=1}^{n} L_i R_i} \tag{4.8}$$

Substituting eq. (4.8) in eq. (4.7) results in

$$M_{lim,j} = p^* T_p \left(\frac{1}{\pi}\right)^{\frac{q}{2}} \frac{R_j^{1-\frac{q}{2}}}{\sum_{i=1}^{n} L_i R_i} \tag{4.9}$$

Transforming this finite difference expression into an integral one at depth z, we obtain:

$$M_{lim}(z) = p^* T_p \left(\frac{1}{\pi}\right)^{\frac{q}{2}} \frac{R(z)^{1-\frac{q}{2}}}{\int_0^D R dz} \tag{4.10}$$

For the special case of $q = 2$ (which is slightly lower than the value of 2.367 determined by De Jong van Lier et al., 2006) and performing a fitting procedure, analogous to De Jong van Lier et al. (2006), between M_{lim} and T_p for several half-distance between roots, $p^* = 5.3$ was found to result in the best fit. Then eq. (4.10) reduces to

$$M_{lim}(z) = \frac{p^* T_p}{\pi \int_0^D R dz} \tag{4.11}$$

If the number of layers is not infinite, eq. (4.11) can be expressed in a finite way as

$$M_{lim}(z) = \frac{p^* T_p}{\pi \sum_{i=1}^{n} R_i L_i} \tag{4.12}$$

In non-hysteretic conditions, M is uniquely correlated to θ and h. M-θ-h relations are available for several standard soil hydraulic property equation systems (DE JONG VAN

LIER et al., 2009; GRANT; GROENEVELT, 2015) and for practical purposes any M_{lim} can be converted in θ_{lim} or h_{lim}.

4.2.2 Evaluation of water availability in some Brazilian soils

In order to illustrate the use of eq. 4.12, soils from two Brazilian climatic zones were studied. From the semiarid zone located in the northeastern part of Brazil, soils at three sites (sites 1, 2, and 3) representative of an integrally-preserved Caatinga watershed in Ceará State were sampled. The sub-humid zone occurs in a vast area covering the south, southeast and central parts of Brazil. To represent this region, eight sites (sites 4-11) in São Paulo State were sampled. At each location, soil samples were collected from the surface layer and from one or more sub-surface layers. Figure 4.1 and Table 4.1 show location and other details of the sampling locations. The ratio between annual rainfall and potential evapotranspiration shows the significant climatic difference regarding water availability among the sampling sites (Table 4.1). Table 4.2 contains information about the particle size distribution for all sampled soil layers. Soils from both zones show significant variation in particle size distribution over depth, and soils from the sub-humid zone generally have a much higher clay content than semiarid zone soils.

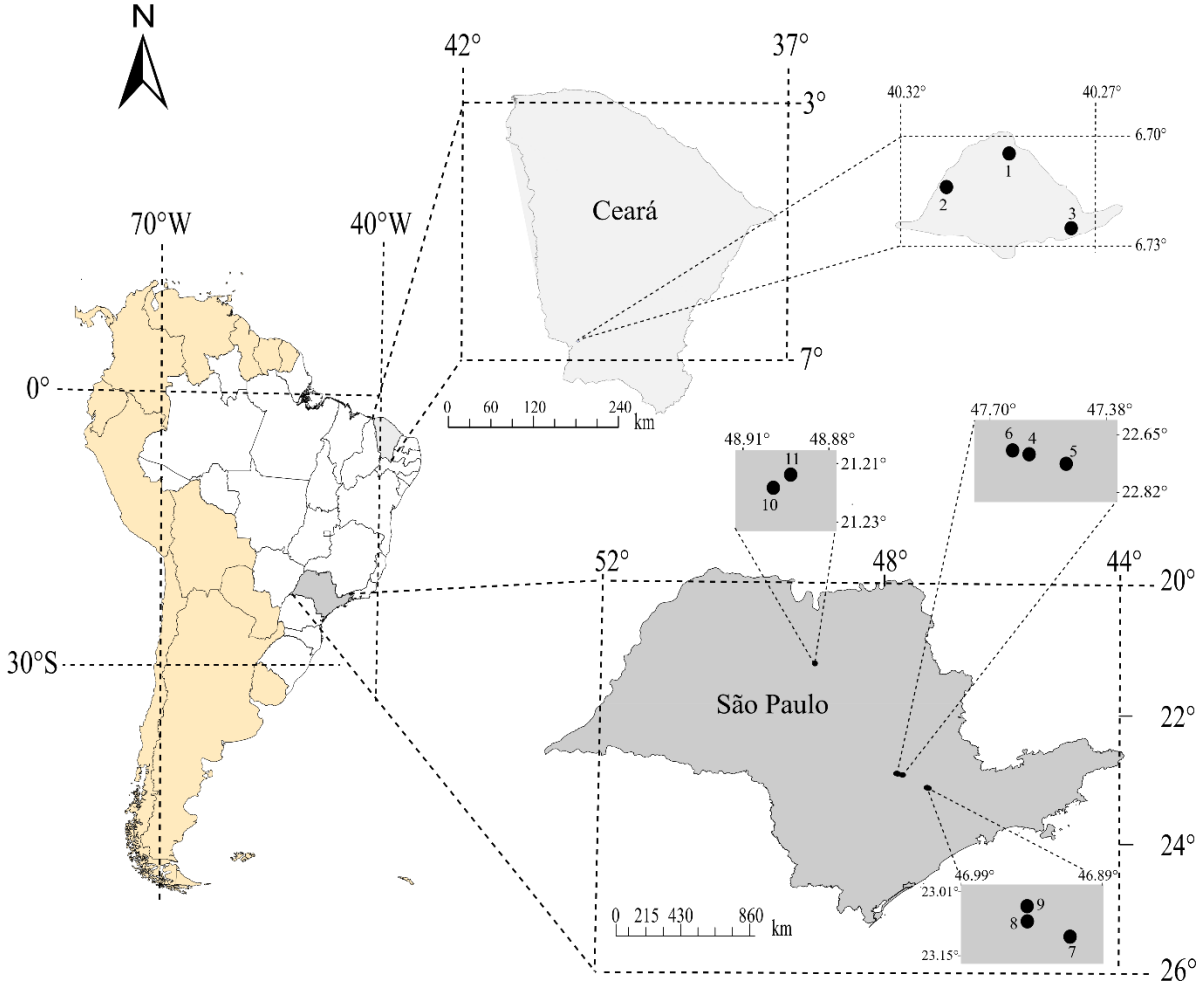

Figure 4.1 - Geographical location of the sampling sites, semiarid zone (1, 2 and 3); sub-humid tropical and subtropical zones (4 to 11)

Table 4.1 – General characteristics of the sampling sites

	Site #			
General characteristics	1, 2, 3	4, 5, 6	7, 8, 9	10, 11
Latitude	6.7° S	22.7° S	23.1° S	21.2° S
Average rainfall (mm y^{-1})	549	1300	1313	1258
Potential evapotranspiration - ETp (mm y^{-1})	2200	960	912	1094
Rainfall/ETp	0.25	1.35	1.44	1.15
Average temperature (ºC)				
annual	26.0	22.3	20.0	21.5
warmest month	28.0	25.3	22.0	23.8
coldest month	24.0	17.9	17.8	19.3
Vegetation type	Caatinga	Fallow	Orchard	Orchard
Climate classification (Köppen)	Bsh	Cwa	Cwa	Aw

Table 4.2 – Sampling sites, soil classification (IUSS, 2015), particle size distribution and texture class for sampled soil layers

	Sampling site #	Great Soil Group according to IUSS (2015)	Depth	Particle size fraction (kg kg^{-1}) Sand	Silt	Clay	Soil texture class
			m	0.05-2.0	0.002-0.05	<0.002	
				----------mm----------			
SEMIARID	1	Lixisol	0.00-0.20	0.38	0.51	0.11	Silt Loam
			0.20-0.40	0.40	0.47	0.13	Loam
			0.40-0.60	0.42	0.43	0.15	Loam
			0.60-0.80	0.45	0.40	0.15	Loam
	2	Luvisol	0.00-0.20	0.31	0.55	0.13	Silt Loam
			0.20-0.40	0.39	0.48	0.12	Loam
	3	Leptosol	0.00-0.20	0.62	0.31	0.07	Sandy Loam
			0.20-0.40	0.56	0.34	0.10	Sandy Loam
SUB-HUMID	4	Ferralsol	0.00-0.20	0.18	0.15	0.67	Clay
			0.20-0.40	0.08	0.10	0.82	Clay
	5	Nitisol	0.00-0.20	0.35	0.27	0.38	Clay Loam
			0.20-0.40	0.26	0.20	0.54	Clay
	6	Luvisol	0.00-0.20	0.20	0.18	0.62	Clay
			0.20-0.40	0.17	0.23	0.60	Clay
	7	Ferralsol	0.00-0.15	0.63	0.04	0.33	Sandy Clay Loam
			0.15-0.30	0.56	0.01	0.43	Sandy Clay
	8	Acrisol	0.00-0.30	0.67	0.18	0.15	Sandy Loam
			0.51-0.68	0.50	0.13	0.37	Sandy Clay
	9	Leptosol	0.40-0.60	0.62	0.12	0.26	Sandy Clay Loam
	10	Cambisol	0.56-0.72	0.77	0.04	0.19	Sandy Loam
	11	Acrisol	0.00-0.15	0.92	0.02	0.06	Fine Sand
			0.45-0.75	0.67	0.04	0.29	Sandy Clay Loam

4.2.3 Evaporation experiments

To determine the unsaturated hydraulic properties for each soil layer, laboratory evaporation experiments were performed. Six rings (0.10 m high and internal diameter 0.145 m) were filled with air-dried and sieved soil material and then slowly saturated with water by capillarity from bottom to top. After wetting, the bottom side was sealed. Two or three days later, three polymer tensiometers were horizontally inserted in the sample through drilled holes with centers at 25, 50 and 75 mm vertical distance from the sample surface. The used tensiometer type measures in the range from -165 m to -1 m with an accuracy of approximately 0.2 m (BAKKER et al., 2006; VAN DER PLOEG et al., 2008). Each ring equipped with three tensiometers was placed on a precision balance (capacity 8.5 kg and resolution 10^{-4} kg).

Measurements of ring sample weight and pressure heads were automatically logged every 10 min. The evaporation experiment was finished when the upper tensiometer reached a pressure head value below -165 m, which took in the order of 3 weeks. At the end of the measurement, the final water content of the soil sample was determined by oven drying at 105 °C.

4.2.4 Inverse solution

Soil hydraulic parameters were obtained from soil evaporation and pressure head measurements by an inverse one-dimensional solution using Hydrus-1D (ŠIMUNEK et al., 2008). The unsaturated soil hydraulic properties were assumed to be defined by *K*-*θ*-*h* relations described by the Van Genuchten-Mualem model (1980):

$$\Theta = \left[1 + |\alpha h|^{n}\right]^{(1/n)-1} \tag{4.13}$$

$$K = K_s \Theta^{\lambda} \left[1 - \left(1 - \Theta^{n/(n-1)}\right)^{1-(1/n)}\right]^2 \tag{4.14}$$

with $\Theta = (\theta - \theta_r)/(\theta_s - \theta_r)$; θ, θ_r and θ_s are water content, residual water content and saturated water content ($m^3\ m^{-3}$), respectively; h is pressure head (m), K and K_s are hydraulic conductivity and saturated hydraulic conductivity, respectively ($m\ d^{-1}$); and α (m^{-1}), n and λ are fitting parameters.

The water flow boundary conditions were set in terms of: (i) surface evaporation flux for each time interval calculated from observed mass difference over a time interval; (ii) pressure heads measured at the three depths over time and the final soil water content. An inverse solution was obtained using Hydrus-1D for each replicate (ring); therefore, for each replicate a set of hydraulic parameters was estimated. To obtain a single set of hydraulic parameters for each soil layer, for each replicate 10 pressure head values in the range of the observed readings (from -165 to -1.5 m) were selected and respective water content and unsaturated hydraulic conductivity were calculated. These data, for all replicates together, were then processed using RETC software (VAN GENUCHTEN et al., 1991) to generate a unique hydraulic parameter set for each soil layer.

4.2.5 Simulation scenarios to estimate M_{lim}

In order to assess the water supply capacity of the investigated soil layers for soils from both climatic regions, we assumed the existence of a vegetation with a vertical root distribution according to Equation (4.15), as proposed by Schenk and Jackson (2002):

$$r_D = \frac{R_{\max}}{\left[1+\left(\frac{D}{D_{50}}\right)^{c}\right]} \tag{4.15}$$

where: r_D (m) is the cumulative amount of roots above profile depth D (m), R_{max} (m) is the total root length in the soil profile, D_{50} is the depth (m) at which $r_D = 0.5R_{max}$, and c is a dimensionless shape-parameter. To calculate the vertical root distribution, we used the parameterization corresponding to a *tropical semi-deciduous and deciduous forest* as listed in table 4 of Schenk and Jackson (2002). In order to match an R_{mean} of 1000 m m^{-3} over a soil profile of 1 m depth, the corresponding R_{max} of 4142 m m^{-3} was assumed for all soils. The adopted mean root length density of a 1000 m m^{-3} was based on average values over rooted zone for different crops types presented by De Willigen and Van Noordwijk (1987).

Limiting hydraulic conditions were evaluated by calculating the value h_{lim} based on M_{lim} using optimized Van Genuchten hydraulic functions for evapotranspiration rates in the range between 0.5 and 6 mm d^{-1}. Two values for the limiting root water potential (h_w) were used: the commonly employed value of -150 m (e.g. DE JONG VAN LIER et al., 2006; JAVAUX et al., 2008; and many others) and a more negative value h_w = -300 m. In this way, insight was obtained in the sensitivity of results to the value of h_w, and whether soil hydraulic properties allow significant water flow at soil pressure heads more negative than -150 m.

Equation (4.15) was used to evaluate all soils under a similar scenario of water demand and root uptake. For the Caatinga biome in the semiarid zone, however, (soils 1, 2 and 3), root length density measurements were carried out by Pinheiro et al. (2016). Therefore, in addition to root length density profiles obtained using eq. (4.15), we also evaluated a scenario using the experimentally observed root length densities for the semiarid zone.

4.3 Results and Discussion

4.3.1 Soil hydraulic parameter estimation

Estimated hydraulic parameter for all analyzed soil layers are given in Table 4.3. Land use and vegetation type play an important role in the formation of soil structure; they mainly affect macroporosity and soil hydraulic properties at and near saturation (GONZALEZ-SOSA et al., 2012; JARVIS et al., 2013; WANG et al., 2013). In our experiment, samples were sieved and natural macrostructure was destroyed. Therefore, the effect of land use and vegetation type on soil hydraulic properties cannot be evaluated by our methodology. On the other hand, as it was our purpose to evaluate soil water availability determined by soil hydraulic properties for the dry water content range, these are not expected to be affected by macrostructural properties (BITTELLI; FLURY, 2009; CRESSWELL et al., 2008; TULI et al., 2005).

Table 4.3 - Optimized Van Genuchten-Mualem parameters (Eq. [4.13] and [4.14]) for soils from the Brazilian semiarid zone (soils 1-3), and from the Brazilian sub-humid zone (soils 4-11) together with their coefficient of determination (R^2)

	Sampling site #	Great Soil Group IUSS (2015)	Depth	α	n	θ_r	θ_s	K_s	λ	R^2
			m	m^{-1}	-	-----m^3 m^{-3}-----		m d^{-1}	-	-
SEMIARID	1	Lixisol	0.00-0.20	0.195	1.752	0.053	0.242	0.339	0.974	0.85
			0.20-0.40	0.171	1.633	0.033	0.200	0.363	1.851	0.93
			0.40-0.60	0.081	2.041	0.087	0.196	0.752	2.466	0.96
			0.60-0.80	0.042	1.796	0.116	0.194	0.008	1.468	0.60
	2	Luvisol	0.00-0.20	0.177	1.436	0.023	0.258	0.147	1.916	0.71
			0.20-0.40	0.243	1.828	0.061	0.259	0.187	0.787	0.92
	3	Leptosol	0.00-0.20	0.086	1.653	0.034	0.096	0.020	3.029	0.77
			0.20-0.40	0.602	1.444	0.031	0.110	3.010	2.691	0.95
SUB-HUMID	4	Ferralsol	0.00-0.20	1.615	1.223	0.055	0.202	0.0004	17.67	0.64
			0.20-0.40	3.575	1.239	0.048	0.324	0.014	2.633	0.60
	5	Nitisol	0.00-0.20	4.832	1.348	0.152	0.319	0.123	10.41	0.99
			0.20-0.40	1.982	1.268	0.061	0.420	0.0052	-0.645	0.89
	6	Luvisol	0.00-0.20	12.506	1.404	0.068	0.377	0.0081	1.414	0.82
			0.20-0.40	1.965	1.205	0.094	0.368	0.0018	3.204	0.75
	7	Ferralsol	0.00-0.15	3.031	1.249	0.075	0.235	0.0033	6.964	0.60
			0.15-0.30	3.276	1.185	0.075	0.353	0.0110	7.930	0.58
	8	Acrisol	0.00-0.30	4.949	1.381	0.103	0.300	0.0217	0.612	0.81
			0.51-0.68	1.979	1.385	0.031	0.219	0.0105	0.004	0.98
	9	Leptosol	0.40-0.60	1.868	1.290	0.078	0.327	0.0028	0.018	0.96
	10	Cambisol	0.56-0.72	1.280	1.168	0.109	0.203	0.0002	27.19	0.73
	11	Acrisol	0.00-0.15	1.637	1.189	0.029	0.194	0.00001	10.53	0.77
			0.45-0.75	8.365	1.565	0.141	0.212	0.03060	3.221	0.96

The measured range of pressure heads during the evaporation experiment was different among samples. Soils from the semiarid zone were analyzed from -10 m to -165 m, whereas sub-humid zone soils allowed analysis from -1.5 m to -165 m. The upper limit of these ranges matches the conditions when the flow in the sample rings was strictly upward, the difference between both groups of soils is probably related to their distinct pore geometry. Dealing with sieved material, the >2 mm soil structure is destroyed, but most of the smaller structure elements, very important in weathered tropical soils, are maintained.

As stressed by Simunek et al. (1998), as long as independent measured information from the analyzed range is not included in the optimization process, extrapolation beyond the range of measurement is associated with a high level of uncertainty. Considering this, the optimized values for saturated conditions (θ_s and K_s) are merely fitting parameters for equations (4.13) and (4.14) and do not correspond to values measured at saturation.

The λ parameter from eq. 4.14 is related to tortuosity and connectivity of the pore space, but its exact physical meaning is unclear (VOGEL, 2000). A higher λ leads to a faster reduction of K with decreasing Θ (eq. 4.14). For the analyzed soils, λ ranged from -0.65 to 27.2 (Table 4.3), showing the arbitrariness of the commonly used value ($\lambda = 0.5$) obtained in a fitting procedure performed by Mualem (1976) on a set of 45 soils. Predictions of K are especially sensitive to λ in the dry range, making its correct determination of utmost importance in plant water availability studies. The average λ ± standard deviation for the semiarid zone soils was 1.9 ± 0.8, for the sub-humid zone soils the value was 6.5 ± 7.9.

4.3.2 Limiting pressure head

The limiting pressure head h_{lim} (the bulk soil pressure head at the onset of the falling-rate phase) calculated from M_{lim} is lower in the semiarid zone soils (soils 1-3) than in sub-humid zone soils 4-11 (Table 4.4), suggesting that hydraulic properties of soils from the semiarid ecosystem allow root water uptake at a potential rate under a wider range of soil pressure heads. The smaller values of λ, on average, in the soils from the semiarid zone (Table 4.3) imply in higher values of K under dry conditions, affecting directly the matric flux potentials used to evaluate h_{lim}. To illustrate the magnitude of this effect, Table 4.4 shows values of K at h_w = -150 m (K_{150}) and at -300 m (K_{300}) calculated using eq. 4.13 and 4.14. Whereas K_{150} for the semiarid zone soils are of the order 10^{-7} to 10^{-9} m d^{-1}, in the sub-humid zone soils this range is between 10^{-10} and 10^{-22} m d^{-1}. Semiarid zone soils show a coarser texture than sub-humid zone soils (Table 4.2). In addition, according to Klein at al. (2014b), coarse layers are the major water source for plant transpiration during dry periods whereas soils with higher clay content hold a large amount of non-transpirable water.

Table 4.4 – Hydraulic conductivities K_{150} at h_w = -150 m and K_{300} at h_w = -300 m together with hydraulic conditions (h_{lim} [m] and Θ_{lim} [m^3 m^{-3}]) at the onset of the falling rate phase calculated for R_{max} = 4142 m m^{-3} and T_p = 6 mm d^{-1} and for limiting root water potentials (h_w) of -150 m and -300 m for all layers of the evaluated soils

Climatic zones	Sampling sites	Great Soil Group IUSS (2015)	Depth	K_{150}	K_{300}	$h_{lim,\ 150}$	$h_{lim\ 300}$	$\Theta_{lim,\ 150}$	$\Theta_{lim,\ 300}$
			m	---m d^{-1}---		---m---		---m^3 m^{-3}---	
SEMIARID	1	Lixisol	0.00-0.20	$3.8 \cdot 10^{-8}$	$2.0 \cdot 10^{-9}$	-78	-81	0.13	0.12
			0.20-0.40	$3.0 \cdot 10^{-8}$	$1.4 \cdot 10^{-9}$	-75	-77	0.21	0.20
			0.40-0.60	$1.2 \cdot 10^{-8}$	$1.2 \cdot 10^{-10}$	-77	-77	0.15	0.15
			0.60-0.80	$2.4 \cdot 10^{-7}$	$9.3 \cdot 10^{-9}$	-118	-135	0.27	0.25
	2	Luvisol	0.00-0.20	$7.0 \cdot 10^{-8}$	$5.4 \cdot 10^{-9}$	-84	-90	0.31	0.30
			0.20-0.40	$7.2 \cdot 10^{-9}$	$3.7 \cdot 10^{-10}$	-47	-47	0.13	0.13
	3	Leptosol	0.00-0.20	$4.0 \cdot 10^{-9}$	$1.1 \cdot 10^{-10}$	-49	-49	0.38	0.38
			0.20-0.40	$2.9 \cdot 10^{-9}$	$1.7 \cdot 10^{-10}$	-33	-33	0.26	0.26
SUB-HUMID	4	Ferralsol	0.00-0.20	$7.9 \cdot 10^{-21}$	$9.4 \cdot 10^{-23}$	>-1.5*	>-1.5	>0.83	>0.32
			0.20-0.40	$1.7 \cdot 10^{-12}$	$2.0 \cdot 10^{-13}$	>-1.5	>-1.5	>0.71	>0.71
	5	Nitisol	0.00-0.20	$7.1 \cdot 10^{-21}$	$8.9 \cdot 10^{-23}$	>-1.5	>-1.5	>0.56	>0.56
			0.20-0.40	$3.3 \cdot 10^{-10}$	$6.5 \cdot 10^{-11}$	-2.0	-2.0	0.69	0.69
	6	Luvisol	0.00-0.20	$5.9 \cdot 10^{-15}$	$5.7 \cdot 10^{-16}$	>-1.5	>-1.5	>0.36	>0.36
			0.20-0.40	$1.4 \cdot 10^{-12}$	$1.6 \cdot 10^{-13}$	>-1.5	>-1.5	>0.81	>0.81
	7	Ferralsol	0.00-0.15	$7.3 \cdot 10^{-16}$	$3.9 \cdot 10^{-17}$	>-1.5	>-1.5	>0.72	>0.72
			0.15-0.30	$1.3 \cdot 10^{-14}$	$8.9 \cdot 10^{-16}$	>-1.5	>-1.5	>0.77	>0.77
	8	Acrisol	0.00-0.30	$4.2 \cdot 10^{-12}$	$5.3 \cdot 10^{-13}$	>-1.5	>-1.5	>0.68	>0.68
			0.51-0.68	$1.1 \cdot 10^{-10}$	$1.7 \cdot 10^{-11}$	-2.0	-2.0	0.61	0.61
	9	Leptosol	0.40-0.60	$6.7 \cdot 10^{-11}$	$1.1 \cdot 10^{-11}$	>-1.5	>-1.5	>0.77	>0.77
	10	Cambisol	0.56-0.72	$7.5 \cdot 10^{-22}$	$6.3 \cdot 10^{-24}$	>-1.5	>-1.5	>0.88	>0.88
	11	Acrisol	0.00-0.15	$9.2 \cdot 10^{-18}$	$4.5 \cdot 10^{-19}$	>-1.5	>-1.5	>0.85	>0.85
			0.45-0.75	$1.8 \cdot 10^{-18}$	$6.0 \cdot 10^{-20}$	>-1.5	>-1.5	>0.30	>0.30

* Limiting pressure head (h_{lim}) higher than -1.5 m

To what extent plants are able to sustain the water demand of their shoot depends on the hydraulic properties of the soil-root system. As long as root system conductance is large enough, root system geometry and root hydraulic properties have a low impact on water uptake. The ability of the soil to keep water flowing towards the roots is then predominantly determined by the soil hydraulic properties (DE JONG VAN LIER et al., 2013; LOBET et al., 2014). As the rhizosphere is highly susceptible to a local drop in hydraulic conductivity (LOBET et al., 2014), a lower limiting soil pressure head will allow plants to withstand a wider range of water content with a lower risk of hydraulic failure due to embolism or cavitation triggered by a soil water potential below a species-specific threshold (CHOAT et al., 2012; KLEIN et al., 2014a). This would allow plants to withstand adverse scenarios of soil drought.

Comparing the calculated values of h_{lim} for h_w= -150 and h_w= -300 m, differences were very small and did not represent a significant increase in soil water availability. These values show the low sensitivity of available water to the lower limiting pressure head, analogous to the low sensitivity of the permanent wilting point to the corresponding pressure head (e.g., SAVAGE et al., 1996). It is therefore suggested that, in order for a vegetation to adapt to dry soils without capillary rise from a water table, natural vegetation is more likely to invest in shallower and denser root systems and in the enforcement of stomatal closure, but not in structures that allow a reduction of the lower suction limit in root tissues (CASTELLANOS et al., 1991; KLEIN et al., 2014b). The optimal strategy under capillary rise scenarios is not answerable by this theory.

4.3.3 Limiting soil pressure head for semiarid zone soils based on in situ measurements of root length density

Although the bulk RLD measurements carried out in this research for the Caatinga biome do not exclusively represent active fine roots (roots able to conduct water), the values measured were higher (Table 4.5) than those used in the previous scenario.

Table 4.5 – Limiting soil pressure head h_{lim} (m) at the onset of the falling rate phase for the Caatinga biome using measured root length densities associated with a transpiration rate of 6 mm d^{-1}

Sampling sites	Great Soil Group IUSS (2015)	Depth (m)	RLD (m m^{-3})	$h_{lim,150}$	$h_{lim,300}$	$\Theta_{lim,150}$	$\Theta_{lim,300}$
				m		m^3 m^{-3}	
1	Lixisol	0.00-0.20	$3.7 \cdot 10^3$	-99	-108	0.11	0.10
		0.20-0.40	$2.8 \cdot 10^3$	-95	-101	0.17	0.16
		0.40-0.60	$2.0 \cdot 10^3$	-91	-92	0.12	0.12
		0.60-0.80	$1.6 \cdot 10^3$	-134	-173	0.25	0.20
2	Luvisol	0.00-0.20	$4.1 \cdot 10^3$	-97	-109	0.29	0.27
		0.20-0.40	$1.8 \cdot 10^3$	-55	-56	0.12	0.12
3	Leptosol	0.00-0.20	$2.8 \cdot 10^3$	-53	-53	0.36	0.36
		0.20-0.40	$1.8 \cdot 10^3$	-36	-37	0.25	0.25

Analyzing the h_{lim} of the soils from semiarid zone for transpiration rates ranging from 0.5 to 6.0 mm d^{-1}, h_{lim} ranged from -36 to -148 m (Figure 4.2).

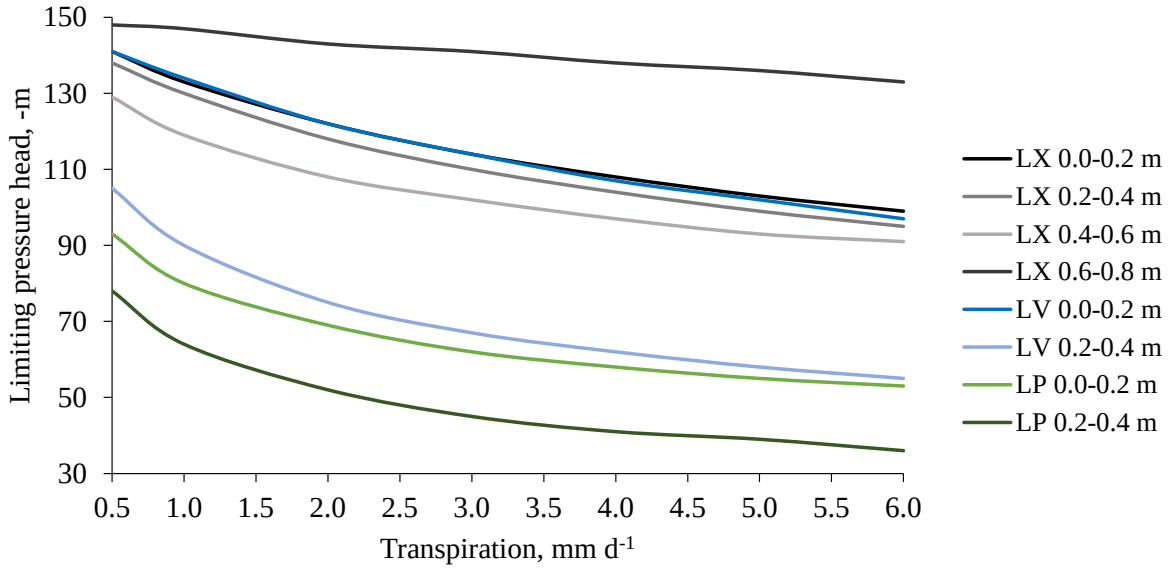

Figure 4.2 – Limiting soil pressure head estimated from M_{lim} over a range of transpiration for soils from semiarid zone. The acronyms LX, LV and LP mean Lixisol (soil 1), Luvisol (soil 2) and Leptosol (soil 3), respectively

As observed by de Jong van Lier et al. (2006), in the case of a high RLD the root pressure head remains similar to the bulk pressure head in the surrounding soil since the flux density toward the root surface to meet the transpiration rate is small compared to a scenario with low RLD. Therefore, hydraulic gradients to meet water demand will be smaller and h_{lim} corresponds to a drier bulk soil condition. The semiarid Leptosol with the lowest RLD and the shallowest rooting depth of Caatinga samples (PINHEIRO; COSTA; DE ARAÚJO, 2013) has the highest h_{lim}, making the vegetation growing on this soil more susceptible to drought stress. In addition to high RLD (Table 4.5), the Caatinga biome typically develops shallow roots (PINHEIRO; COSTA; DE ARAÚJO, 2013) and, according to an earlier study, these shallow root systems may allow to maximize uptake of ephemeral pulses of water in the upper soil layers (PINHEIRO et al., 2016). The concept of pulse water availability of short duration for arid regions has been reported, e.g., by Lauenroth et al. (2014), Reynolds et al. (2000), Sala and Lauenroth (1982) and Williams et al. (2009).

Klein et al. (2014b) found that variability of hydraulic properties with soil depth plays an important role in water availability for plants, particularly in water-limited ecosystems. Table 4.5 and Figure 4.2 suggest that for the Caatinga biome the surface layer allows root water uptake to occur at lower (more negative) water potentials than in deeper layers. This supports the idea that the surface layer is the most important layer regarding water availability in the Caatinga biome for several reasons: it receives ephemeral pulses of rainfall; it contains the highest root length density; and it shows the most favorable hydraulic properties for water

flow to plant roots. These results corroborate an earlier study carried out for the same Caatinga forest, where the upper layer supplied up to 90% of the total water requirement (PINHEIRO et al., 2016). Other authors have also found transpiration to be controlled by soil water content of the surface layer (GAINES et al., 2015; KLEIN et al., 2014b; LIU et al., 2011; RAZ-YASEEF et al., 2012).

Similar to results discussed before, when considering h_w= -300 m instead of -150 m, only a slight decrease in h_{lim} is observed, corresponding to a minimal increase in transpirable water for forest survival. According to Klein et al. (2014a), the remarkable changes in hydraulic properties among soil types that are mostly independent of the forest biome type, introduce additional variation among forests in terms of their susceptibility to soil drought. Many plant strategies can be recognized in the Caatinga biome, which allow the vegetation to cope with low soil-water ranges, e.g. spreading of shallow roots, reduced leaf area and shedding of leaves (PINHEIRO et al., 2016; PINHEIRO; COSTA; DE ARAÚJO, 2013). There are indications that the ability of woody plants to survive and recover from periods of sustained drought is strongly related to their resistance to embolism (CHOAT et al., 2012). Possibly, some strategy regarding hydraulic failure, i.e. protection of the xylem from extensive embolism, may then be part of Caatinga species strategy. However, our results suggest that soil hydraulic properties allowing maintenance of water supply to plants under low soil pressure heads is also a very important feature in determining establishment and survival of plants in the Caatinga biome.

4.4 Conclusions

Using measured soil hydraulic properties of Brazilian soils from different climate zones under unsaturated conditions to determine a limiting matric flux potential of total crop water availability we conclude that:

1. Given characteristic rooting density patterns, the matric flux potential approach extended to multi-layer scenarios allows to identify soil hydraulic vulnerability for different ecosystems, identifying climate zones that are likely to be more harmed by water shortage enhanced by soil drought.

2. Soils from the Brazilian semiarid zone are able to deliver water to plants under a wide range of soil-water content, with limiting pressure heads between -36 and -148 m. In contrast, in the used experimental setup, soils from the sub-humid zone showed stronger hydraulic restrictions for supplying transpirable water.

3. For the analyzed soils, a negligible increase in available water results from decreasing the root water potential (h_w) below -150 m. It is generally suggested that species in semiarid ecosystems are adapted to allow lower root water potentials, but our results indicate that this would not be an efficient evolutionary adaptation.

References

BAKKER, G.; VAN DER PLOEG, M.J.; DE ROOIJ, G.H.; HOOGENDAM, C.W.; GOOREN, H.P.A.; HUISKES C.; KOOPAL, L.K.; KRUIDHOF, H. New polymer tensiometers: measuring matric pressures down to the wilting point. **Vadose Zone Journal**, Madison, v. 6, n. 1, p. 196-202, 2007.

BITTELLI, M.; FLURY, M. Errors in water retention curves determined with pressure plates. **Soil Science Society of America Journal**, Madison, v. 73, n. 5, p. 1453-1460, 2009.

CASTELLANOS, J.; MAASS, M.; KUMMEROW, J. Root biomass of a dry tropical forest in Mexico. **Plant and Soil**, Dordrecht, v. 131, n. 131, p. 225-228, 1991.

CHOAT, B.; JANSEN, S.; BRODRIBB, T.J.; COCHARD, H.; DELZON, S.; BHASKAR, R.; BUCCI, S.J.; FEILD, T.S.; GLEASON, S.M.; HACKE, U.G.; JACOBSEN, A.L.; LENS, F.; MAHERALI, H.; MARTÍNEZ-VILALTA, J.; MAYR, S.; MENCUCCINI, M.; MITCHELL, P.J.; NARDINI, A.; PITTERMANN, J.; PRATT, R.B.; SPERRY, J.S.; WESTOBY, M.; WRIGHT, I.J.; ZANNE, A.E. Global convergence in the vulnerability of forests to drought. **Nature**, London, v. 491, p. 752–755, 2012.

CRESSWELL, H.P.; GREEN, T.W.; MCKENZIE, N.J. The adequacy of pressure plate apparatus for determining soil water retention. **Soil Science Society of America Journal**, Madison, v. 72, n. 1, p. 41-49, 2008.

DE ARAÚJO J.C.; GÜNTNER, A.; BRONSTERT, A. Loss of reservoir volume by sediment deposition and its impact on water availability in semiarid Brazil. **Hydrological Sciences Journal**, Wallingford, v. 51, n. 1, p. 157-170, 2006.

DE JONG VAN LIER, Q.; DOURADO NETO, D.; METSELAAR, K. Modeling of transpiration reduction in Van Genuchten–Mualem type soils. **Water Resources Research**, Washington, v. 45, n. 2, p. 1-9, 2009.

DE JONG VAN LIER, Q.; METSELAAR, K.; VAN DAM, J.C. Root water extraction and limiting soil hydraulic conditions estimated by numerical simulation. **Vadose Zone Journal**, Madison, v. 5, n. 4, p. 1264–1277, 2006.

DE JONG VAN LIER, Q.; VAN DAM, J.C.; DURIGON, A.; DOS SANTOS, M.A.; METSELAAR, K. Modeling water potentials and flows in the soil-plant system comparing hydraulic resistances and transpiration reduction functions. **Vadose Zone Journal**, Madison, v. 12, n. 3, p. 1-20, 2013.

DE WILLIGEN, P.; VAN NOORDWIJK, M. **Roots, plant production and nutrient use efficiency**. 1987. 282 p. Thesis (PhD) - Wageningen University, 1987.

DOMEC, J.C.; KING, J.S.; NOORMETS, A.; TREASURE, E.; GAVAZZI, M.J.; SUN, G.; MCNULTY, S.G. Hydraulic redistribution of soil water by roots affects whole-stand evapotranspiration and net ecosystem carbon exchange. **New Phytologist,** Malden, v. 187, p. 171–183, 2010.

DURIGON, A.; GOOREN, H.P.A.; DE JONG VAN LIER, Q.; METSELAAR, K. Measuring hydraulic conductivity to wilting point using polymer tensiometers in an evaporation experiment. **Vadose Zone Journal**, London, v. 10, n. 2, p. 741–746, 2011.

GAINES, K.P.; STANLEY, J.W.; MEINZER, F.C.; MCCULLOH, K.A.; WOODRUFF, D.R.; CHEN, W.; ADAMS, T.S.; LIN, H.; EISSENSTAT, D.M. Reliance on shallow soil water in a mixed-hardwood forest in central Pennsylvania. **Tree Physiology**, Oxford, v. 00, p. 1-15, 2015.

GARDNER, W.R.; MIKLICH, F.J. Unsaturated conductivity and diffusivity measurements by a constant flux method. **Soil Science**, Philadelphia, v. 93, n. 4, p. 271–274, 1962.

GONZALEZ-SOSA, E.; BRAUD, I.; DEHOTIN, J.; LASSABATÈRE, L.; ÂNGULO-JARAMILLO, R.; LAGOUY, M.; BRANGER, F.; JACQUEMINET, C.; KERMADI, S.; MICHEL, K. Impact of land use on the hydraulic properties of the topsoil in a small French catchment. **Hydrological Processes**, Chichester, v. 24, n. 17, p. 2382–2399, 2010.

GRANT, C.D.; GROENEVELT, P.H. Weighting the differential water capacity to account for declining hydraulic conductivity in a drying coarse-textured soil. **Soil Research**, Sidney, v. 53, n. 4, p. 386–391, 2015.

IDEN, S.C.; PETERS, A.; DURNER, W. Improving prediction of hydraulic conductivity by constraining capillary bundle models to a maximum pore size. **Advances in Water Resources**, Oxford, v. 85, p. 86-92, 2015.

IUSS WORKING GROUP WRB. **World Reference Base for Soil Resources 2014:** international soil classification system for naming soils and creating legends for soil maps. Rome: FAO, 2015. 203 p. (FAO. World Soil Resources Reports, 106).

JARVIS, N.; KOESTAL, J.; MESSING, I.; MOEYS, J.; LINDAHL, A. Influence of soil, land use and climatic factors on the hydraulic conductivity of soil. **Hydrology And Earth System Sciences**, Gottingen, v. 17, p. 5185–5195, 2013.

JAVAUX, M.; SCHRÖDER, T.; VANDERBORGHT, J.; VEREECKEN, H. Use of a three-dimensional detailed modeling approach for predicting root water uptake. **Vadose Zone Journal**, London, v. 7, n. 3, p. 1079-1088, 2008.

KLEIN, T.; YAKIR, D.; BUCHMANN, N.; GRÜNZWEIG, J.M. Towards an advanced assessment of the hydrological vulnerability of forests to climate change-induced drought **New Phytologist**, Malden, v. 201, n. 3, p. 712-716, 2014a.

KLEIN, T.E.; ROTENBERG, E.; COHEN-HILALEH, E.; RAZ-YASEEF, N.; TATARINOV, F.; PREISLER, Y.; OGÉE, J.; COHEN, S.; YAKIR, D. Quantifying transpirable soil water and its relations to tree water use dynamics in a water-limited pine forest. **Ecohydrology**, Hoboken, v. 7, n. 2, p. 409–419, 2014b

LAUENROTH, W.K.; SCHLAEPFER, D.R.; BRADFORD, J.B. Ecohydrology of dry regions: storage versus pulse soil water dynamics. **Ecosystems**, New York, v. 17, n. 8, p. 1469–1479, 2014.

LIU, Y.; XU, Z.; DUFFY, R.; CHEN, W.; AN, S.; LIU, S.; LIU, F. Analyzing relationships among water uptake patterns, rootlet biomass distribution and soil water content profile in a subalpine shrubland using water isotopes. **European Journal of Soil Biology**, Paris, v. 47, p. 380–386, 2011. doi:10.1016/j.ejsobi.2011.07.012.

LOBET, G.; COUVREUR, V.; MEUNIER, F.; JAVAUX, M.; DRAYE, X. Plant water uptake in drying soils. **Plant physiology**, Rockville, v. 164, p. 1619-1627, 2014.

MARENGO, J.A.; CHOU, S.C.; KAY, G.; ALVES, L.M.; PESQUERO, J.F.; SOARES, W.R.; SANTOS, D.C.; LYRA, A.A.; SUEIRO, G.; BETTS, R.; CHAGAS, D.J.; GOMES, J.L.; BUSTAMENTE, J.F.; TAVARES, P. Development of regional future climate change scenarios in South America using the Eta CPTEC/HadCM3 climate change projections: climatology and regional analyses for the Amazon, São Francisco and the Paraná River basins. **Climate Dynamics**, New York, v. 38, n. 9, p. 1829–1848, 2012.

MUALEM, Y. A new model for predicting the hydraulic conductivity of unsaturated porous media. **Water Resources Research**, Washington, v. 12, n. 3, p. 513-522, 1976.

PINHEIRO, E.A.R.; COSTA, C.A.G.; DE ARAÚJO, J.C. Effective root depth of the Caatinga biome. **Journal of Arid Environments**, London, v. 89, p. 1-4, 2013.

PINHEIRO, E.A.R.; METSELAAR, K.; DE JONG VAN LIER, Q.; DE ARAÚJO, J.C. Importance of soil water to the Caatinga biome, Brazil. **Ecohydrology**, Hoboken, 2016. In press.

PULLAN, A.J. The quasilinear approach for unsaturated porous media flow. **Water Resources Research**, Washington, v. 26, n. 6, p. 1219–1234, 1990.

RAATS, P.A.C. Laterally confined, steady flows of water from sources and to sinks in unsaturated soils. **Soil Science Society of America Journal**, Madison, v. 41, n. 2, p. 294–304, 1977.

_____. Uptake of water from soils by plant roots. **Transport in Porous Media**, New York, v. 68, n. 1, p. 5-28, 2007.

RAZ-YASEEF, N.; YAKIR, D.; SCHILLER, G.; COHEN, S. Dynamics of evapotranspiration partitioning in a semi-arid forest as affected by temporal rainfall patterns. **Agricultural and forest meteorology**, Amsterdam, v. 157, p. 77-85, 2012.

REYNOLDS, J.F.; KEMP, P.R.; TENHUNEN, J.D. Effects of long-term rainfall variability on evapotranspiration and soil water distribution in the Chihuahuan Desert: a modeling analysis. **Plant Ecology**, Dordrecht, v. 150, n. 1, 145–59, 2000.

SALA, O.E.; LAUENROTH, W.K. Small rainfall events: an ecological role in semiarid regions. **Oecologia**, New York, v. 53, n. 3, p. 301–304, 1982.

SAVAGE, M.J.; RITCHIE, J.T.; BLAND, W.L.; DUGAS, W.A. Lower limit of soil water availability. **Agronomy Journal**, Madison, v. 88, n. 4, p. 844-651, 1996.

SCHENK, H.J.; JACKSON, R.B. The global biogeography of roots. **Ecological Monographs**, Washington, v. 72, n. 3, p. 311-328, 2002.

SENEVIRATNE, S.I.; NICHOLLS, N.; EASTERLING, D.; , GOODESS, C.M.; KANAE, S.; KOSSIN, J.; LUO, Y.; MARENGO, J.; MCINNES, K.; RAHIMI, M.; REICHSTEIN, M.; SORTEBERG, A.; VERA, C.; ZHANG, X. Changes in climate extremes and their impacts on the natural physical environment. In: FIELD, C.B., BARROS, V.; STOCKER, T.F.; QIN, D.; DOKKEN, D.J.; EBI, K.L.; MASTRANDREA, M.D.; MACH, K.J.; PLANTTNER, G.-K, ALLEN, S.K.; TIGNOR, M.; MIDGLEY, P.M. (Ed.). **Managing the risks of extreme events and disasters to advance climate change adaptation:** a special report of Working Groups I and II of the Intergovernmental Panel on Climate Change (IPCC). Cambridge; New York: Cambridge University Press, 2012. p. 109-230.

ŠIMŮNEK, J.; VAN GENUCHTEN, M. TH.; ŠEJNA, M. Development and applications of the HYDRUS and STANMOD software packages and related codes. **Vadose Zone Journal**, Madison, v. 7, n. 2, p. 587-600, 2008.

ŠIMŮNEK, J.; WENDROTH, O.; VAN GENUCHTEN, M. TH. Parameter estimation analysis of the evaporation method for determining soil hydraulic properties. **Soil Science Society of America Journal**, Madison, v. 62, n. 4, p. 894–905, 1998.

TULI, A.; HOPMANS, J.W.; ROSLTON, D.E.; MOLDRUP, P. Comparison of air and water permeability between disturbed and undisturbed soils. **Soil Science Society of America Journal**, Madison, v. 69, n. 5, p. 1361-1371, 2005.

VAN DER PLOEG, M.J.; GOOREN, H.P.A.; BAKKER, G.; DE ROOIJ, G.H.. 2008. Matric potential measurements by polymer tensiometers in cropped lysimeters under water-stressed conditions. **Vadose Zone Journal**, Madison, v. 7, n. 3, p. 1048–1054, 2008.

VAN GENUCHTEN, M.TH. A closed-form equation for predicting the hydraulic conductivity of unsaturated soils. **Soil Science Society of America Journal**, Madison, v. 44, n. 5, 892-898, 1980.

VAN GENUCHTEN, M. TH.; LEIJ, F. J.; YATES, S. R. **The RETC code for quantifying the hydraulic functions of unsaturated soils**: version 1.0. Robert S. Riverside: Kerr Environmental Research Laboratory, 1991. 8 p. (EPA Report, 600/2-91/065).

VOGEL, H.J. A numerical experiment on pore size, pore connectivity, water retention, permeability, and solute transport using network models. **European Journal of Soil Science**, Malden, v. 51, n. 1, p. 99-105, 2000.

WANG, Y.; SHAO, M.; LIU, Z.; HORTON, R. Regional-scale variation and distribution patterns of soil saturated hydraulic conductivities in surface and subsurface layers in the loessial soils of China. **Journal of Hydrology**, Amsterdam, v. 487, p. 13–23, 2013.

WENDROTH, O.; EHLERS, W.; HOPMANS, J.W.; KAGE, H.; HALBERTSMA, J.; WÖSTEN, J.H.M. Reevaluation of the evaporation method for determining hydraulic functions in unsaturated soils. **Soil Science Society of America Journal**, Madison, v. 57, n. 6, p. 1436–1443, 1993.

WILLIAMS, C.A.; HANAN, N.; SCHOLES, R.J.; KUTSCH, W. Complexity in water and carbon dioxide fluxes following rain pulses in an African savanna. **Oecologia**, New York, v. 161, n. 3, p. 469–480, 2009

WIND, G.P. Capillary conductivity data estimated by a simple method. In RIJTEMA, P.E.; WASSINK, H. (Ed.). **Water in the unsaturated zone**. Gentbrugge: IASAH, 1968. p. 181–191.

APPENDIX

Appendix A

Biomass growth on basis of incoming radiation *I* is calculated as:

$$\frac{dB_t}{dt} = f(t)\varepsilon_I f_I (1-\alpha_v) I \tag{A1.1}$$

where B_t is woody biomass of the tree; $f(t)$ is the proportion of incoming radiation (I) intercepted by the vegetation; ε_t is the radiation use efficiency of the vegetation; f_I is the resources use efficiency and α_v is the albedo of the vegetation.

Biomass growth on basis of water use efficiency is calculated as:

$$\frac{dB_t}{dt} = f(t)\varepsilon_w f_w ET_P \tag{A1.2}$$

where ET_P is the potential evapotranspiration.

Assuming $f(t)$ to be equal for both approaches and equating these biomass growth rates, yields an estimate for ET_P:

$$\frac{\varepsilon_I f_I (1-\alpha_v) I}{f_w \varepsilon_w} = ET_P \tag{A1.3}$$

Dividing eq. A1.3 by the potential evapotranspiration of a reference crop, eq. A1.4:

$$\frac{\varepsilon_{Irc} f_{Irc} (1-\alpha_{rc}) I}{f_{wrc} \varepsilon_{wrc}} = ET_{\mathrm{Prc}} \tag{A1.4}$$

results in:

$$\frac{ET_P}{ET_{\mathrm{Prc}}} = \left(\frac{1-\alpha_v}{1-\alpha_{rc}}\right) \frac{f_{wrc}\varepsilon_{wrc}}{f_w \varepsilon_w} \frac{\varepsilon_I f_I}{\varepsilon_{Irc} f_{Irc}} \tag{A1.5}$$

$$\frac{ET_P}{ET_{\mathrm{Prc}}} = K_c \tag{A1.6}$$

Assuming

$$\frac{f_{wrc}\varepsilon_{wrc}}{f_w \varepsilon_w} \frac{\varepsilon_I f_I}{\varepsilon_{Irc} f_{Irc}} = 1 \tag{A1.7}$$

results in a ratio of:

$$K_c = \left(\frac{1-\alpha_v}{1-\alpha_{rc}}\right) \tag{A1.8}$$

where:

$$\alpha_v = \alpha_v(1-e^{-kLAI}) + \alpha_s e^{-kLAI} \tag{A1.9}$$

$$\alpha_{rc} = \alpha_{rc}(1-e^{-kLAI_{rc}}) + \alpha_{src} e^{-kLAI_{rc}} \tag{A1.10}$$

where: α_v and α_s are the albedo of the vegetation and bare soil of the vegetation, respectively; α_{rc} and α_{rcs} are the albedo of the reference crop and bare soil, respectively; *k* is the radiation extinction coefficient of the canopy; *LAI* is the leaf area index.

Rearranging eq. A1.9 and A1.10 in A1.8 results in:

$$K_c = \frac{1-\alpha_v(1-e^{-kLAI}) - \alpha_s e^{-kLAI}}{1-\alpha_{rc}(1-e^{-kLAI_{rc}}) - \alpha_{src} e^{-kLAI_{rc}}} \tag{A1.11}$$

Eq. A1.11 can be written as:

$$K_c = \frac{1-\alpha_v - (\alpha_s - \alpha_v)e^{-kLAI}}{1-\alpha_{rc} - (\alpha_{src} - \alpha_{rc})e^{-kLAI_{rc}}} \tag{A1.12}$$

For a reference crop the leaf area index is 2.88, and the crop albedo is 0.23. The soil albedo is not assumed to play a part, so 0.23 will be assumed to be the overall albedo, then:

$$K_c = \frac{1-\alpha_v - (\alpha_s - \alpha_v)e^{-kLAI}}{1-0.23} \tag{A1.13}$$